AD-751 757

TURBULENT MODELS FOR STRONGLY HEATED, DEVELOPING GAS FLOWS

Donald M. McEligot

Arizona University

Prepared for:

Army Mobility Equipment Research and Development Center

August 1972

DISTRIBUTED BY:

NTIS

National Technical Information Service
U. S. DEPARTMENT OF COMMERCE
5285 Port Royal Road, Springfield Va. 22151

AD751757

Unclassified

AD _ _ _ _ _ _ _ _

TURBULENT MODELS FOR STRONGLY HEATED, DEVELOPING GAS FLOWS

FINAL REPORT

Compiled by

Professor Donald M. McEligot, Principal Investigator
Aerospace and Mechanical Engineering Department

August 1972

Prepared for Electrical Equipment Division
U. S. Army Mobility Equipment Research and Development Center
Fort Belvoir, Virginia

by

University of Arizona, Tucson, Arizona

under

Contract DAAK 02-69-C-0282

Unclassified

Approved for Public Release; Distribution Unlimited.

187

NOTICES

DESTROY THIS REPORT WHEN IT IS NO LONGER NEEDED. DO NOT RETURN IT TO THE ORIGINATOR.

THE FINDINGS IN THIS REPORT ARE NOT TO BE CONSTRUED AS AN OFFICIAL DEPARTMENT OF THE ARMY POSITION UNLESS SO DESIGNATED BY OTHER AUTHORIZED DOCUMENTS.

THE CITATION IN THIS REPORT OF TRADE NAMES OF COMMERCIALLY AVAILABLE PRODUCTS DOES NOT CONSTITUTE AN OFFICIAL ENDORSEMENT OR APPROVAL OF THE USE OF SUCH PRODUCTS.

Unclassified
Security Classification

DOCUMENT CONTROL DATA - R & D

(Security classification of title, body of abstract and indexing annotation must be entered when the overall report is classified)

1. ORIGINATING ACTIVITY (Corporate author)
Aerospace and Mechanical Engineering Department
College of Engineering
University of Arizona, Tucson, Arizona 85721

2a. REPORT SECURITY CLASSIFICATION
Unclassified

2b. GROUP

3. REPORT TITLE

Turbulent Models for Strongly Heated, Developing Gas Flows

4. DESCRIPTIVE NOTES (Type of report and inclusive dates)

Scientific Final

5. AUTHOR(S) (First name, middle initial, last name)

Donald M. McEligot

6. REPORT DATE	7a. TOTAL NO. OF PAGES	7b. NO. OF REFS
August 1972	175	45

8a. CONTRACT OR GRANT NO.
DAAK02-69-C-0282

b. PROJECT NO.

c.

d.

9a. ORIGINATOR'S REPORT NUMBER(S)

9b. OTHER REPORT NO(S) (Any other numbers that may be assigned this report)

10. DISTRIBUTION STATEMENT

Approved for public release; distribution unlimited

11. SUPPLEMENTARY NOTES

12. SPONSORING MILITARY ACTIVITY
U. S. Army Mobility Equipment
Research and Development Center
Fort Belvoir, Virginia 22060

13. ABSTRACT

As bases for studies in the design of compressors and turbines and for turbulent flow in magnetohydrodynamic channels, basic numerical and experimental investigations were made towards developing an operational three-dimensional treatment of turbulent transport processes, with consideration of fluid property variation and body forces. Two-dimensional numerical programs were developed and applied for gaseous, internal, turbulent, boundary layer flow in circular tubes and wide rectangular ducts. Measurements under strong heating were: (a) heat transfer and friction parameters for flow through square ducts, (b) wall temperatures for mixed convection in the laminarization region in circular tubes, (c) velocity and temperature profiles in a wide rectangular duct, and (d) velocity and temperature profiles in laminarizing flow in a circular tube.

DD FORM 1 NOV 65 1473

Unclassified
Security Classification

AGO 5698A

14 KEY WORDS	LINK A		LINK B		LINK C	
	ROLE	WT	ROLE	WT	ROLE	WT
Turbulent flow						
Turbulent models						
Laminarization						
Reverse transition						
Heat transfer						
Internal flow						
Numerical methods						
Variable properties						
Laminar flow						
Thermocouples						
Surface roughness						
Forced convection						
Mixed convection						

Unclassified

AD _ _ _ _ _ _ _ _ _

TURBULENT MODELS FOR STRONGLY HEATED, DEVELOPING GAS FLOWS

FINAL REPORT

Compiled by

Professor Donald M. McEligot, Principal Investigator
Aerospace and Mechanical Engineering Department

August 1972

Prepared for Electrical Equipment Division
U. S. Army Mobility Equipment Research and Development Center
Fort Belvoir, Virginia

by

University of Arizona, Tucson, Arizona

under

Contract DAAK 02-69-C-0282

Unclassified

Approved for Public Release; Distribution Unlimited.

NOTICES

DESTROY THIS REPORT WHEN IT IS NO LONGER NEEDED. DO NOT RETURN IT TO THE ORIGINATOR.

THE FINDINGS IN THIS REPORT ARE NOT TO BE CONSTRUED AS AN OFFICIAL DEPARTMENT OF THE ARMY POSITION UNLESS SO DESIGNATED BY OTHER AUTHORIZED DOCUMENTS.

THE CITATION IN THIS REPORT OF TRADE NAMES OF COMMERCIALLY AVAILABLE PRODUCTS DOES NOT CONSTITUTE AN OFFICIAL ENDORSEMENT OR APPROVAL OF THE USE OF SUCH PRODUCTS.

E R R A T A

1. p. 86, $Gr_q = Gr^* q^+ Re$

2. p. 91, Test Section, line 8: convection effects

3. p. 117, REYNOLDS: GD_h/μ_m

SUMMARY

As bases for studies in the design of compressors and turbines and for turbulent flow in magnetohydrodynamic channels, basic numerical and experimental investigations were made towards developing an operational three-dimensional treatement of turbulent transport processes with consideration of fluid property variation and body forces. The eventual application was intended to be flow through the passages between blades of axial turbomachines. The report covers two years, supported by the U. S. Army Mobility Equipment Research and Development Center, Fort Belvoir, Virginia, of a program expected to require about five years.

Two-dimensional numerical programs were developed and applied for gaseous, internal, turbulent, boundary layer flow in circular tubes and in wide rectangular ducts with fluid property variation including provision for longitudinal buoyancy forces and gaseous radiation interaction. Of the turbulent models tested, the van Driest-wall properties model presently appears most practical. Measurements conducted with strong heating were: (a) heat transfer and friction parameters for vertical flow through square ducts, (b) wall temperatures for mixed convection in the laminarization region in circular tubes, (c) mean velocity and temperature profiles in a wide rectangular duct, and (d) mean velocity and temperature profiles in laminarizing flow in a circular tube.

FOREWARD

The author wishes to acknowledge the encouragement and assistance of MERDC Contracting Officer's Representatives, Dr. F. E. McDonald and Mr. J. T. Broach, Jr.

It is obvious upon reading this report that much of the work was accomplished by Mssrs. Kenneth R. Perkins and Karl W. Schade, graduate students in our Department. Less apparent, but also important, was the ground work laid by Dr. C. A. Bankston of Los Alamos Scientific Laboratory and our own earlier graduates, Drs. T. B. Swearingen, R. W. Shumway, H. C. Reynolds and C. W. Coon. Further, the modest amount completed would not have been approached without a sabbatical leave granted to the Principal Investigator by the University of Arizona. Throughout, the assistance of my colleagues, Professors H. C. Perkins and R. B. Kinney, has been invaluable.

At the University of Arizona, MERDC support was supplemented by funds from the Engineering Experiment Station, National Science Foundation Institutional Grant and the Graduate College. Much of the apparatus and some of the computer routines were consequences of earlier support by the U. S. Army Research Office - Durham. Several collaborators in Great Britain were supported by their Science Research Council. Professor R. Greif, of the University of California, was supported by the National Science Foundation. The University Computer Center of the University of Arizona and the Computer Centre at Imperial College provided computing assistance.

TABLE OF CONTENTS

NOMENCLATURE

A_{cs}	cross sectional area
b	plate spacing
c_p	specific heat at constant pressure
F_b'''	body force per unit volume
g_c	dimensional constant
h	convective heat transfer coefficient, $q'_w/P(T_w-T_m)$
k_{eff}	effective thermal conductivity
$\dot{m}$	mass flow rate
p	pressure
P	perimeter
q''	heat transfer per unit area
r_w	tube radius
T	absolute temperature
u	local axial velocity
v	local transverse velocity
V	bulk velocity

x	axial coordinate
y	transverse coordinate

Symbols

μ_{eff}	effective viscosity
ν	kinematic viscosity
ρ	density
τ	shear stress

Non-dimensional parameters

Re	Reynolds number, $4\dot{m}/(\mu P)$
q^+	turbulent wall heat flux parameter, $q''_w A_{cs}/(\dot{m}\, c_{p,i} T_i)$

Subscripts

i	inlet
m	evaluated at local bulk temperature
t	turbulent component
w	evaluated at the wall

INTRODUCTION

While a large number of adequate computational procedures have been developed for incompressible, turbulent boundary layers on flat plates, provided an initial turbulent profile is well known, the problem of predicting flow through turbomachinery is much more complicated. Figure 1 demonstrates a number of additional considerations which must be added to the calculation procedure and which may affect the development of turbulent processes. Separate boundary layers develop on the rotor hub, on the blades, and on the shroud so the flow is definitely three-dimensional. In order to increase performance, turbine inlet temperatures are raised well above blade temperatures causing strong fluid property variation. The effects of non-circular passages, the fixed shroud and rotationally induced body forces, all lead to significant secondary flows. Varying pressure gradients - both favorable and adverse, and possibly severe - occur due to the longitudinal variation in cross section. In addition, combustion products may cause radiative exchange between the gas and the surfaces to become important. Further complicating the situation is the periodically transient flow condition, produced by the motion of the rotor. The investigator has chosen to treat only the steady-state problem (as have most of his predecessors), in order to make the problem tractable.

Computer technology is reaching the degree of development where numerical solutions can be obtained for flow in complicated geometries

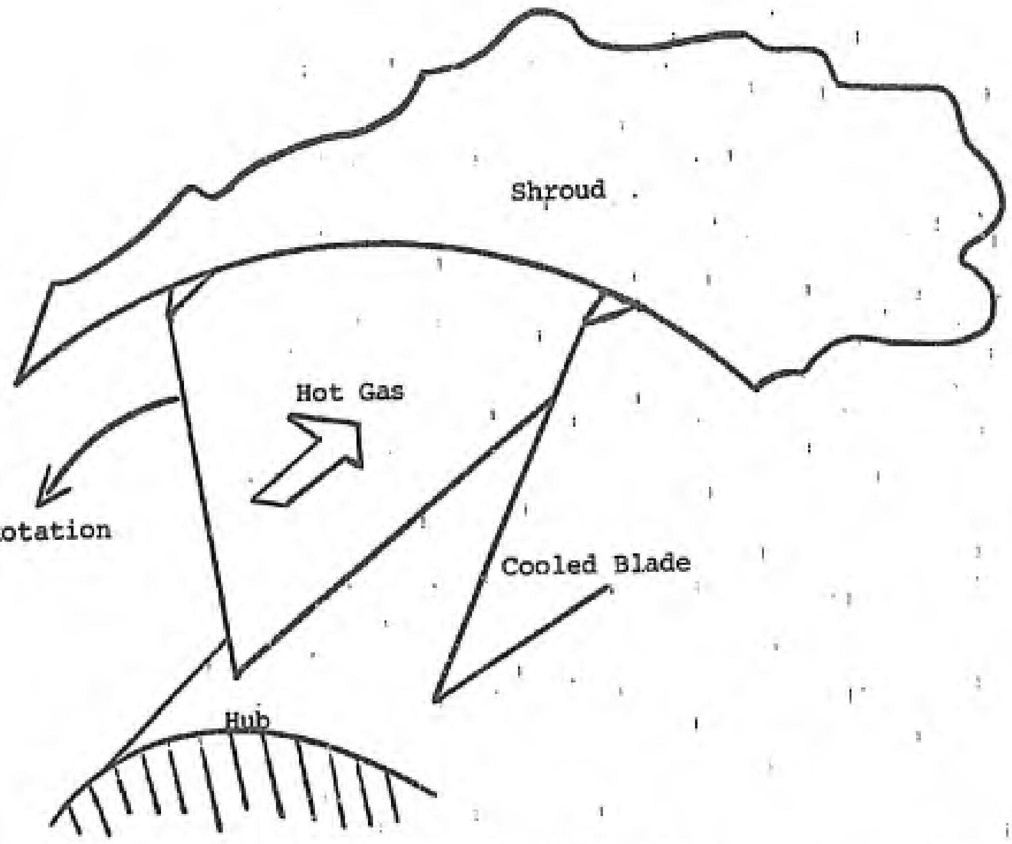

Figure 1. Schematic Diagram of Flow Through Axial Turbomachines.

and with strong variation of the fluid properties. The main difficulty in prediction is no longer in the mathematical approach - instead it is in describing the basic turbulent behavior in a form which will be valid as the flow conditions change radically along and across the fluid stream. Accordingly, a basic objective of the present work is to find a useful generalization of transport phenomena in turbulent flows.

For a two-dimensional flow, for example, the problem might be described by the coupled boundary layer equations,

$$\rho u \frac{\partial u}{\partial x} + \rho v \frac{\partial u}{\partial y} = - g_c \frac{dp}{dx} + \frac{\partial}{\partial y} (\mu_{eff} \frac{\partial u}{\partial y}) + g_c F_b'''$$

$$\rho u \frac{\partial h}{\partial x} + \rho v \frac{\partial h}{\partial y} = \frac{\partial}{\partial y} (k_{eff}) \frac{\partial T}{\partial y}$$

$$\frac{\partial}{\partial x} (\rho u) + \frac{\partial}{\partial y} (\rho v) = 0$$

and

$$\rho_i v_i b = \int_{A_{cs}} \rho u dy$$

with appropriate boundary and entrance conditions. In our terminology, we refer to the means of predicting the effective viscosity and thermal conductivity as the "turbulent model." Once the turbulent model is described these equations can be readily solved using an advanced digital computer. With an adequate, operational turbulent model and a computer program to solve the appropriate governing equations, it should be possible to develop design predictions for flow through turbines and compressors, for flow in magnetohydrodynamic ducts or for flow within heat exchangers in atomic power plants.

Previous Work

During the 1960's the Principal Investigator conducted basic experimental and analytical studies of internal gas flows with strong property variation [1,2]. For the Army Research Office, Durham, such studies concentrated on laminar flow with circular tubes [3,4], flat ducts [5] and annuli [6], and predictions were obtained by the numerical solution of the property-coupled system of partial differential equations which governs the problems. The analysis for laminar flow in circular tubes was verified in the laboratory [7] and measurements were obtained for turbulent flow through triangular tubes [8], both with gas property variation.

Initial turbulent analyses [2] centered on improving the prediction of heat transfer to low Reynolds number turbulent flow at low heating rates. In this flow regime, the accepted descriptions of the turbulent behavior - such as the "universal" velocity profile - no longer held. Experimental measurements improved our knowledge of the turbulent transport processes in this region [9]; then analyses were conducted and the heat transfer results were verified in the laboratory [10].

More recently the emphasis was shifted to obtaining analytical predictions of the heat transfer and pressure drop for strongly heated turbulent gas flows in circular tubes. Previous approaches treated a fictitious "fully developed" condition [11,12] or assumed a velocity profile for the solution of the energy equation in the thermal entry [13,14,15]. In contrast to this, we developed a reliable, flexible numerical method which solves the coupled governing equations - energy equation, x-momentum equation, continuity equation and integral continuity equation - to give both heat transfer and pressure drop predictions for strongly heated turbulent flows [4,16]. Real gas properties may be employed and the wall heat flux variation may be specified arbitrarily. The turbulent model is contained in a sub-program which may be easily modified to include new or different hypotheses.

The basic problem is describing the turbulent behavior. Reliable measurements are available for fully developed flow without heating. Under such conditions many models - eddy diffusivity distributions, mixing length treatments, generalized velocity profiles - have been adequate [17,18]. But when extending this sort of information to more complicated problems, one does not know which phenomena (if any) should remain invariant in adding effects not present in the original profile data. In our early investigations [4,16], about eleven models were compared to an experiment with strong heating of nitrogen entering at about 180° R. The model showing the best agreement was chosen for further prediction.

While the trends of the experiments - including an unexpected early maximum in wall temperature - were predicted by the numerical program, a systematic discrepancy was observed. Immediately after the start of heating, wall temperatures were overpredicted and further downstream they were consistently underpredicted. While a number of experimental difficulties might explain the difference in the immediate thermal entry, the difference downstream would require a substantial error in the measured heating rate or mass flow rate if experimental error is claimed as the explanation. It was concluded that the adopted turbulence model was not completely adequate to describe the real flow behavior. Neither the one used nor comparable approaches in the literature [18,19,20] accounted for the longitudinal growth or decay of turbulence within the scope of the model. Instead only dependence on functional behavior across the cross section is treated and the longitudinal variation enters indirectly via the other variables. In a sense, such approaches imply instantaneous development of the turbulence rather than allowing a finite length for growth and decay.

Such difficulties may be expected to occur in any analysis which attempts to treat turbulent flows undergoing readjustment - either due to changes in the fluid properties by heating or due to changes in the cross section of the flow passage. Both these causes appear in flow through turbines and compressors and their ductwork. Existing turbulent models failed in another sense when applied to channels such as rectangular ducts for magnetohydrodynamics studies - the models were essentially one dimensional and, thus, did not include consideration of the effects of a second surface in the immediate vicinity, so the corners were not treated well. Further, the effects of body forces are not generally included. In passages for rotating machinery, both these latter difficulties may be more severe than in the MHD duct.

Goals of the Present Study

The long-range goal is to develop an operational three-dimensional treatment of turbulent transport processes which would also account for effects of property variation and body forces. Numerical methods are to be applied to develop predictions for gross parameters, such as wall temperature or wall heating rate and pressure drop, for comparison to small scale experiments. Profile measurements are to be made in turbulent flows undergoing readjustment in an effort to determine features of the model directly. Thus, the main tasks of this work may be broken down into three categories:

1. *Development of a general computer program for calculation of developing flows in non-circular ducts of varying cross sections with body forces,*

2. *Development of models for turbulent flow behavior, and*

3. *Conducting experiments (a) to aid in the development of the turbulent model, and (b) to test the overall predictions for turbulent flows.*

Since only the first two years - of an estimated five or more - were supported under the present contract, only intermediate tasks were completed and the main emphasis was directed towards categories 2 and 3.

Organization

Results of the study are summarized briefly in the following section under the individual categories. Further details may be found in referenced publications in the open literature or in internal technical reports which are reproduced as self-contained Appendices to this report.

RESULTS

Computer Program Development

During the contract period programs were developed only for two-dimensional flows.

The methods of our earlier numerical program for variable property, turbulent flow through circular tubes [4] were applied to flow in non-circular ducts of infinite aspect ratio by Schade [21]. His program solves the coupled boundary layer equations for turbulent flow with variable wall temperature or variable wall heat flux as the boundary conditions on the walls. As posed, the thermal energy equation and the x-momentum equation are parabolic with transport behavior represented by "effective" viscosity and "effective" thermal conductivity, which are calculated in a separate subroutine. Boundary conditions may be asymmetric (Appendix G). The program is generally reliable when mixing length or eddy diffusivity models are used in the subroutine for effective viscosity although care must be exercised at the initial calculation step for severe cooling of a laminar gas flow [22].

In addition to turbulent flows, the program was used to obtain solutions for laminar flow with strong property variation. Three new cases were treated: (a) heating and cooling at constant wall temperature with a fully developed velocity profile at entry, (b) heating and cooling at constant wall temperature with a uniform velocity profile at entry, and (c) heating with constant wall heat flux and a uniform velocity profile at the entrance [22].

In order to examine problems involving the flow of infrared radiating gases, the program was extended to include an energy source term. First, sets of solutions were obtained for optically thin conditions, where the source term is of a non-linear algebraic form [23]. An electrically conducting gas could be treated with a comparable source term. Next, non-grey conditions were represented by the more realistic band absorptance model which leads to an integral relationship in the source term [24]. This extension increased the running time significantly but led to no other difficulty.

Three unsuccessful attempts were made to incorporate the turbulence energy equation of Bradshaw, Ferris and Atwell [25] into the program as a means of evaluating the effective velocity. Finally, Bradshaw's method-of-characteristics approach was extended directly to the symmetric internal duct situation by introducing a pseudo-boundary layer from the opposite wall and approximately superposing the turbulent shear stresses from the two walls [26]. Since viscous effects are omitted from the governing equations in the Bradshaw approach, this program is not suitable for low Reynolds number flows in its present form.

Our original program for circular tubes [4] was extended to include a body force in the momentum equation in order to permit calculations where significant natural convection effects may occur. The addition may also be useful for some magnetohydrodynamic flows. The revision was tested against Worsoe-Schmidt's predictions [27] for mixed convection in laminar flow and close agreement was found. The program was then applied to examine the predicted effects of "buoyancy forces" in the relaminization flow region (Appendix A). It must be emphasized, however, that inclusion of a body force in the momentum equation is not expected to answer the question of the effects of body forces on the turbulent model itself.

Turbulent Models

Schade's program [21], predicting gas flow through a rectangular duct with infinite aspect ratio, was applied to turbulent flows readjusting due to strong cooling [28]. Four turbulent transport models were tested and the numerical predictions were compared to the experiments of Dr. Frank Muller, Mobility Equipment Research and Development Center, Fort Belvoir, Virginia. The best agreement between predictions and measurements was obtained with the same "van Driest-wall properties" mixing length model which had worked well in our earlier circular tube study [4]. The previous study considered severe heating at an approximately constant wall flux; under such conditions there was a much stronger influence on the Nusselt number than on the friction factor. On the other hand, with cooling the effects of property variation on friction were about the same as on heat transfer and the results could be approximately predicted by quasi-developed analyses. Further, the results for cooling were less sensitive to the choice of the turbulence model.

In an investigation at Imperial College, partially supported by this contract, Morse [29] applied a version of the Patankar-Spalding program [30] to data from a number of high Reynolds number experiments involving severe heating and cooling. He tested a number of eddy diffusivity models and mixing length models, and he confirmed that the "van Driest-wall properties" model was the best of those attempted. He also improved the treatment of the core region slightly.

Numerical analyses were conducted for turbulent gas flows adjusting towards laminar behavior due to heating in circular tubes. The van Driest-wall properties model was modified by adding consideration of longitudinal growth and decay of turbulence in the form of a rate equation as proposed by Nash and McDonald [31]. In comparison to several experiments available in the literature, the additional treatment of growth and decay appeared to yield significant improvement for strongly heated flow at high Reynolds numbers but only slight improvement for laminarizing flows [32]. Later modifications improved the prediction of laminarizing flows further, but the turbulent model still could not be considered universally acceptable (Appendix A includes further description). This study did show that the behavior of the viscous sublayer can explain observations of laminarization and that such behavior is strongly dependent on the description of the turbulent transport model and the manner in which the variables within the model are evaluated.

Revisions were made to the computer calculation of effective viscosity in the wall region (high shear layer) of turbulent flows. Incorporated in the revisions was a relaminarization criterion which allows for the viscous sublayer thickness to be determined by a critical value of the turbulence Reynolds number as suggested by Launder and Jones [33]. Two interpretations of the model were tested with two values of the suggested parameter for axial lag. None worked well for strong heating of a gas at high Reynolds number; the Nusselt number was 20 percent too high in the thermal entrance region and near the exit, while at $50 \lesssim x/D \lesssim 100$ results for two versions crossed the data and exhibited sharp minima. Predictions were also compared to Bankston's data for laminarizing and laminarescent flows [34] and again failed to exhibit the proper behavior. A modification of the exponential decay term in the van Driest model suggested by Cebeci overpredicted Stanton numbers substantially in the low Reynolds number range.

Each of the models mentioned above uses an algebraic representation of mixing length or eddy diffusivity to evaluate the effective viscosity. Bradshaw, previously at the National Physical Laboratory and now at Imperial College, has developed a model which treats the turbulent shear stress ($\tau_t = \nu_t \, \partial u/\partial y$) as the dependent variable in a partial differential equation derived from the turbulence kinetic energy equation [25] and has applied it to a variety of two-dimensional flows [35]. As a first step towards utilization in turbomachinery and duct flow problems, with Bradshaw's help we extended the treatment to adiabatic flow between symmetric parallel plates using the same empirical functions to evaluate the governing equation as Bradshaw had originally used for external flows. A pseudo-superposition technique was introduced to treat interaction across the centerplane. Results compare well with high Reynolds number data for wide rectangular ducts [26]. Attempts to extend the method to low Reynolds number, adiabatic, turbulent flow - where viscous effects change the character of the governing equations from hyperbolic to parabolic for a significant portion of the cross section - were unsuccessful. The primary difficulty was the behavior of the turbulent shear stress equation in the vicinity of the wall.

We next considered phenomenological models of the physical behavior in the viscous sublayer. Initial attempts to develop stability criteria for Black's model [36] of the viscous sublayer were unsuccessful. Likewise, a simple cyclic description of the transient velocity field near the wall was found to be inappropriate.

Experiments with significant buoyancy forces in the axial direction demonstrated that further modifications of turbulent models will be necessary to predict the proper trends of the effects due to body forces (Appendix A).

Experiments with Three-Dimensional Flows

Measurements of wall parameters for gas flows developing due to strong heating in a small, vertical, square duct were obtained by K. R. Perkins. This work was initiated under a previous contract with the Army Research Office - Durham. The flow range spanned laminar, turbulent and laminarizing regimes, with emphasis on the latter. Details of the experiment are reported in Appendix C and the data are tabulated in Appendix D. The cross sectional shape had a significant rounding of the internal corners so that rectangular coordinates are not completely appropriate. The data should then provide additional crucial tests of general, three-dimensional, internal boundary layer programs expected to be developed in the coming years. For design purposes the effects of property variation are seen to correspond essentially to our previous results for symmetrical circular tubes.

Experiments with Mixed Convection (Effect of Body Forces)

The experiments of Hall and co-workers [37,38] at the University of Manchester have shown that an "aiding" body force apparently interferes with heat transfer in turbulent flow of supercritical fluids if natural convection becomes significant. In explanation, they hypothesize that the effect of a "buoyancy force" in the same direction as the turbulent forced flow is to cause a partial relaminarization. It is possible that the same effect would occur when an axial electromagnetic or electrostatic body force or a longitudinally directed centrifugal force is involved.

In the laminar flow of air an "aiding" buoyancy force improves heat transfer. To examine whether our turbulence model for low Reynolds number flow would lead to predictions in agreement with the trends noticed and hypothesized by Hall, the revised computer program was applied to air flow at Re_i = 6000 and non-dimensional heating rates q^+ = 0.002 and 0.004. In our profile data at these conditions (Appendix B) and "low" Grashoff numbers, the former flow showed turbulent behavior, while a heating rate of $q^+ \simeq 0.004$ appeared to cause laminarization. In contrast to Hall's experimental observations, our numerical model predicts that the effect of an "aiding" body force is to improve heat transfer.

Experiments were conducted with air flowing in a 1/2 inch diameter vertical tube at several flow rates in the low Reynolds number range and at several pressure levels. Since the Grashoff number varies as density-squared, this size tube and flow range leads to negligible natural convection effects at atmospheric pressure and significant, but not dominant, buoyancy forces at pressures around seven atmosphere. Details of the experiments are presented in Appendix A. By selecting experimental procedure so that comparisons could be made with only the Grashoff number differing between successive runs, the effect of the body force could be isolated dramatically. The procedure was essentially the same as that employed by Hall and Jackson [37] in their demonstration with supercritical CO_2.

For rapidly laminarizing conditions, the measurements show a slight improvement in heat transfer parameters with aiding buoyancy forces as in laminar flow. However, for gradual laminarization and for turbulent flow the aiding buoyancy force inhibits heat transfer; that is, the measurements refute the trends of body force effects which are predicted by the numerical turbulent model.

Experiments with Property Variation in Fully Developed Flow

When a gas is heated in a circular tube, fully established conditions are not obtained because the viscosity continually increases in the axial direction and the density continually drops. Consequently, a number of processes operate simultaneously to affect the turbulent behavior. In a parallel plate duct, fully established conditions may eventually be reached if it is heated asymmetrically and if one wall is maintained at a fixed temperature. Dr. B. E. Launder and his students at Imperial

College have constructed such a duct in order to examine flows with significant variation of fluid properties across the flow but no time-mean variation in the longitudinal direction.

While on sabbatical leave at Imperial College, the Principal Investigator obtained preliminary data on this duct with an electrically-heated upper surface and a water-cooled lower surface. With this configuration a fully developed flow could eventually be established downstream with $T_{hot} \approx 400°F$ and $T_{cold} \approx 60°F$ and with the heat flux in a direction perpendicular to the walls. Schade's program [21] was applied with asymmetric boundary conditions to predict the duct length necessary to approach fully-established conditions (Appendix G). As initially constructed, the apparatus supported the upper hot plate with 2 x 1 x 1/4 aluminum channels which were insulated from the main plates by 1/8 inch thick strips of "Sindanyo", an insulator. However, analysis of the heat losses revealed that most of the energy from the resistance heating blanket of the hot plate would pass to the cold plate via these side channels rather than through heat transfer to the gas. It was recommended that the side channels be replaced by better insulation. Before modifications were completed the Principal Investigator returned to Arizona from sabbatical leave.

The experiment has been continued by Launder with partial support from this contract. One of his students, Mr. A. F. Morse, obtained time-mean velocity and temperature profiles for Reynolds numbers between 10^4 and 10^5 at wall-to-bulk temperature ratios up to 1.53 [29]. The present apparatus has eliminated the aluminum supports in favor of

Marinite 36 (an asbestos based insulating material) and has an aspect ratio of 7.5. Although none of the runs conducted achieved a complete fully developed thermal flow the measurements have shown that definite changes in the dimensionless velocity and temperature profiles are evident when compared to isothermal flow at the same Reynolds number. The sublayer resistance appears to decrease somewhat when the temperature gradient is negative at the wall, but only slightly when the gradient is positive.

Profile Measurements in Laminarizing Flow

Time-mean velocity and temperature profiles were measured by R. J. Pederson for air flow through a strongly heated, 1/2 inch circular-tube (Appendix B). The entering Reynolds number was 6000, and fully developed turbulent flow was established prior to heating. An impact tube and thermocouple served as the velocity and temperature probes, respectively. A hot film anemometer was employed to examine the intermittency approaching the viscous sublayer.

Two heating rates were chosen for the experiments. Run 46 corre-

Run	q^+	x/D	T_w/T_b	Re_b	Re_w
46	$\sim$ *0.002*	*37.6*	*1.43*	*5000*	*3900*
33	$\sim$ *0.004*	*38.6*	*1.84*	*4300*	*2800*

sponded to the lower heating rate and was chosen to yield "laminaresent" conditions. By that, it is meant that heat transfer and friction parameters were expected to be less than those for adiabatic flow at the same

Reynolds number, but the flow was essentially turbulent with the transport parameters adjusting toward the adiabatic values as the flow continued downstream. Run 33 corresponded to the higher heating rate and was expected to yield laminar predictions, although the local bulk Reynolds number indicates turbulent flow.

Velocity profiles are shown in Figure 2. For the lower heating rate, Run 46, the velocity profile appears to display a logarithmic variation near the tube wall characteristic of the "law of the wall" for adiabatic flow. The slight flattening at the tube centerline is due to axial symmetry. In the absence of definite information about the viscous wall layer, which might be expected to be thickened by heating, the results of Run 46 appear to follow the pattern for normal adiabatic flow. On the other hand, at the higher heating rate (Run 33) there appears to be a predominantly viscous profile near the tube wall, with a rather extensive and approximately constant velocity region in the center. Temperature limitations prevented hot film anemometer measurements closer to wall than 0.09 inches for this run. However, at this closest approach to the wall, oscilloscope traces show the flow to be completely turbulent. Thus, it appears that for strong heating the turbulent shear stress in a substantial core region is approximately zero while the turbulent kinetic energy is non-zero. Therefore, difficulty can be expected in trying to apply to this flow,turbulent models which relate the turbulent shear and kinetic energy to one another, such as Bradshaw's technique. Though uncalibrated, the anemometer traces apparently show a high turbulence level for this run (Appendix B).

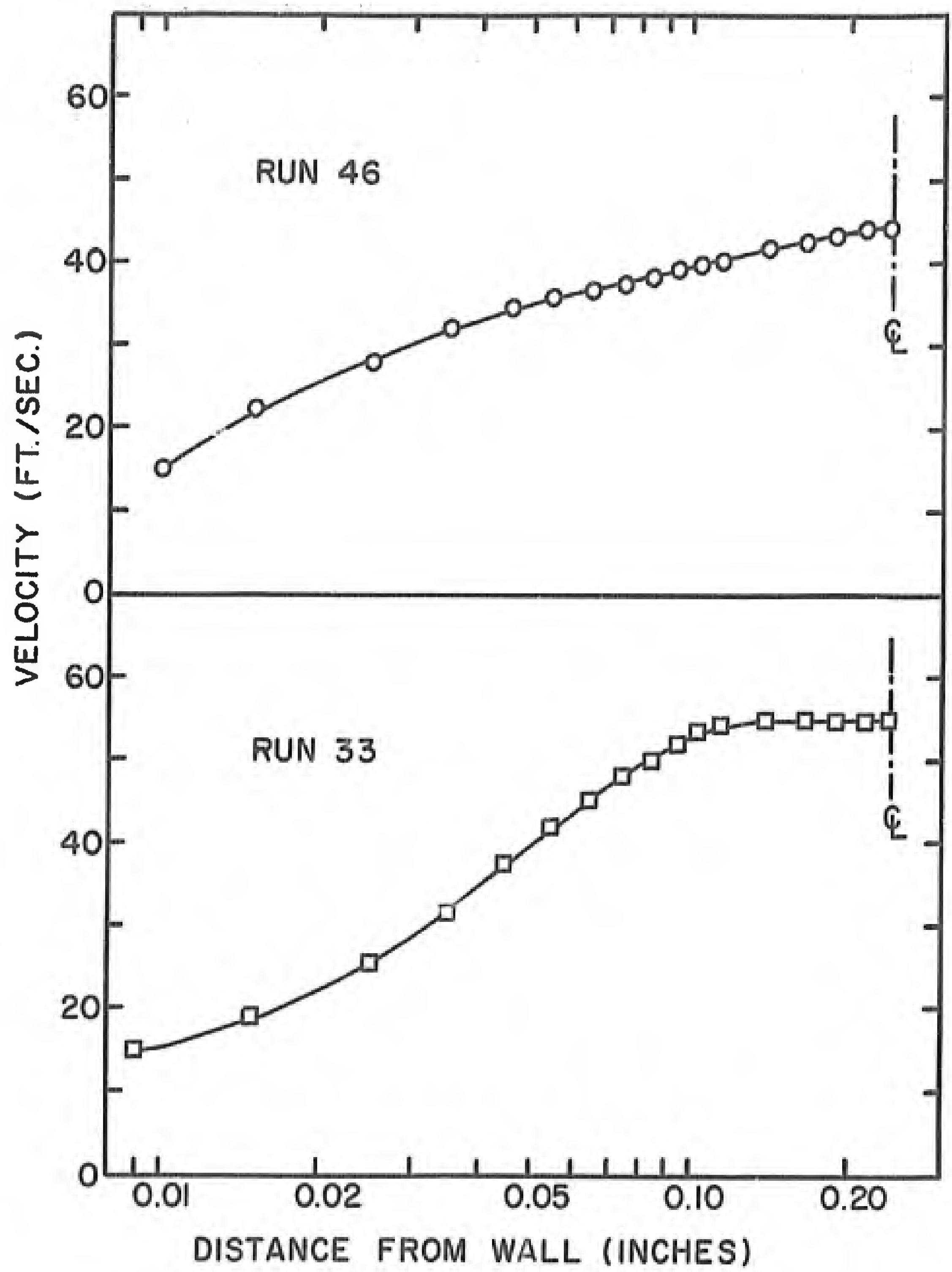

Figure 2. Measured Velocity Profiles in Laminarescent and Laminarizing Heated Air Flow.

The temperature profiles of Figure 3 support the tenative conclusions from the velocity profiles. In the case of low heating, the temperature varies rapidly only in the region close to the wall. This behavior is typical of turbulent flow. For the higher heating rate, the temperature varies gradually from the wall to the centerline. This implies that the "thermal resistance", although still high, is spread uniformly as in laminar flow. This is in contrast to turbulent flows where it is concentrated near the wall. Perhaps the most striking effect of the greater resistance for the high heating run is that the centerline temperature is slightly less than that for the low heating condition, whereas approximately twice as much energy has been added to the same flow.

Technical Papers and Reports Completed*

K. W. Schade, "A Numerical Solution for the Turbulent Flow of a Gas with Strong Property Variation Between Parallel Plates," M. S. Report, Aerospace-Mechanical Engineering Department, University of Arizona, 1969.

D. M. McEligot and C. A. Bankston, "Numerical Predictions for Circular Tube Laminarization by Heating," ASME paper 69-HT-52, presented at National Heat Transfer Conference, August 1969.

C. A. Bankston and D. M. McEligot, "Turbulent and Laminar Heat Transfer to Gases with Varying Properties in the Entry Region of Circular Ducts," *Int. J. Heat Mass Transfer*, 13, 319-344, 1970.

D. M. McEligot, S. B. Smith and C. A. Bankston, "Quasi-Developed Turbulent Pipe Flow with Heat Transfer, *J. Heat Transfer*, 92, 641-650, 1970.

---

*As noted in the Foreward a number of these have been partially supported by other agencies as well.

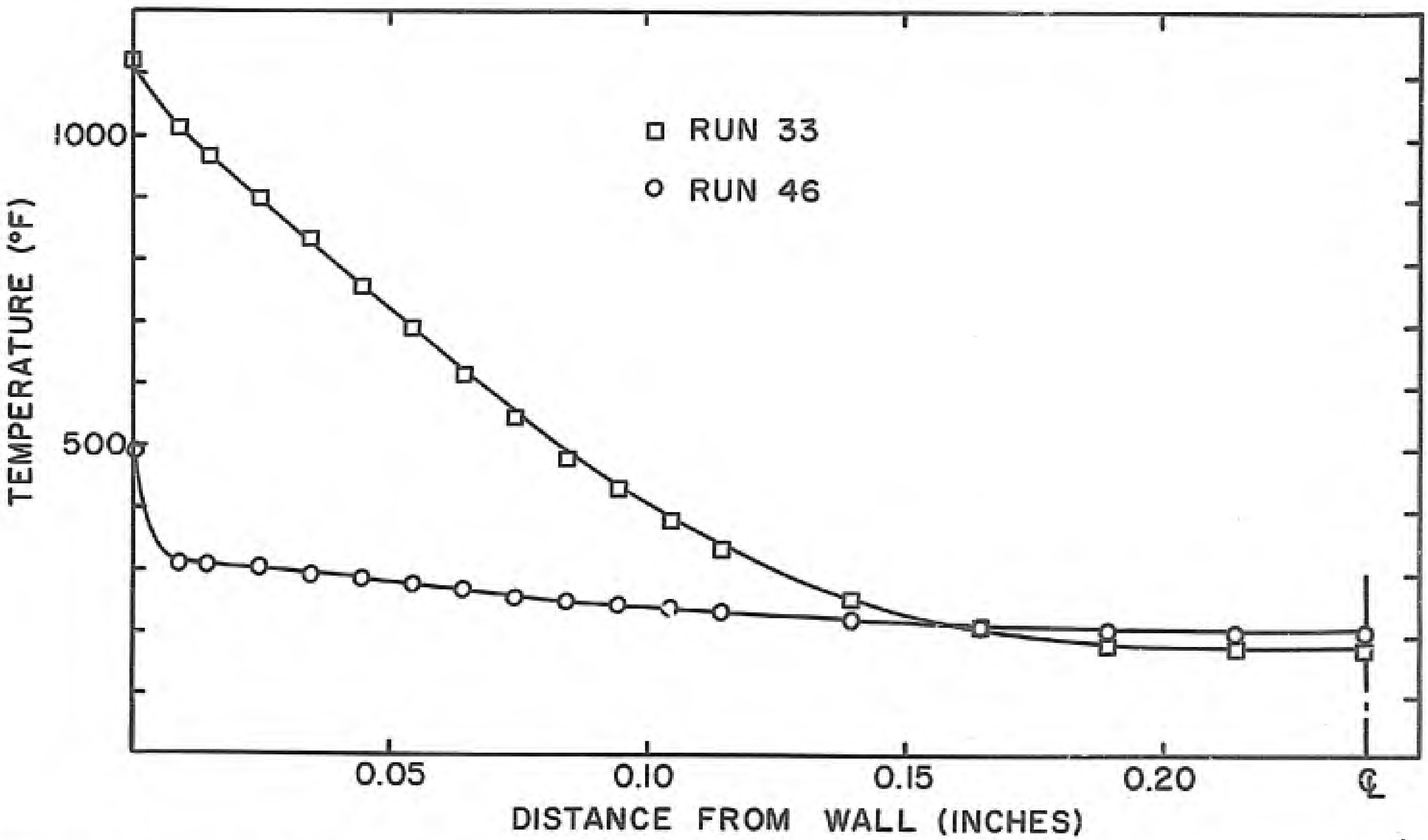

Figure 3. Measured Temperature Profiles for Laminarescent (Run 46) and Laminarizing (Run 33) Heated Air Flow.

R. Greif and D. M. McEligot, "Heat Transfer in Thermally Developing Laminar Flows with Optically Thin Radiation," *J. Heat Transfer*, 93, 473-475, 1971.

K. W. Schade and D. M. McEligot, "Cartesian Graetz Problems with Air Property Variation," *Int. J. Heat Mass Transfer*, 14, 653-666, 1971.

R. Greif and D. M. McEligot, "Thermally Developing Laminar Flows with Radiative Interaction Using the Band Absorptance Model," *Appl. Sci. Research*, 25, 234-244, 1971.

K. W. Schade and D. M. McEligot, "Turbulent Flow Between Parallel Plates with Gas Property Variation," ASME paper 71-FE-38 presented at ASME Fluids Engineering Conference, May 1971.

P. Bradshaw, R. B. Dean and D. M. McEligot, "Calculations of Interacting Turbulent Shear Layers: Duct Flow," Imperial College Aero. Rpt. 71-14, 1971. Submitted to ASME. Also *J. Basic Eng.*, (in press).

A. F. Morse, "Heat Transfer in Turbulent Flow in Pipes and Plane Channels with Steep Property Gradients," Imperial College, Mech. Eng. Rept. ON/6/13, December 1971.

K. R. Perkins and D. M. McEligot, "Roughness of Heat Transfer Surfaces," *Int. J. Heat Mass Transfer* (in press).

J. A. Bates, R. A. Schmall, G. A. Hasen and D. M. McEligot, "Mixed Convection in the Relaminarization Region," Appendix A.

K. R. Perkins, K. W. Schade and D. M. McEligot, "Measurement of Three-Dimensional Gas Flow," Appendix C.

K. R. Perkins and D. M. McEligot, "Use of Scanning Electron Microscope to Examine Heat Transfer Surfaces," Appendix E.

W. G. Hess, A. F. Deardorff and D. M. McEligot, "Radiating Thermocouple Conduction Error," Appendix F.

D. M. McEligot and K. W. Schade, "Effects of Inlet Temperature on Thermal Development for Turbulent Flow in Ducts Heated Asymmetrically with Air Property Variation," Appendix G.

K. R. Perkins, K. W. Schade and D. M. McEligot, "Heated Laminarizing Gas Flow in a Square Duct," *Int. J. Heat Mass Transfer*, (in press).

RELATED WORK

Currently, extensive efforts are taking place at Imperial College and other institutions to develop and apply partial differential equations for various turbulence properties with the aim of identifying "universal" aspects and, thus, to ease extension to a wide variety of flows. Their 1-, 2- and 3-equation turbulence models provide means of calculating the longitudinal rate of change of the turbulence properties which are taken as dependent variables. As mentioned, Bradshaw uses the turbulent shear stress as a dependent variable; Spalding's group has used turbulence kinetic energy, length scale, the product of two, dissipation of turbulence kinetic energy, and a quantity related to fluctuating vorticity-squared as dependent turbulence variables. Harlow and Nakayama of Los Alamos have also examined an equation predicting the turbulence energy decay rate. Nee at Notre Dame solves an equation for the effective viscosity itself.

For external incompressible and compressible turbulent boundary layers which are less complicated than those considered under the present contract, Ng and Spalding [39] and Bradshaw, Sivasegaram and Whitelaw [40] have shown there is little value in solving a kinetic energy or length scale equation compared to using predictions based on a simple mixing length model. A common feature of the above approaches is their acceptance of a form of universal velocity profile near the wall. Thus, they are not likely to work well for low Reynolds number flows or for strongly heated flows, even at high Reynolds numbers, since our successful numerical predictions imply a much thicker viscous region than is represented in the usual "law of the wall" behavior. Observations of the same weakness in strongly accelerated flows - as in nozzles and turbomachine blading - have led Jones and Launder [41] to extend partial differential equations for the turbulence structure to $y^+ \approx 1$. They solve an equation for turbulence kinetic energy in conjunction with one for dissipation of turbulence kinetic energy - a so-called k-ε model. The model predicts experimental trends properly and generally agrees in magnitude with the observed data. It has not yet been successfully applied to strongly heated internal flows. Their program is available from the National Research Development Corporation in Great Britain.

An exciting new development of promise is a series of solutions by Deardorff at the National Center for Atmospheric Research [42,43]. He solves the three-dimensional time-dependent Navier Stokes equations for fully developed turbulent flow fields by introducing empirical "sub-grid-scale" treatment of the smaller scale behavior and then examining the resulting statistics. The method is not yet appropriate for design purposes with the sort of problems treated under this contract but it bears watching. Boundary conditions are taken as cyclic for non-rigid boundaries so the program is constrained to fully developed mean flows or approximations thereof, such as the planetary boundary layer, rather than continually developing flows. Treating three space dimensions also leads to rather coarse grid distributions with present day computers; for a length of four characteristic thicknesses, Reference 43 uses a 40 by 40 by 20 uniform grid so the "wall" region still requires assumption of a law-of-the-wall. Despite solving the transient Navier-Stokes equations the approach does, in fact, rely on a number of adjustable empirical constants in its evaluation. For four cases, approximately 150 hours of CDC 6600 time were used; at our academic rates this would correspond to about $75,000 per case on our CDC 6400. This operational program demonstrates that three-dimensional turbulent solutions are feasible but that some form of turbulent model is still necessary.

Spalding's group has developed numerical programs for steady three-dimensional laminar boundary layers in rectangular ducts [44,45] and has exercised them for the following pertinent situations:

a. *Entrance flow in a rectangular duct.*

b. *Flow development in a square duct with an axial jet.*

c. *Flow in a rectangular duct with a moving wall (shroud).*

d. *Transverse natural convection in a developing forced flow (body force).*

For simple turbulent models the extension to handle turbulent flows is conceptually straight forward. With coarse grids, computer time has been of the order of a few minutes of IBM 7094 time since the three-dimensional steady boundary layer is approximately equivalent to a two-dimensional transient problem for computational purposes.

CONCLUSIONS

Each of the aspects mentioned in the Introduction as additional complications necessary in a general three-dimensional boundary layer program has been handled separately in operational computer programs. Thus, combination into a general computational program for turbomachinery is now feasible. However, no general turbulent model is yet available to predict the transport processes in a completely reliable fashion. For design purposes at present, the best choice appears to be the van Driest-wall properties model with empirical modifications as necessary.

RECOMMENDATIONS

Each of the present tasks should be continued. In particular, more knowledge is necessary for reducing the empiricism in turbulence models so that design calculations may be extended to new flow situations with confidence.

In general computation programs, a wide variety of geometries must be accomodated. Accordingly, a selection of control volume shapes, in addition to the current rectangular parallelepiped, should be developed and should be available on call within the program; some of the automatic finite element techniques of structural engineers may prove valuable in this respect.

REFERENCES

1. D. M. McEligot, P. M. Magee and G. Leppert, *J. Heat Transfer*, 87, 67, 1965.

2. D. M. McEligot, L. W. Ormand and H. C. Perkins, *J. Heat Transfer*, 88, 239, 1966.

3. D. M. McEligot and T. B. Swearingen, *Int. J. Heat Mass Transfer*, 9, 1145, 1966.

4. C. A. Bankston and D. M. McEligot, *Int. J. Heat Mass Transfer*, 13, 319-344, 1970.

5. T. B. Swearingen and D. M. McEligot, *J. Heat Transfer*, 93, 432-440, 1971.

6. R. W. Shumway, Ph.D. Thesis, University of Arizona, 1969.

7. T. B. Swearingen, Ph.D. Thesis, University of Arizona, 1969.

8. D. A. Campbell and H. C. Perkins, *Int. J. Heat Mass Transfer*, 11, 1003, 1968.

9. H. C. Reynolds, M. E. Davenport and D. M. McEligot, "Velocity Profiles for Fully Developed, Turbulent Low Reynolds Number Pipe Flow," ASME paper 68-WA/FE-34, 1968.

10. H. C. Reynolds, T. B. Swearingen and D. M. McEligot, *J. Basic Eng. Trans.*, 91, 87, 1969.

11. R. G. Deissler, NACA Report 1210, 1955.

12. J. B. Botje, Ph.D. Thesis, Purdue University, 1956.

13. R. G. Deissler, NACA TN 3016, 1953.

14. H. Wolf, *J. Heat Transfer*, 81, 267, 1959.

15. P. M. Magee and D. M. McEligot, *Nuc. Sci. Eng.*, 31, 337, 1968.

16. D. M. McEligot, S. B. Smith and C. A. Bankston, *J. Heat Transfer*, 92, 641, 1970.

17. D. B. Spalding and S. W. Chi, *J. Fluid Mech.*, 18, 117, 1964.

18. R. M. Kendall et al., DDC AD 619 209, 1964.

19. G. L. Mellor, *AIAA J.*, 5, 1570, 1967.

20. A. M. O. Smith, N. A. Jaffe and R. C. Lind, AD 631 329, 1963.

21. K. W. Schade, M.S.E. Report, Aerospace and Mechanical Engineering Department, University of Arizona, 1969.

22. K. W. Schade and D. M. McEligot, *Int. J. Heat Mass Transfer*, 14, 653, 1971.

23. R. Greif and D. M. McEligot, *J. Heat Transfer*, 93, 473, 1971.

24. R. Greif and D. M. McEligot, *Appl. Sci. Research*, 25, 234, 1971.

25. P. Bradshaw, D. H. Ferris and H. P. Atwell, *J. Fluid Mech.*, 28, 593, 1967.

26. P. Bradshaw, R. B. Dean and D. M. McEligot, Imperial College, Aero Rpt. 71-14, 1971. Submitted to ASME. Also *J. Basic Eng.*, (in press).

27. P. M. Worsoe-Schmidt, Ph.D. Thesis, Stanford University, 1964.

28. K. W. Schade and D. M. McEligot, "Turbulent Flow Between Parallel Plates with Gas Property Variation," ASME paper 71-FE-38, 1971.

29. A. F. Morse, "Heat Transfer in Turbulent Flow in Pipes and Plane Channels with Steep Property Gradients, Imperial College, Mech. Eng. Rpt. ON/G/13, December 1971.

30. S. V. Patankar and D. B. Spalding, *Int. J. Heat Mass Transfer*, 10, 1389, 1967.

31. J. F. Nash and A. G. J. MacDonald, NPL Aero. Rpt. 1234, ARC 29088, FM 3844, 1967. NASA N68-20516.

32. D. M. McEligot and C. A. Bankston, "Numerical Predictions for Circular Tube Laminarization by Heating," ASME paper 69-HT-52, 1969.

33. B. E. Launder and W. P. Jones, "On the Prediction of Laminarescent Turbulent Boundary Layers," ASME paper 69-HT-13, 1969.

34. C. A. Bankston, Ph.D. Thesis, University of New Mexico, 1965.

35. P. Bradshaw and D. H. Ferris, "Applications of a General Method of Calculating Turbulent Shear Layers," ASME paper 71-WA/FE-8, 1971.

36. T. J. Black, NASA CR-888, 1968.

37. W. B. Hall and J. D. Jackson, "Laminarization of a Turbulent Pipe Flow by Buoyancy Forces," ASME paper 69-HT-55, 1969.

38. W. B. Hall and P. H. Price, "Mixed Forced and Free Convection from a Vertical Plate to Air," 4th International Heat Transfer Conf., 1970.

39. K. H. Ng and D. B. Spalding, Imperial College, Mech. Eng. Rpt. BL/TN/A/27, 1970.

40. P. Bradshaw, S. Sivasegaram and J. H. Whitelaw, Imperial College, Mech. Eng. Rpt. BL/TN/A/34, 1970.

41. W. P. Jones and B. E. Launder, *Int. J. Heat Mass Transfer*, 15, 301, 1972.

42. J. W. Deardorff, *J. Fluid Mech.*, 41, 453, 1970.

43. J. W. Deardorff, *J. Atmos. Sci.*, 30, 91, 1972.

44. D. Sharma and D. B. Spalding, Imperial College, Mech. Eng. Rpt. BL/TN/A/47, 1971.

45. R. M. Curr, D. Sharma and D. G. Tatchell, Imperial College, Mech. Eng. Rpt. EF/TN/A/41, 1971.

APPENDIX A

MIXED CONVECTION IN THE RELAMINARIZATION REGION

J. A. Bates[1], R. A. Schmall[2], G. A. Hasen[3] and D. M. McEligot[4]

An exploratory study into the effect of buoyancy forces on predominantly forced upflow in heated circular tubes is reported. By operating in the low Reynolds number range both laminarizing flows and flows which remain essentially turbulent may be examined. Numerical solutions of the property-coupled, governing internal boundary layer equations predict that in both cases when the buoyancy force acts in the direction of an air flow the heat transfer performance is improved. However, a simple experiment demonstrates that in turbulent air flow, this so called "aiding" situation can inhibit heat transfer instead.

---

1. Major, U.S.A.F. Graduate student.

2. Teaching Assistant.

3. Graduate student.

4. Professor.

1. Introduction

Recently Hall and Jackson (1969) hypothesized that buoyancy forces can modify turbulence production near the wall in the forced upward flow of fluids at supercritical pressure under strong heating. They suggest that the modification leads to laminarization which, in turn, causes the "deterioration" phenomena reported by many for internal flow in the neighborhood of the pseudocritical temperature [see Hall, Jackson and Watson (1968) or Shiralkar and Griffith (1969)]. By "deterioration" one means a large and localized reduction in the heat transfer coefficient for a turbulent flow. The consequences are unexpected peaks appearing in the wall temperature distribution when the heating rate is controlled as it is in most experimental measurements of such flows.

Comparable unexpected temperature peaks have also been observed in the severe heating of common gases, well removed from the critical point, by Perkins and Worsoe-Schmidt (1965). However, with the aid of modern digital computers, Bankston and McEligot (1970) found they could predict this behavior by a simple, empirical extension of the van Driest turbulence model (1956). With further empirical modification McEligot and Bankston (1969) were also able to predict relaminarization in a number of heated, trubulent gas flows. Accordingly, one might suggest handling the problem for turbulent flow near the critical point by applying the same turbulence model and numerical program, but using the appropriate description of fluid properties in the critical region rather than those of common gases.

The present paper examines a companion problem: will significant buoyancy forces modify the turbulence behavior in the heating of common gases or can the same turbulence model be used for mixed convection as for pure forced convection? After reviewing the pecularities of internal flow with significant property variation for the reader, we apply the numerical program of Bankston and McEligot to turbulent upflow and downflow of air in a circular tube and then we conduct a simple experiment to test the predictions. A second, included question is whether buoyancy forces aid or hinder heat transfer in forced, vertical upflow.

2. Background

The idealized geometry considered is a vertical, circular tube with an adiabatic flow development region preceeding a section where a constant wall heat flux is applied. In experiments this thermal boundary conditon is approximated by resistive heating, but since both electrical resisitivity and external heat losses vary with temperature; the idealized condition, q''_w = constant, is usually not attained. The forced internal gas flow is generally upward.

(a) Effects of transport property variation

The transport properties of fluids near their critical points vary severely and rather irregularly with both temperature and pressure. However, most of the physical phenomena involved occur with air if the temperature variation is severe. Air properties can be conveniently modeled by power laws of the form

$$\mu \sim T^a,\ k \sim T^b,\ c_p \sim T^d,\ \rho \sim p/T \qquad (1)$$

for analysis. Pressures may be kept high so that the Mach number is low, but the density still varies strongly due to its temperature dependence.

In the situation to be considered, the temperature varies significantly both along and across the tube. Thus, definition of a local Reynolds number becomes ambiguous unless investigators specify the location at which the properties are to be evaluated. A bulk Reynolds number,

$$Re_b = \frac{GD}{\mu_b} = \frac{4\dot{m}}{\pi D \mu_b} \qquad (2)$$

wall Reynolds number,

$$Re_w = \frac{GD}{\mu_w} \qquad (3)$$

and modified wall Reynolds number,

$$Re_{w,m} = \frac{V_b D}{\nu_w} \qquad (4)$$

and others are all commonly used. It can be seen that with heating Re_b will continually decrease along the tube while others may pass through maxima. An example of such severe heating is provided by Run 140 in the experiments of Perkins and Worsoe-Schmidt (1965). In their one-eighth inch tube an inlet Re of 2.7 x 10^5, nitrogen was heated to about eight times its inlet temperature, the wall temperature peaked to about twelve times the inlet gas temperature, and the ratio T_w/T_b reached about seven. The Nusselt number "deteriorated" by about sixty per cent.

Early variable property analyses by Deissler (1955), Sze (1957) and others considered the flow as fully-developed, thereby neglecting advection terms in the same manner as in equilibrium turbulent boundary layer studies. In a recent investigation, Schade and McEligot (1971) essentially confirmed Sze's predictions for turbulent air flow being cooled in a parallel plate duct with approximately constant wall temperature; since this boundary condition approximates an equilibrium layer, the confirmation is not surprising. However, with a constant wall heat flux, the axial variation of the wall viscosity invalidates the similarity assumption. Further, as the bulk temperature increases, the gas accelerates, so advection terms must be included in the analyses. Consequently, the early analytical predictions deviated from experimental observations as the heating rate was increased.

Adapting features of the numerical analyses of Worsoe-Schmidt and Leppert (1965) and Patankar and Spalding (1967), Bankston and McEligot (1970) developed a computer program to solve the property-coupled internal boundary layer equations for turbulent flow in a circular tube. Their studies showed that - by solving the complete boundary layer equations, including axial and radial advection terms, with a suitable choice of turbulence model - the experimental observations could be predicted. In the process they found the predictions to be highly sensitive to the turbulence model and the manner in which properties appearing in its definition were evaluated.

(b) Laminarization or reverse transition

In a sense, all heated turbulent gas flows apparently "laminarize." That is, for those cases where the numerical predictions agree with the data, the predictions show a thicker viscous sublayer than an unheated flow at the same local Re_b would possess. The result is a reduction in heat transfer parameters compared to constant property predictions. This situation is comparable to that described by Schraub and Kline (1965) as "laminarescent." In this paper we will consider it as normal turbulent behavior; the heat transfer and friction parameters are described by standard empirical correlations for turbulent gas flow with variable properties as developed by Perkins and Worsoe-Schmidt (1965) and others.

For an unheated turbulent internal flow, as the Reynolds number is reduced, eventually the viscous sublayer begins to occupy a substantial portion of the cross section and the turbulence model must be modified in the wall region in order to predict reasonable velocity profiles and friction factors. McEligot, Ormand and Perkins (1966) showed simple modifications suffice. Since the friction factors still agree with the Drew, Koo, and McAdams (1932) turbulent prediction, we also consider this regime as turbulent (though others might term it laminarescent because the viscous sublayer is thicker, in nondimensional terms, than for asymptotic turbulent flow).

Now if heating of a gas continues indefinitely, Re_b eventually decreases below 2300 (or such) and one expects the flow to revert to laminar. However, McEligot (1963) detected this transition to laminar flow occuring at successively higher values of Re_b as the heating rate (nondimensional) was increased. For heated gas flows, this retransition may be detected by deviation below variable properties turbulent correlations and eventual agreement with the downstream laminar Nusselt number, the criteria used by Coon and Perkins (1970). Bankston (1965) applied hot wire anemometry in tubes about 0.1 inch in diameter and demonstrated (1970) that laminarization as well as reversion to turbulent flow, could be recognized on a plot of the variation of local Stanton number versus local Re_b axially along the tube. The gross behavior can be categorized for these small tube experiments in terms of the locus on a graph of non-dimensional heating rate,

$$q^+ = q_w''/(Gc_pT_i) \tag{5}$$

and entering Reynolds number. Bankston (1966) pointed out that the flow regime classification can also be presented in terms of a thermal version of the acceleration parameter, K, which has the same order of magnitude as in the external flow, acceleration experiments of Moretti and Kays (1965). Most internal flow measurements have been in small tubes so transverse profile measurement has not been possible. However, R. J. Pederson has conducted preliminary, unpublished, temperature and velocity profile measurements at the University of Arizona; by considering the classification plot, he selected two heating conditions at $Re_i = 6000$ to give "laminarescent" and "laminarizing" flows, respectively, and found that the profiles confirmed his expectations.

In this paper we consider laminarizing conditions as those which would yield agreement with laminar heat transfer predictions downstream well before Re_b is reduced to the usual (laminar-to-turbulent) transition Reynolds number. However, since the thermal entry length for laminar flow increases with Reynolds number, laminar downstream results may not be reached within the length of tube available even though we conclude that a particular run is laminarizing.

McEligot and Bankston (1969) conducted numerical experiments to match data obtained by various investigators for both laminarizing and essentially turbulent conditions. For runs which were laminarizing the viscous sublayer, defined as the radial location at which the turbulence Reynolds number (ϵ/ν) reached unity, rapidly filled the tube after the initiation of heating. Thus, while there would still be turbulent fluctuations, the viscous effects would dominate. The turbulence model which was most successful is described below under Numerical Predictions for Turbulent Mixed Convection.

(c) Mixed convection

The low velocity flow of a non-reacting gas undergoing strong heating symmetrically in a circular tube may be described, under the usual boundary layer approximations, by the following governing equations for the mean quantities:

continuity,

$$\frac{\partial\, \overline{\rho u}}{\partial \bar{x}} + \frac{2}{\bar{r}} \frac{\partial}{\partial \bar{r}} (\overline{\rho v r}) = 0 \tag{6a}$$

x - momentum,

$$\overline{\rho u} \frac{\partial \bar{u}}{\partial \bar{x}} + 2\overline{\rho v} \frac{\partial \bar{u}}{\partial \bar{r}} = \frac{d\bar{p}}{d\bar{x}} + \frac{4}{Re_i} \frac{1}{\bar{r}} \frac{\partial}{\partial \bar{r}} (\bar{r}\bar{\mu}_{eff} \frac{\partial \bar{u}}{\partial \bar{r}}) + \frac{Gr_i^*}{Re_i^2} \bar{\rho} \tag{6b}$$

thermal energy,

$$\overline{\rho u} \frac{\partial \bar{h}}{\partial \bar{x}} + 2\overline{\rho v} \frac{\partial \bar{h}}{\partial \bar{r}} = \frac{4}{Re_i Pr_i} \frac{1}{\bar{r}} \frac{\partial}{\partial \bar{r}} (\bar{r} \frac{\bar{k}_{eff}}{\bar{c}_p} \frac{\partial \bar{h}}{\partial \bar{r}}) \tag{6c}$$

and integral continuity,

$$\int_0^1 \overline{\rho u r d r} = \frac{1}{2} \tag{6d}$$

plus the no-slip and impermeable wall boundary conditions. (While the quantities are time-mean values, the overbars represent nondimensionalization - usually in terms of inlet properties.) The effective transport properties, $\bar{\mu}_{eff}$ and $\bar{k}_{eff}$, may be provided by solution of auxiliary equations, such as those for kinetic energy of turbulence and/or dissipation of kinetic energy of turbulence and additional assumptions, or may be taken from mixing length or eddy diffusivity descriptions. The body force is taken as positive when in the direction of flow; consequently, the modified Grashoff number, $Gr_i^* = g\, D^3/\nu_i^2$, will have a negative sign for upflow.

In the present study the thermal boundary condition is

$$\left.\frac{\partial \bar{h}}{\partial \bar{r}}\right|_w = \frac{q_i^+(\bar{x}) Re_i Pr_i \bar{c}_{p,w}}{2\bar{k}_w} \tag{7}$$

ie., a specified wall heat flux distribution. Thus, the parameters determining the flow and resulting wall temperature distribution are Re_i, Pr_i, Gr_i^*, and $q_i^*(\bar{x})$.

For laminar flow the stipulation of μ_{eff} and k_{eff} is unambiguous. Worsoe-Schmidt and Leppert (1965) treated the laminar, upward flow of air in the thermal entry region by a numerical technique which included property variation and showed that the effect of "buoyancy" forces in the flow direction (so-called aiding flow) is to improve heat transfer. Thus, for laminar upflow and a specified wall heat flux, wall temperatures are less for mixed convection than for pure forced convection at the same conditions. With laminar cooling experiments, Biggs and Stachiewicz (1970) qualitatively confirmed the predictions of Worsoe-Schmidt and Leppert.

Investigations of turbulent mixed convection have been limited. Eckert and Diaguila (1954) examined entry flow in a short tube at high Grashoff numbers and categorized the flow regimes as forced, free or mixed. Hall and Price (1970) measured the effect of a laminar freestream flow imposed on a turbulent natural convective boundary layer with Gr/Re^2 of the order of ten. Ojalvo, Anand and Dunbar (1967) developed a numerical procedure for a hypothesized fully-developed, combined forced and free flow with the usual constant properties assumptions. From pure forced convection results, they chose an eddy diffusivity expression to be invariant with y^+. However, since the maximum value of Gr/Re^2 which they treated was about 5×10^{-5}, their tabulated predictions do not actually include the mixed convection regime. There appear to be no analytical predictions available which consider developing, turbulent mixed convective flows with significant property variation; while feasible, the validity of solutions to equations (6) will be primarily dependent on the choice of a turbulence model.

The most extensive source of data for the present problem - natural convective effects in a predominantly forced, turbulent flow - is the literature on fluids heated strongly near their critical point as mentioned earlier. Howevever, a number of interrelated complications preclude easy generalization of such measurements.

3. Numerical predictions for turbulent mixed convection

By solving the governing equations numerically, one eliminates uncertainties about the analysis other than those concerned with the turbulence model itself. It is believed that all other aspects which are significant in the current problem are included properly by equations (6) and (7) and the equation-of-state idealizations, equations (1).

The numerical method we apply has been presented elsewhere by Bankston and McEligot (1969, 1970) and will not be detailed here. The approach is similar to that proposed by Patankar and Spalding (1967) in that a finite control volume analysis is employed to generate a set of implicit, finite difference equations. These algebraic equations are solved successively and are then iterated to handle the non-linearities caused by the temperature-dependent property variation and by the axial advection term in the momentum equation. Mesh spacing is varied in both radial and axial directions with the node adjacent to the wall usually in the range $0.2 < y^+ < 0.5$. The primary difference from the earlier work of Bankston and McEligot is the addition of a body force term to account for buoyancy effects. In laminar flow, the predictions agree with Worsoe-Schmidt and Leppert (1965). For turbulent flow the program has used only mixing length or eddy diffusivity models, to date, but it could be extended readily to solve additional parabolic, partial differential equations for turbulence quantities as done by Spalding's group, if such an extension were warranted.

(a) Turbulence model

For less complicated, external incompressible and compressible turbulent boundary layers, Ng and Spalding (1970) and Bradshaw, Sivasegaram and Whitelaw (1970) have shown there is little value in solving a kinetic energy or length scale equation compared to using predictions based on a simple mixing length model. In their comparisons, initial conditions were taken to be the same and essentially equivalent wall laws were employed; the main difference among them was in the treatment of the outer region of the boundary layer. Launder (1969) demonstrated that such predictions are more sensitive to the treatment of the immediate wall layer. At present, it appears that only Launder and Jones (1970) have developed an advanced model which (1) solves turbulence equations into the viscous sublayer and (2) is suitable for laminarization problems in accelerated flows. Their model predicts experimental trends properly and generally agrees in magnitude with the observed data except that the model reverts back to a turbulent boundary layer again after laminarization more rapidly than the measurements; this is about the same level of agreement obtained for our internal, heated laminarization problems by empirically modifying a mixing length model.

For the comparative purposes of the present paper a tested mixing length model is applied. It should suffice to show predicted trends induced by buoyancy effects. The model is an extension of van Driest's (1956) mixing length,

$$\ell_{fd} = \kappa y[1 - \exp(-y^+/y_\ell^+)] \tag{8}$$

adjusted, for low Reynolds number turbulent flow, by defining

$$y_\ell^+ = fn(Re^*) \tag{9}$$

for gaseous variable properties, by evaluating with a modified Reynolds number,

$$Re^* = Re_w \sqrt{T_b/T_w} \tag{10}$$

and for axial development, by a rate equation,

$$\frac{\partial \ell(x,r)}{\partial x} = \frac{C\sqrt{\tau/\rho}}{\nu}[\ell_{fd}(x,y) - \ell(x,y)] \tag{11}$$

The function y_ℓ^+ approaches a constant value of 26 as Re^* is increased and y^+ is defined as

$$y^+ = \frac{y\sqrt{\tau_w/\rho_w}}{\nu_w} \tag{12}$$

Following Nash and McDonald (1967) we give the growth coefficient, C, a higher value (more rapid readjustment) when ℓ is decreasing than when ℓ is growing.

For limiting conditions of high Reynolds number flow with variable properties, this model yields a slight improvement to the version used successfully by Bankston and McEligot (1970). For adiabatic, low Reynolds number turbulent flow it provides essentially the same predictions as the effective Reichardt model of Reynolds, Swearingen and McEligot (1969). The data from which this model was derived were taken for forced convection without significant free convection effects.

(b) Predictions

Results are presented for two heating rates, $q_i^+ = 0.002$ and 0.004, at a flow rate given by $Re_i = 6000$. Calculations cover an adiabatic length of twenty diameters at the tube entrance so that a fully developed flow is approached, particularly in the wall region. Thus, at the initiation of heating the viscous sublayer thickness, y_s/r_w (ie., location where $\varepsilon=\nu$), is about 0.06. The heated region is also twenty diameters long. At each heating rate, results are calculated for three Grashoff number: $Gr_i^* = -2 \times 10^7$ (upflow), 0 (pure forced convection), and $+2 \times 10^7$ (downflow). With $|Gr_i^*/Re_i^2| = 5/9$ one expects forced convection to dominate but free convection effects to be significant. For the most part we concentrate on upflow to conform to the conditions in our apparatus.

From the work of Bankston (1970) and McEligot, Coon and Perkins (1970) it appears that a forced convection run with $q_i^+ = 0.002$ and $Re_i = 6000$ would remain essentially turbulent. The shapes of Pederson's unpublished profile measurements at $x/D \approx 38$ agree with this expectation. Likewise, the predicted trace of $St(x)$ versus $Re_b(x)$ shows the characteristic form for turbulent gas flow with moderate heating. A maximum value of about 1.4 is calculated for T_w/T_b, so properties vary significantly but not severely. The program also predicts y_s/r_w will approximately double to 0.12 in the twenty diameter heated length for both $Gr_i^* = 0$ and -2×10^7, in further agreement.

For the turbulent conditions, predicted velocity profiles are shown in Figure 1 to demonstrate the effects of buoyancy forces in upflow. Velocities have been normalized with the local bulk velocity. Initially, when the thermal boundary layer is still close to the wall and the buoyancy forces are concentrated in that region, the viscous sublayer is predicted to be slightly thicker than for forced convection alone. As one would expect, the natural convection increases the axial velocity in this region. Near $x/D = 7$, y_s becomes equal for the two cases and then further downstream y_s is slightly thinner with natural convection than without. The location y_s is indicated on Figure 1 by short vertical lines intersecting the profiles; at $x/D = 20$, y_s/r_w is 0.117 with body forces and 0.120 for forced convection alone. The curly vertical lines indicate the extent of the thermal boundary layer; it propagates towards the centerline more rapidly with $Gr = 0$.

Resulting wall temperatures are shown in Figure 2a. With the buoyancy forces, in the immediate thermal entrance region the increased velocity near the wall (rather than the slightly thicker viscous sublayer which would increase thermal resistance) evidently dominates the convective heat transfer. After about seven diameters both processes - increased velocities and thinner y_s - act to improve heat transfer. The general conclusion from Figure 2a is a prediction that for upward turbulent flow the net effect of substantial buoyancy forces would be to improve heat transfer but only slightly.

Laminarizing conditions are expected when the heating rate is revised to $q^+ = 0.004$ at the same Re_i. For forced convection alone, y_s/r_w increases rapidly and is predicted to reach 0.66 by twenty diameters. However, the characteristics induced by significant superposed buoyancy forces are predicted to be qualitatively the same as at the lower heating rate but are more exaggerated. Again y_s is thicker than for forced convection in the immediate entry and becomes thinner downstream. The dominant effect is still the increase of velocity due to buoyant forces in the thermal boundary layer so that wall temperatures are reduced, as shown in Figure 2b. Thus, for laminarizing upward flows the predictions lead to the same conclusion as for turbulent flow and for laminar flow: the net effect of buoyancy forces is to improve heat transfer.

For flow in the opposite direction to the buoyancy force, program calculations ceased at both heating rates when negative velocities were predicted near the wall, since the parabolic program is not valid for recirculating flows. However, such results can probably be interpreted as showing that separation is likely to occur as it does in comparable "fully developed" laminar flow solutions.

4. Experiment

As with the numerical predictions, the experiments are operated at conditions for laminarizing flows and for turbulent flows. To examine the effects of natural convection on predominantly forced flows, we wish to vary the Grashoff number while maintaining all other parameters at fixed values. From the definition

$$Gr_i^* = \frac{g\rho_i^2 D^3}{\mu_i^2} \qquad (13)$$

it is seen that we can adjust the importance of the body force term in the momentum equation (6b) by varying ρ_i. Existing apparatus for studying the low Reynolds number range is modified to do so. The same tube was used for all runs. Operating procedures were then chosen so that all other control parameters remained the same during comparative runs at the same Re_i and heating rate.

In the measurements γM_i^2 was less than 1.2×10^{-3} in all runs so that the variation of the density, during a single run, was predominantly caused by the temperature variation. From run to run the pressure level was adjusted to vary ρ_i in Gr_i^*.

(a) Apparatus

The test section is a vertical tube of thin, 1/2 inch diameter, Inconel 600 heated resistively and surrounded by "Eccosphere" insulation. Wall thickness is 0.010 inch. The lower electrode is attached above a fifty diameter section which serves as an adiabatic flow development region. The useful heated length is about thirty diameters before exit effects become important. Chromel-alumel thermocouples of 0.005 inch wire are welded to the outside of the tube to measure wall temperatures. Pressure taps consist of 12 mil holes which were drilled by the electric discharge technique.

A compressor and storage tank supply air at pressures up to 125 psig. As shown in Figure 3, a pressure regulator reduces the air pressure to the value desired at the variable area flowmeter. Flow then passes through a throttling valve to the test section. Gas inlet temperature is approximately room temperature. An adjustable conical plug at the test section exit provides the primary control for the pressure in the test section. Test section pressure and flowmeter pressure are determined with mercury manometers or Heise bourdon tube gages, as appropriate.

Electrical power is provided from a Sorenson line voltage stabilizer via a 20-to-1 transformer and an adjustable transformer in series. Current and voltage are measured with a Weston Model 370 ammeter and a John Fluke Model 883AB differential voltmeter. Thermocouple voltages are read with a Hewlett Packard Model 3450A digital voltmeter.

Measurements are obtained by conducting a pair of runs sequentially. Usually the higher pressure, therefore higher Grashoff number, run is taken first. The pressure regulator, throttling valve and exit cone are set to give the desired test section pressure and the mass flow rate for the desired Reynolds number. The adjustable transformer is set to the current for the desired heating rate. After steady state is reached the readings are taken. Then the exit cone is removed for a run with atmospheric pressure which gives the lowest Grashoff number possible in the test section. At the same time the throttling valve is readjusted until the pressure at the flowmeter and the float level yield the same readings as for the higher pressure run; it is not usually necessary to readjust the pressure regulator. The transformer setting is not normally touched. Thus, the inlet flow and thermal conditions are essentially the same for both runs and only Gr_i^* changes. Since the mass flow rate and heating rate are unchanged, the axial variations of bulk temperature and bulk transport properties along the test section also remain essentially unchanged.

(b) Experimental results

Three sets of experimental data will be presented as representative of the measurements: two at laminarizing conditions and one with turbulent flow. Other preliminary data also support the observations to be presented. Table 1 lists the control parameters for the three comparative runs.

The forced convection run at $Re_i = 3250$ and $q_i^+ = 0.0051$ would be expected to laminarize according to the indicators mentioned earlier; a plot of preliminary data for St(x) versus $Re_b(x)$ confirms the expectation.

With $|Gr_i^*/Re_i^2|$ only about 0.08 for the higher pressure run, one might question whether any natural convection effects should be discerned. For turbulent flow of supercritical carbon dioxide Shiralkar and Griffith (1970) suggest 10^{-2} as the critical value of a local Gr/Re^2 parameter at which free convection effects will become important; Hall (1970) recommends $|Gr_b/Re_b^{1.8}| \approx 0.1$ as a criterion, where

$$Gr_b = \left(\frac{\rho_b - \rho_w}{\rho_b}\right) \frac{gD^3}{\nu_b^2} \qquad (14)$$

For the run in question, Hall's parameter has a value about 0.13 near the entrance and it drops to 0.05 downstream, so significant effects might be expected at the entrance. For laminar flow, at $Q^+ = 5$, Worsoe-Schmidt and Leppert (1965) show a slight improvement in Nusselt number for Gr_i^*/Re_i of 100 and a considerable improvement at Gr_i^*/Re_i of 1000. (Their Q^+ equals our q^+ times $Re_i Pr_i/2$.) For our run, Q^+ is 5.8 and Gr_i^*/Re_i is 250 so a slight improvement would be expected if it were laminar. Measured wall temperature distributions are compared in Figure 4 and the higher Grashoff number run does show slightly lower temperatues, despite a marginally higher heating rate. Thus, the heat transfer parameters are improved in agreement with the laminar prediction.

McEligot, Coon and Perkins (1970) predict that a forced convection flow at $Re_i = 5840$ and $q^+ = 0.0031$ will also laminarize and, again, our experimental $St(x)$-$Re_b(x)$ trace agrees. However, with a higher Re_i and lower q_i^+ than the previous set of runs, the viscous sublayer thickness would be less at the inlet and the laminarization process would be expected to take place more slowly. With $|Gr_i^*/Re_i^2| \approx 0.02$ and $|Gr_b/Re_b^{1.8}| \approx 0.035$ for the higher pressure run, natural convection effects are expected to be slight or negligible. The wall temperature data on Figure 5 surprise one since there is a noticeable difference between the two runs. Further, with greater buoyancy forces the heat transfer parameters are reduced rather than improved. Thus, this comparison is in agreement with the Hall and Jackson (1969) observation for turbulent flow of supercritical fluids rather than with the laminar prediction.

The last pair of runs compared is for turbulent flow at a moderate heating rate. For the high pressure run, the parameter $|G_i^*/Re_i^2|$ is about 0.09 and $|Gr_d/Re_d^{1.8}|$ approaches 0.1 so buoyancy forces are in the range where they are expected to begin to be important. As shown in Figure 6 there is a definite effect; upward buoyancy forces interfere with heat transfer. In comparison to the previous figure the temperature scale has been expanded. The increases in wall temperatures downstream, apparently due to the buoyancy forces, are about thirty to forty degrees F in both cases, but the percentage increase is considerably greater for the conditions of Figure 6. Of the pair of turbulent runs, the heating rate was purposely set about one percent higher for the "forced convection" run and yet the wall temperature at $x/D \approx 28$ is about fifteen percent lower. The percentage reduction in the Nusselt number is even greater since the bulk temperature increases along the tube.

5. Discussion

Though not exhaustive, the experiments show that buoyancy forces acting in the same direction as the flow can interfere with heat transfer to air. This observation is in concert with the Hall and Jackson (1969) experiments on heated, turbulent flow of supercritical fluids. Further, the effect can be observed at lower values of the $|Gr_d/Re_d^{1.8}|$ parameter than normally expected. For laminarizing flows, forces may either aid or interfere with heat transfer in heated upflow.

Numerical predictions - with the turbulence model being the only significant aspect in doubt - show a trend opposite to that observed in two of the experiments. That is, the numerical calculations suggest that so-called "aiding" flow does enhance heat transfer processes in both laminarizing and turbulent flows, but the measurements refute these predictions. To correct this feature with the present turbulent model would require further empirical modification. Other approaches of promise might be to extend the two-equation turbulence model of Jones and Launder (1970) or to add a buoyancy force to the unsteady Stokes flow model of Cebeci (1970). However, such attempts are beyond the scope of this exploratory paper.

Barring consideration of a complete change of flow pattern, two explanations for the reduction in heat transfer parameters in turbulent, "aiding" flow appear reasonable. The region between the predicted peak in the velocity profile and the tube centerline could be considered a mixing layer rather than a wall shear layer; as the velocity gradient is reduced over this region the production of turbulence is reduced in comparison to normal turbulent pipe flow. A second explanation might be that the buoyancy force acts to stabilize the region in the immediate vicinity of the wall causing an effective thickening of the viscous sublayer beyond that predicted by the turbulence model.

The numerical predictions with a mixing length model qualitatively show some of the phenomena involved in the two explanations. The buoyancy forces arise in the thermal boundary layer, which grows from zero thickness at the start of heating to almost filling the tube in twenty diameters. For the first several diameters the thermal boundary layer is only slightly thicker than the viscous sublayer so the region where the velocity is increased is primarily within the sublayer as seen in Figure 1. (With lower Re_i this effect will be exaggerated further since the sublayer is thicker.) Thus, near the edge of the sublayer the velocity gradient is reduced by the buoyant effects and the sublayer is predicted to thicken since

$$\frac{\varepsilon}{\nu} = \frac{\ell^2}{\nu}\left|\frac{du}{dy}\right| \tag{15}$$

As noted earlier, the numerical calculations predict that this thickening has less effect than the increase in velocity near the wall. As the thermal boundary layer grows, the region of increased velocity moves inward away from the wall causing the velocity gradient to be increased near the edge of the sublayer and to be decreased, and even zero or negative, further out in the core. The sublayer becomes thinner and a wake-like region forms at the center. However, in the numerical predictions the turbulence scale is still determined by the distance from the wall rather than mixing layer or wake characteristics; ε is reduced due to the change in velocity gradient but a modification of ℓ has not been included (other than the effects via property variation). Accordingly, the predicted ε may still be too high in the central region.

The experiments of Hall and Price (1970) on the effect of an imposed freestream velocity on a turbulent, natural convection boundary layer on a flat plate examine a flow pattern comparable to the central mixing region. As the imposed velocity approached the maximum velocity of the natural convection boundary layer, the turbulence level was reduced and therefore their heat transfer was reduced. At some stages the core of a turbulent mixed convection flow can become analogous to the moving belt experiment of Uzkan and Reynolds (1967), with the increase in velocity due to buoyancy filling the role of the moving belt and the flow along the centerline acting as the grid turbulence. In the shear free region there is no production of new turbulence. On the other hand, in most pipe flow experiments phenomena near the wall dominate the heat transfer.

To see whether reduction in turbulence in the central region could overcome the improvement in heat transfer from increased velocities nearer the wall, two numerical experiments were performed. First, ℓ_{fd} in the turbulence model was set to zero whenever $\partial u/\partial y$ was negative and the dela effect of the rate equation (11) then allowed ℓ to decay to zero. Applied for $q^+ = 0.002$, this artificial model gave no significant change in wall temperature up to twenty diameters and at $x/D = 30$ the prediction was still below that for pure forced convection. A second artificial model simply set ℓ to zero directly whenever $\partial u/\partial y$ was negative. The results were essentially the same as with the first artificial version, so we conclude that reduction of turbulence in the central region alone could not explain the inhibited heat transfer observed in our experiments. (Further, buoyancy forces in the measurements were considerably less than those that led to the velocity maxima in Figure 1; it is unlikely that such peaks existed in the actual flows.)

The other explanation - stabilizing of the wall region by buoyancy forces - is largely unexplored. However, some experimental evidence suggests it is possible. Scheele, Rosen and Hanratty (1960) identified the early stages of transition in heated upflow and downflow. They show that transition occurs at higher Reynolds number in upflow indicating that an effect of buoyancy forces in the direction of flow is to stabilize the viscous flow in comparison to flow in the opposite direction. Likewise Biggs and Stachiewicz (1970) found that, in aiding flow, no transition to turbulent flow occurred in spite of the fact that a range of inlet Reynolds numbers up to 3500 was covered. If the phenomena in the viscous sublayer of a turbulent flow are comparable to the normal transition from laminar to turbulent flow as suggested by the work of Kline, Reynolds, Schraub and Runstadler (1967), then one might expect effects which inhibit transition also to stabilize the viscous sublayer.

ACKNOWLEDGMENTS

The University Computer Center provided the CDS-6400 with which the numerical calculations were performed, and Mssrs. K. R. Perkins and J. Sherfesse aided in the experiments and construction.

REFERENCES

Bankston, C.A. 1965 Fluid Friction, Heat Transfer, Turbulence and Inter-channel Flow Stability in the Transition from Turbulent to Laminar Flow in Tubes. Sc.D. thesis, University of New Mexico.

Bankston, C.A. 1966 personal communication. 4 November 1966.

Bankston, C.A. 1970 The Transition from Turbulent to Laminar Gas Flow in a Heated Pipe. J. Heat Transfer, 92, 569-579.

Bankston, C.A. and McEligot, D.M. 1969 A Numerical Method for Solving the Boundary Layer Equations for Gas Flow in Circular Tubes with Heat Transfer and Property Variations. Los Alamos Scientific Laboratory Tech. Report LA-4149.

Bankston, C.A. and McEligot, D.M. 1970 Turbulent and Laminar Heat Transfer to Gases with Varying Properties in the Entry Region of Circular Ducts. Int. J. Heat Mass Transfer, 13, 319-344.

Biggs, R.C. and Stachiewicz, J.W. 1970 Combined Free and Forced Convective Heat Transfer of Gases. 4th International Heat Transfer Conference. Vol. IV, Paper NC 3.3.

Bradshaw, P., Sivasegaram, S. and Whitelaw, J.H. 1970 An Assessment of Procedures for the Prediction of Turbulent, Supersonic, Two-dimensional Boundary Layer Flows. Imperial College, Mech. Eng. Report BL/TN/A/34.

Cebeci, T. 1970 Calculation of Compressible Turbulent Boundary Layers with Heat and Mass Transfer. AIAA Paper 70-741.

Coon, C.W. and Perkins, H.C. 1970 Transition from the Turbulent to the Laminar Regime for Internal Convective Flow with Large Property Variation. J. Heat Transfer, 92, 506-512.

Deissler, R.G. 1955 Analysis of Turbulent Heat Transfer, Mass Transfer and Friction in Smooth Tubes at High Prandtl and Schmidt Numbers. NACA Rept. 1210.

Drew, T.B., Koo, E.C. and McAdams, W.H. 1932 The Friction Factor for Clean, Round Pipes. Trans. AIChE, 28, 56.

Eckert, E.R.G. and Diaguila, A.J. 1954 Convective Heat Transfer for Mixed Free and Forced Flow Through Tubes. Trans. ASME, 76, 497-504.

Hall, W.B. 1970 Variable Property Effects in Forced Convection Heat Transfer. University of Manchester short course, 9 July 1970.

Hall, W.B. and Jackson, J.D. 1969 Laminarization of a Turbulent Pipe Flow by Buoyancy Forces. ASME paper 69-HT-55.

Hall, W.B., Jackson, J.D. and Watson, A. 1968 A Review of Forced Convection Heat Transfer to Fluids at Supercritical Pressures. Proc. Symposium on Heat Transfer and Fluid Dynamics of Near Critical Fluids, I. Mech. Eng., Vol. 182, Part 3I, 10.

Hall, W.B. and Price, P.H. 1970 Mixed Forced and Free Convection from a Vertical Heated Plate to Air. 4th International Heat Transfer Conference, Vol. IV, Paper NC 3.3.

Jones, W.P. and Launder, B.E. 1969 On the Prediction of Laminarescent Turbulent Boundary Layers. ASME paper 69-HT-13.

Jones, W.P. and Launder, B.E. 1970 The Prediction of Laminarization with a Two-Equation Model of Turbulence. Imperial College, Mech. Eng. Rept. BL/TN/A/40.

Kline, S.J., Reynolds, W.C., Schraub, F.A. and Runstadler, P.W. 1967 The Structure of Turbulent Boundary Layers. J. Fluid Mech, 30, 741-773.

Launder, B.E. 1969 Oral comments while presenting ASME paper 69-HT-13 at National Heat Transfer Conference, Minneapolis.

McEligot, D.M. 1963 The Effect of Large Temperature Gradients on Turbulent Flow of Gases in the Downstream Regions of Tubes. Ph.D. thesis Stanford University. TID-19446.

McEligot, D.M. and Bankston, C.A. 1969 Numerical Predictions for Circular Tube Laminarization by Heating. ASME paper 69-HT-52.

McEligot, D.M., Coon, C.W. and Perkins, H.C. 1970 Relaminarization in Tubes. Int. J. Heat Mass Transfer, 13, 431-433.

McEligot, D.M., Ormand, L.W. and Perkins, H.C. 1966 Internal Low Reynolds Number Turbulent and Transitional Gas Flow with Heat Transfer. J. Heat Transfer, 88, 239.

Moretti, P.M. and Kays, W.M. 1965 Heat Transfer through an Incompressible Turbulent Boundary Layer with Varying Freestream Velocity and Varying Surface Temperature - an Experimental Study. Int. J. Heat Mass Transfer, 8, 1187-1202.

Nash, J.F. and MacDonald, A.G.J. 1967 A Calculation Method for Incompressible Turbulent Boundary Layers including the Effect of Upstream History on the Turbulent Shear Stress. NPL Aero Rept. 1234.

Ng, K.H. and Spalding, D.B. 1970 A Comparison of Three Methods of Predicting the Hydrodynamic Behavior of Two-dimensional Turbulent Boundary Layers on Smooth Walls. Imperial College, Mech. Eng. Rept. BL/TN/A/27.

Ojalvo, M.S., Anand, D.K. and Dunbar, R.P. 1967 Combined Forced and Free Turbulent Convection in a Vertical Circular Tube with Volume Heat Sources and Constant Wall Heat Addition. J. Heat Transfer, 89, 328-334.

Patankar, S.V. a Spalding, D.B. 1967 A Finite Difference Procedure for Solving the Equations of the Two-dimensional Boundary Layer. Int J. Heat Mass Transfer, 10, 1389-1411.

Perkins, H.C. and Worsoe-Schmidt, P.M. 1965 Turbulent Heat and Momentum Transfer for Gases in a Circular Tube at Wall-to-Bulk Temperature Ratios to Seven. Int. J. Heat Mass Transfer, 8, 1011-1031. Data tabulated in Tech. Rept. SU 247-7, Mech. Eng. Dept., Stanford University, September, 1964.

Reynolds, H.C., Swearingen, T.B. and McEligot, D.M. 1969 Thermal Entry for Low Reynolds Number Turbulent Flow. J. Basic Eng., 91, 87-94.

Schade, K.W. and McEligot, D.M. 1971 Turbulent Flow Between Parallel Plates with Gas Property Variation. ASME paper 71-FE-38.

Scheele, G.F., Rosen, E.M. and Hanratty, T.J. 1960 Effect of Natural Convection on Transition to Turbulence in Vertical Pipes. Can. J. Ch. Eng., 38, No.3 67-73.

Schraub, F.A. and Kline, S.J. 1965 A Study of the Structure of the Turbulent Boundary Layer With and Without Longitudinal Pressure Gradients. Stanford University, Thermoscience Div. Rept. MD-12.

Shiralkar, B.S. and Griffith, P. 1969 Deterioration in Heat Transfer to Fluids at Supercritical Pressure and High Heat Fluxes. J. Heat Transfer, 91, 27-36.

Shiralkar, B.S. and Griffith, P. 1970 The Effect of Swirl, Inlet Conditions, Flow Direction and Tube Diameter on the Heat Transfer to Fluids at Supercritical Pressure. J. Heat Transfer, 92, 465-474.

Sze, B.S. 1957 The Effect of Temperature Dependent Fluid Properties on Heat Transfer in Circular Tubes. Ph.D. thesis, Mechanical Engineering, Stanford University.

Uzkan, T. and Reynolds, W.C. 1967 A Shear-free Turbulent Boundary Layer. J. Fluid Mech., 28, 803-821.

Van Driest, E.R. 1956 On Turbulent Flow Near a Wall. J. Aero. Sci., 23, 1007-1011 & 1036.

Worsoe-Schmidt, P.M. and Leppert, G. 1965 Heat Transfer and Friction for Laminar Flow of a Gas in a Circular Tube at High Heating Rate. Int. J. Heat Mass Transfer, 8, 1281-1301.

Table 1. Conditions of Experimental Runs Discussed

Nominal Re_i	Nominal q_i^+	$\lvert Gr_i^*/Re_i^2 \rvert$	Current amps	p(flowmeter) psig	Float level mm	p(test section) psig	Remarks
3250	0.0059	0.0059	62.5	35.7	50.5	0	Laminarizing
		0.078	62.6	35.7	50.0 to 50.5	35.6	-
5840	0.0031	0.0019	61.4	30.2	114.0	0	Laminarizing
		0.018	61.4	30.2	114.0	28.5	-
6900	0.0010	0.0013	40.6	103.7	77.0	0	Turbulent
		0.092	40.4	103.4	77.0	103.2	-

FIGURE CAPTIONS

1. Predicted velocity profiles for turbulent flow.
2. Predicted effect of natural convection on tube wall temperature distribution.
3. Schematic diagram of experimental apparatus.
4. Measured wall temperatures in heated laminarizing flows.
5. Measured wall temperatures in heated laminarizing flows.
6. Measured wall temperatures in heated turbulent flows.

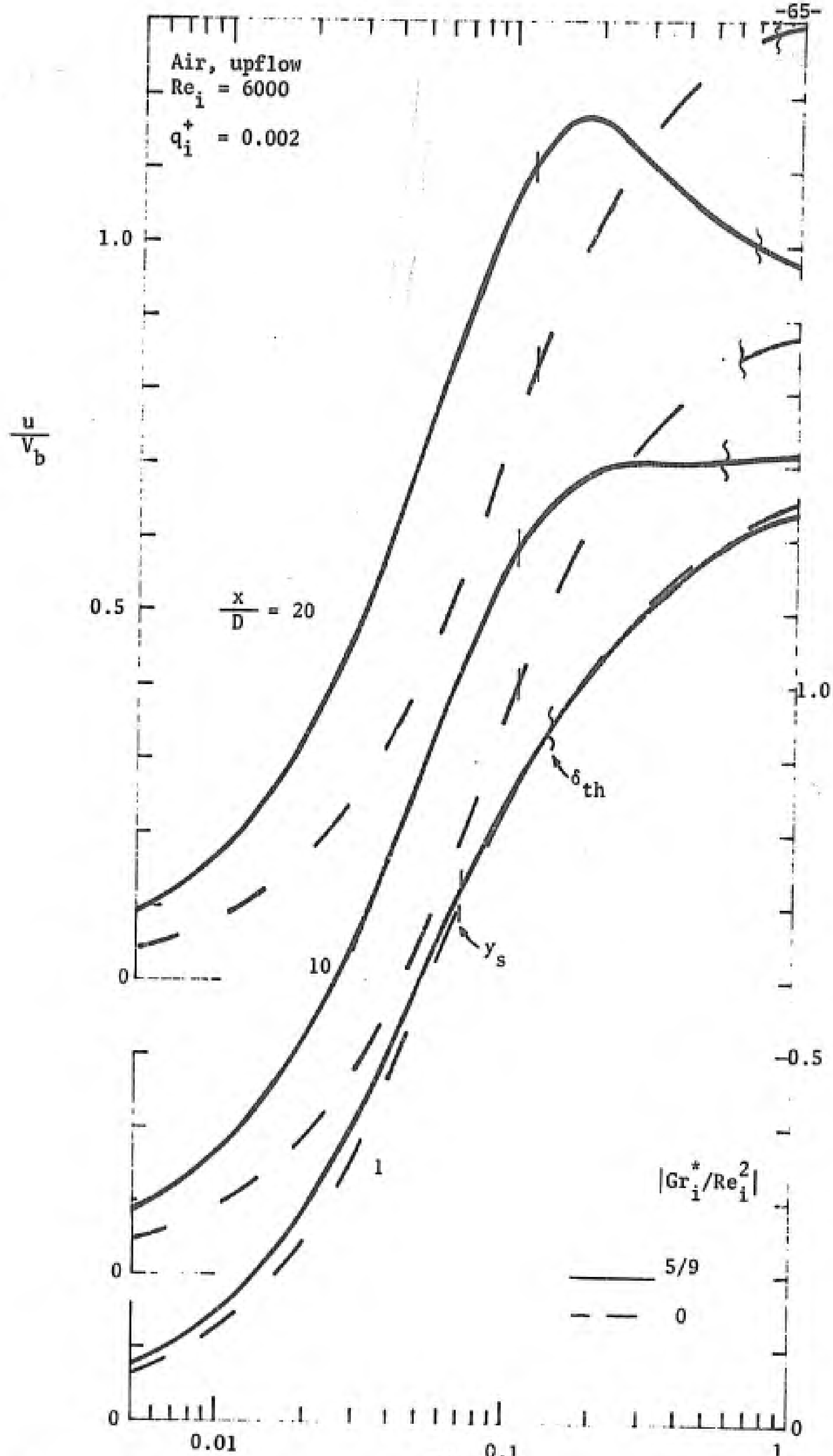

Figure 1. Predicted Velocity Profiles for Turbulent Flow.

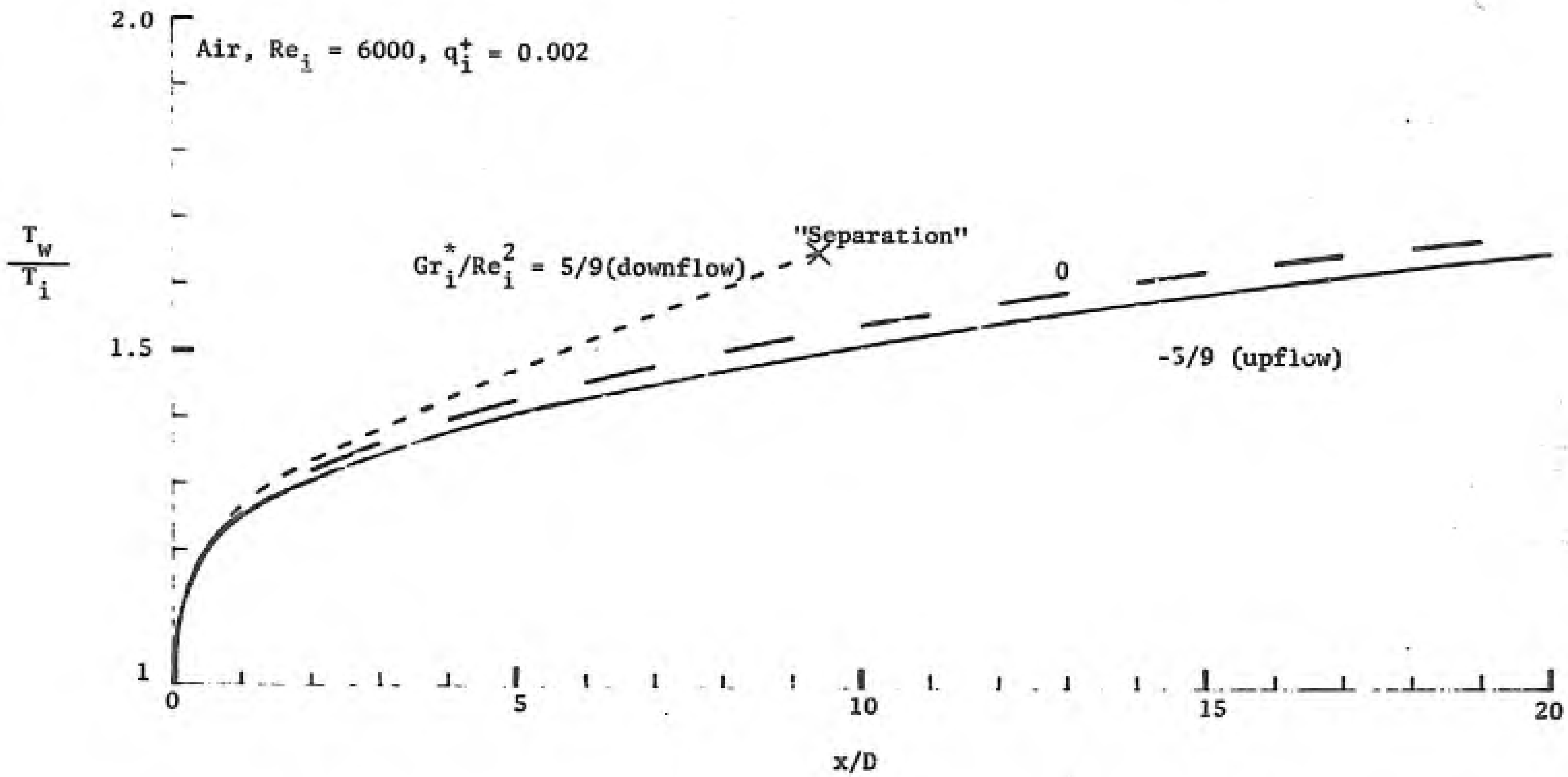

Figure 2a. Predicted Effect of Natural Convection on Tube Wall Temperature Distribution.

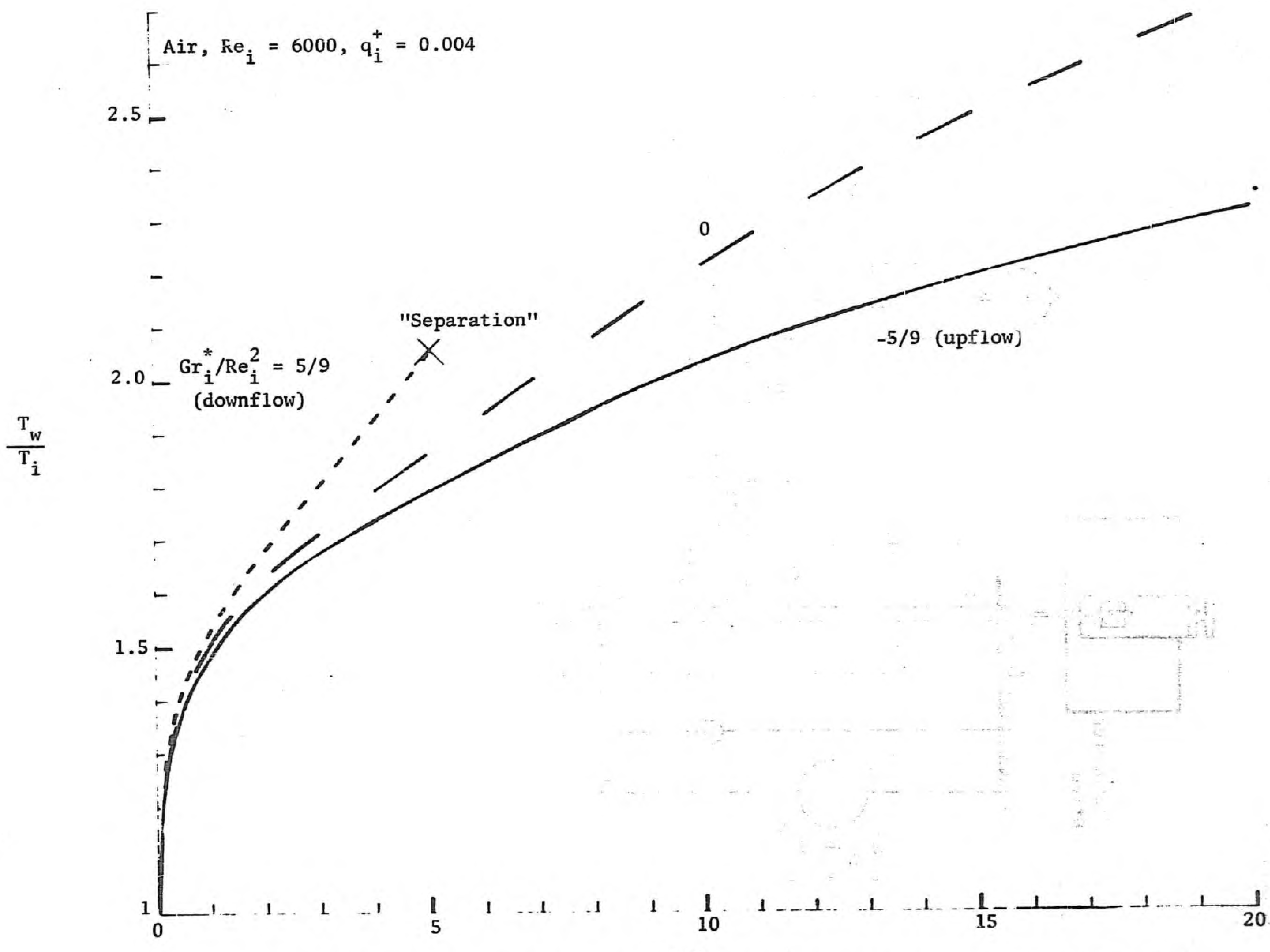

Figure 2b. Predicted Effect of Natural Convection on Tube Wall Temperature Distribution.

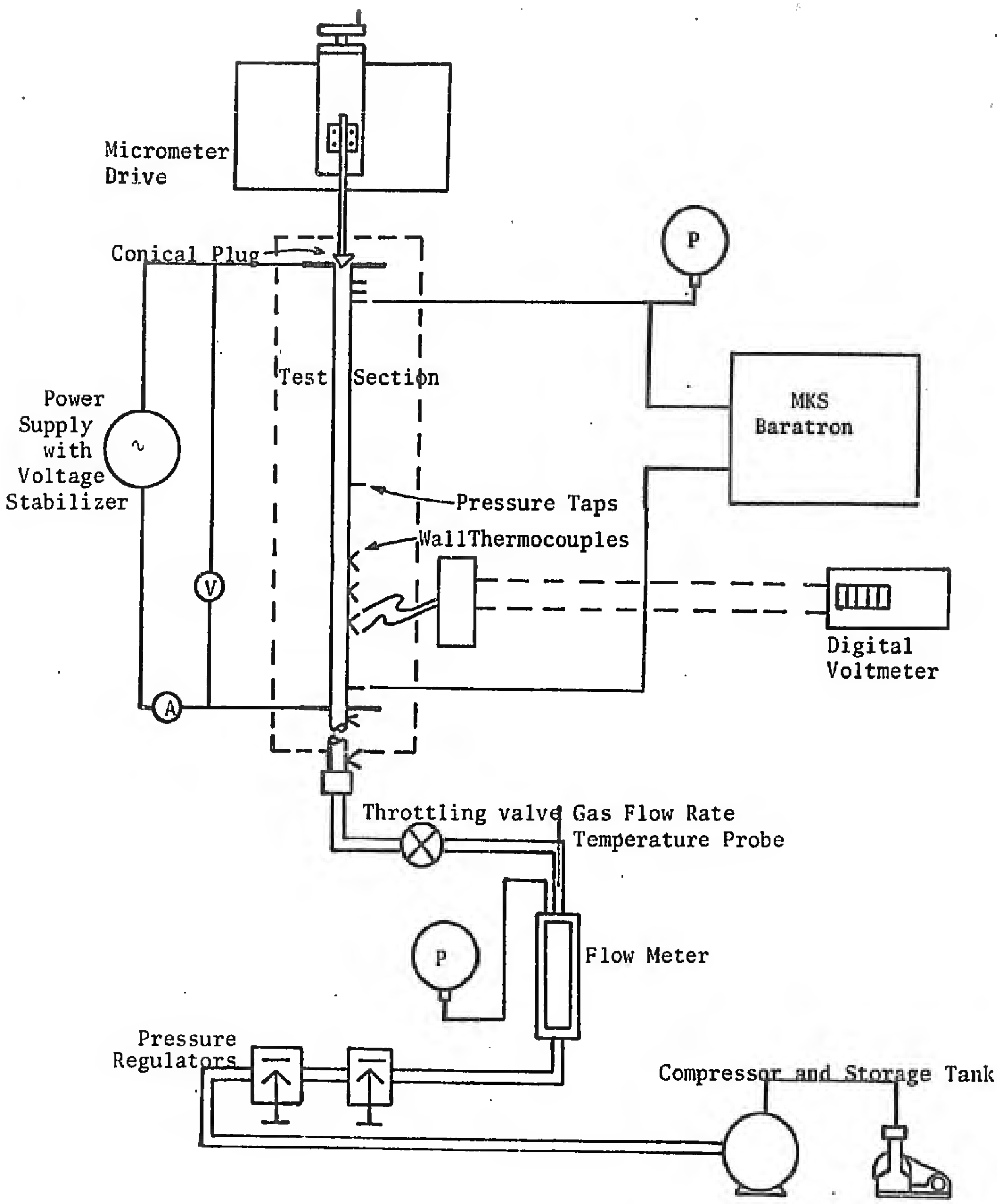

Figure 3. Schematic Diagram of Experimental Apparatus.

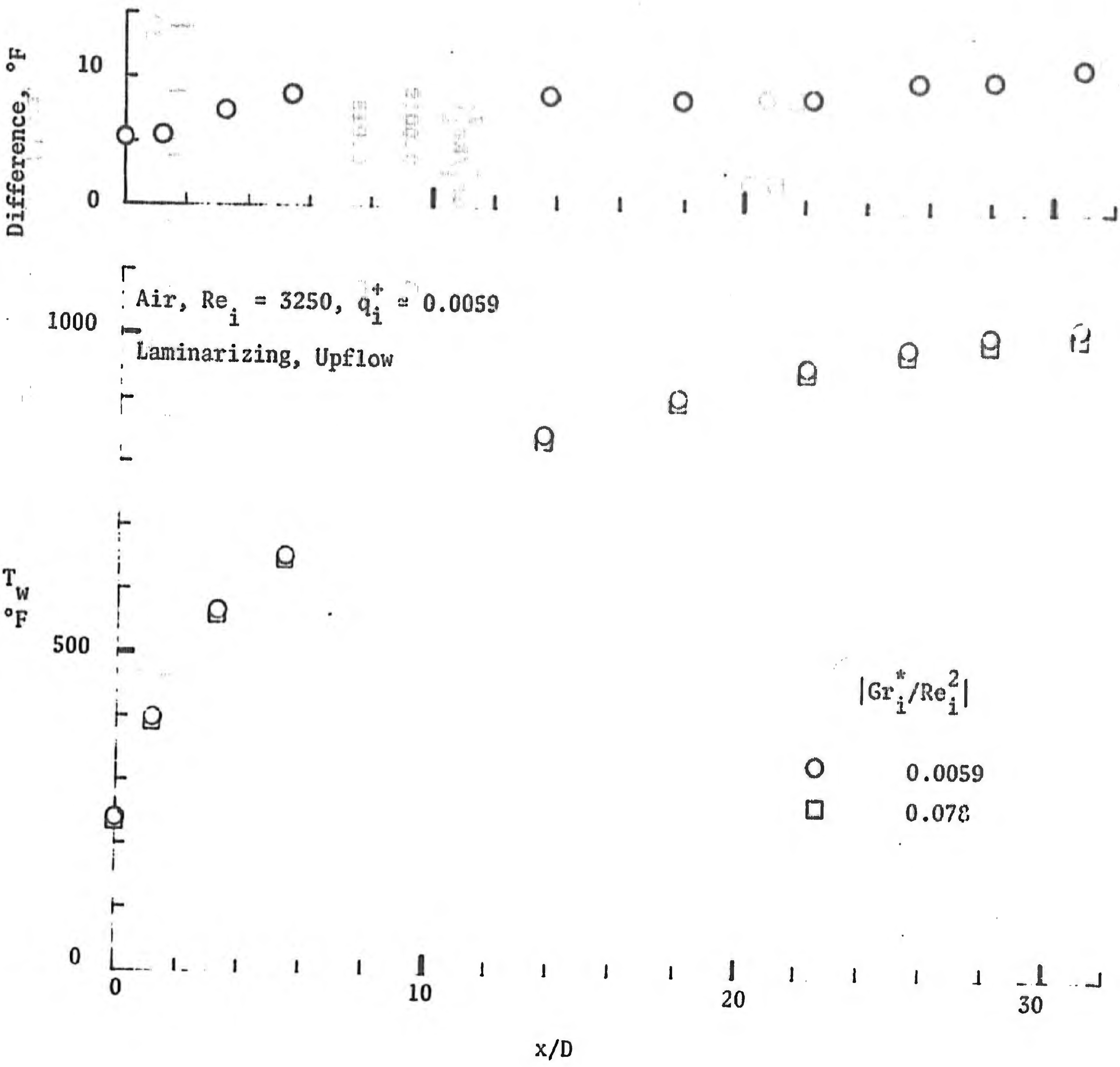

Figure 4. Measured Wall Temperatures in Heated Laminarizing Flows.

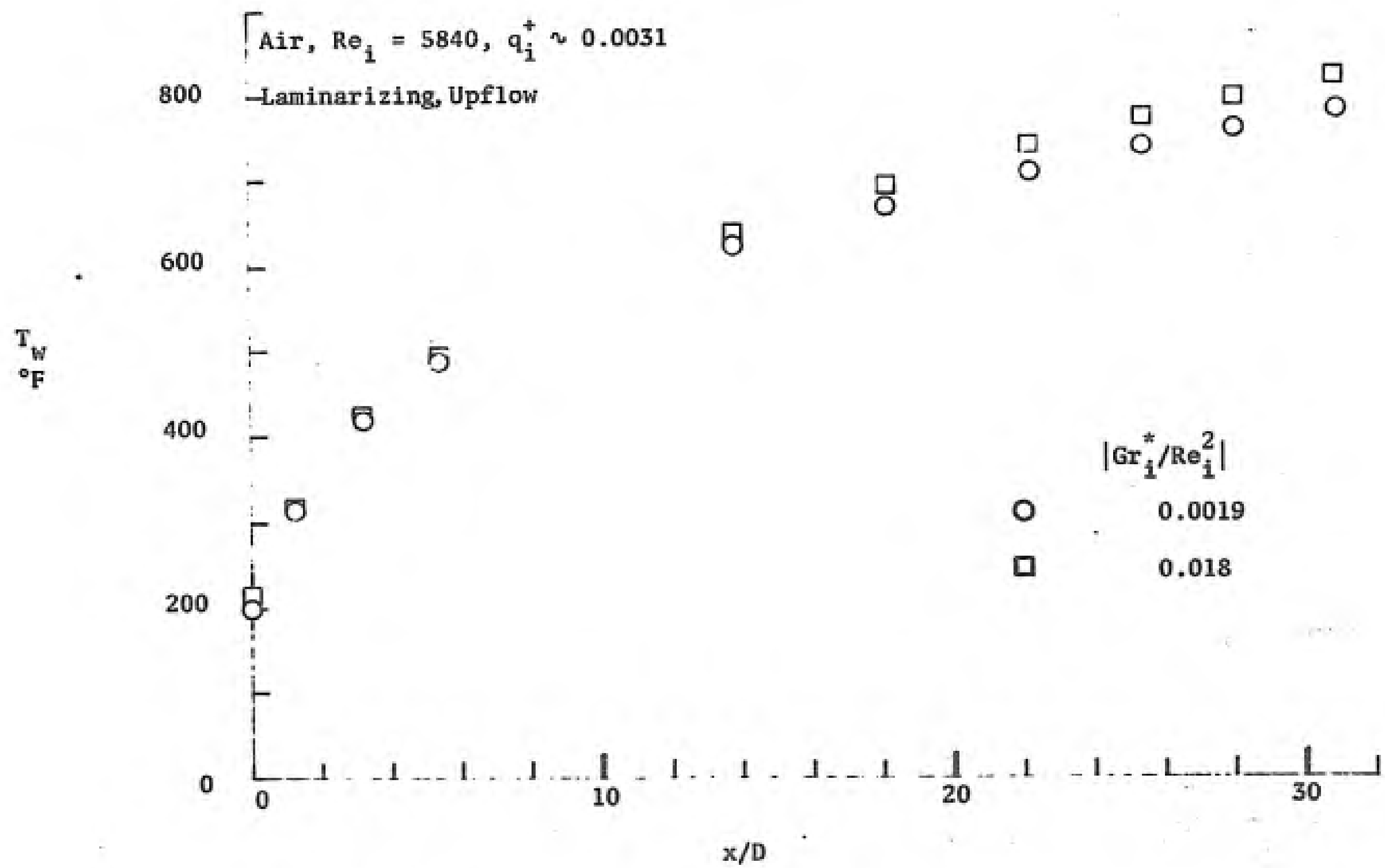

Figure 5. Measured Wall Temperatures in Heated Laminarizing Flows.

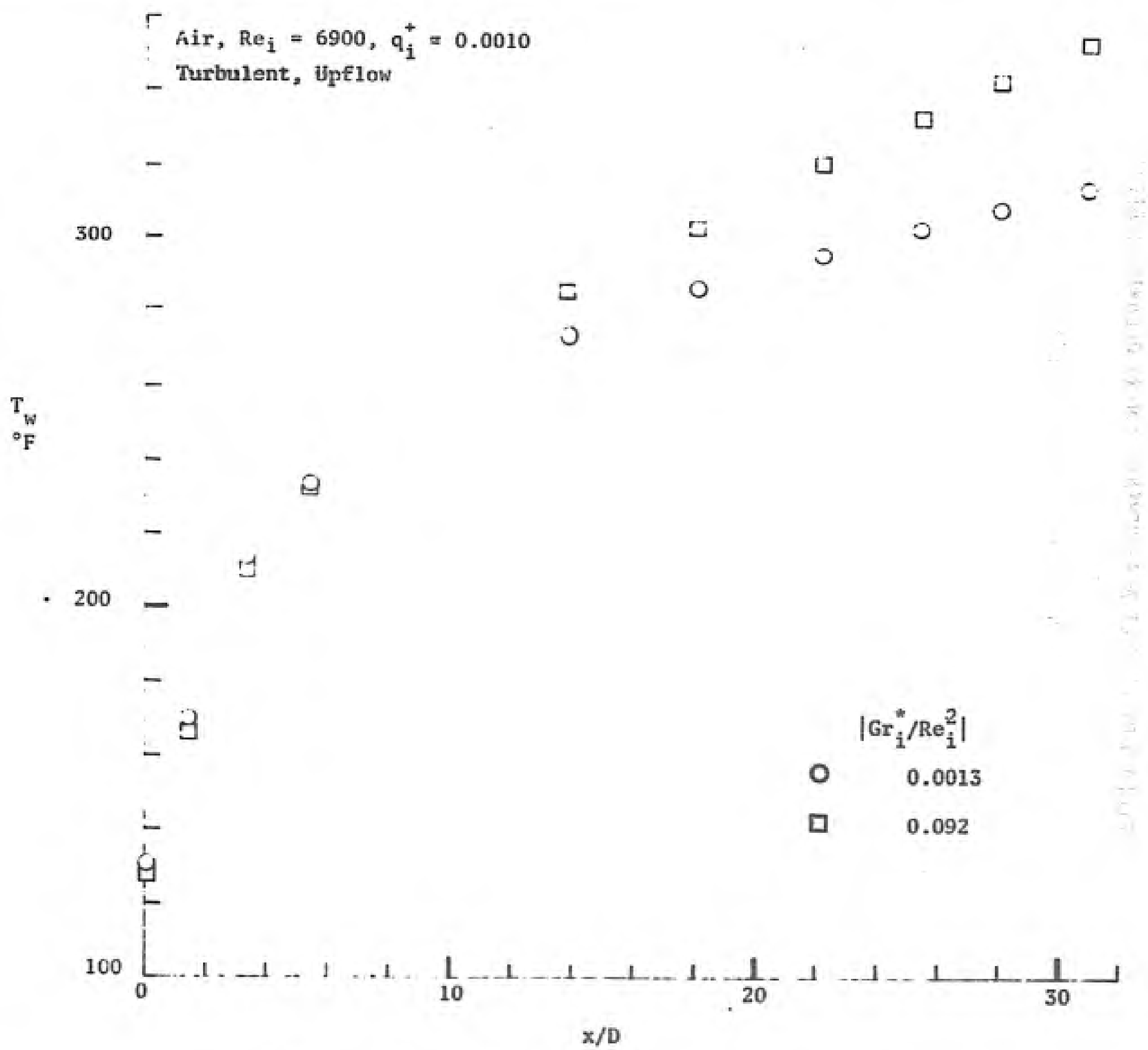

Figure 6. Measured Wall Temperatures in Heated Turbulent Flows.

APPENDIX B

PRELIMINARY PROFILE MEASUREMENTS DURING RELAMINARIZATION

R. J. Pederson[1] and D. M. McEligot[2]

The apparatus of Appendix A was used to conduct profile measurements at atmospheric pressure by mounting a transverse micrometer drive and probe holder on the axial micrometer drive shown in Figure 3 of Appendix A. A test section of the same dimensions was employed.

For mean temperatures, a boundary layer thermocouple probe was constructed of premium grade chromel and alumel wire as shown in Figure 7. By locating the impact tube of Figure 8 opposite a static pressure tap and measuring the pressure difference with the MKS "Baratron," mean velocities could be deduced. A short iterative computer program calculated the local density from the static pressure and the measured temperature in order to determine the local mean velocity and, then, modified the mean fluid temperature estimate via a radiation correction which is dependent on the velocity via the convective heat transfer coefficient. No "displacement" corrections were applied for the probe positions.

With an inlet Reynolds number of about 6000, test section power was set for two experiments:

---

1. NDEA Fellow. Now at the University of Minnesota.
2. Professor.

a. Heating rate, q_i^+*, approximately 0.002 which would be expected to remain turbulent, and*

b. q_i^+ *approximately 0.004 which would be expected to laminarize.*

(Substantial heat losses from the tube precluded a more detailed description of $q_w''(x)$). Deduced downstream profiles are presented in Table 1.

To measure the intermittency distribution at the measuring station, a Thermo-Systems miniature hot film probe, 1275-10A, was also employed with their Model 1010A constant temperature anemometer system. Maximum operating temperature of the hot film probe was limited by the materials of the probe body rather than the prongs or sensor so the probe was introduced at a slight angle which would allow the probe body to remain in the cooler region of the flow. Even with this precaution, in the run at the higher heating rate the sensor could not be brought closer to the wall than 0.09 inches, $y/r_w \approx 0.4$. The oscilloscope traces of the signals were photographed with a Polaroid camera and are reproduced as Figures 1 to 6; Table 2 lists the conditions of each photograph. All traces, except the test cases with no flow and with adiabatic laminar flow, appear fully turbulent. Since the sensor was uncalibrated and simultaneous, fluctuating temperature measurements were not feasible, turbulence intensities could not be calculated. However, the ratio between the bridge voltage fluctuations and the mean bridge voltage (Table 2) can yield some rough indications of orders-of-magnitude.

-74-

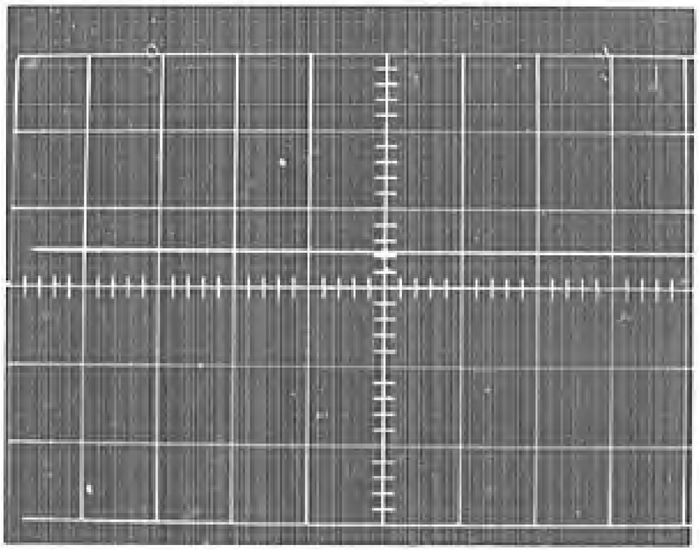

No Flow

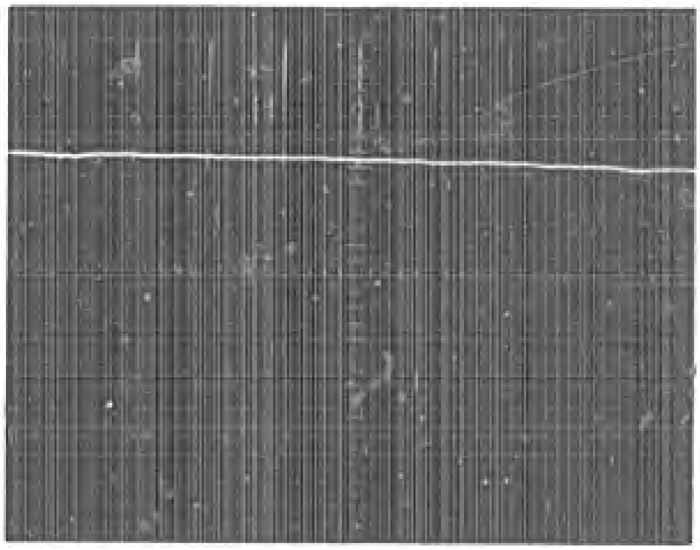

Laminar Flow (Re = 2000)

Figure B-1. Oscilloscope traces of the anemometer output under adiabatic conditions at the centerline of the tube.

Distance
(inches)

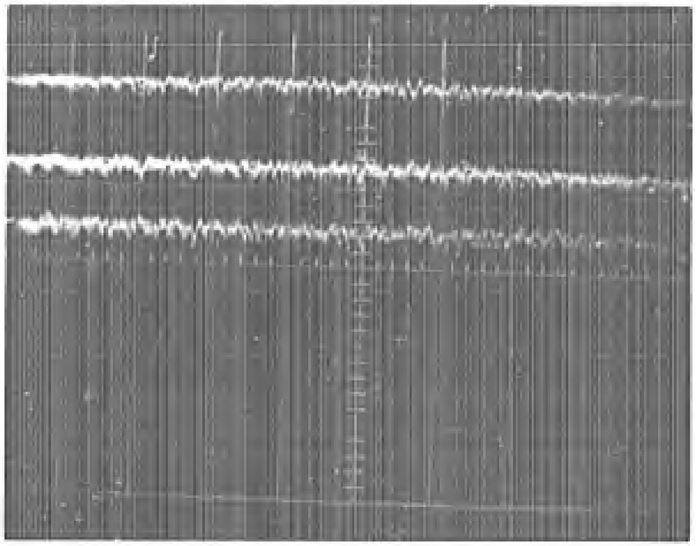

A - 0.24

B - 0.215

C - 0.190

Distance
(inches)

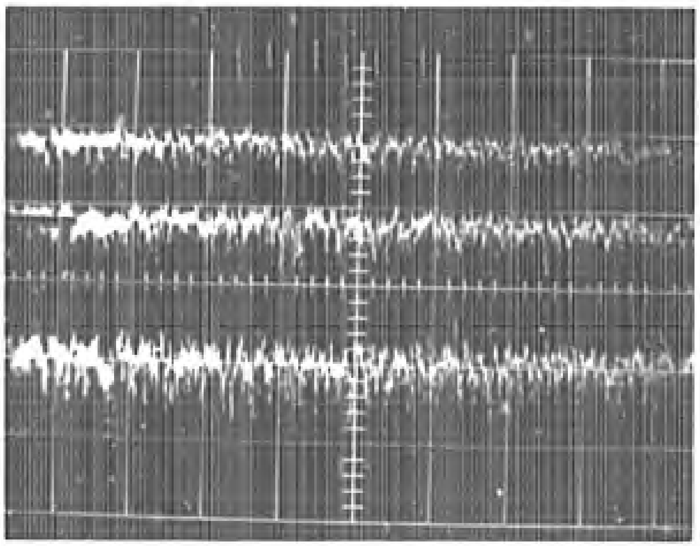

a - 0.090

b - 0.065

c - 0.040

Figure B-2. Oscilloscope traces of the anemometer output for adiabatic, turbulent flow at varying distances from the wall with a Reynolds Number of 6000.

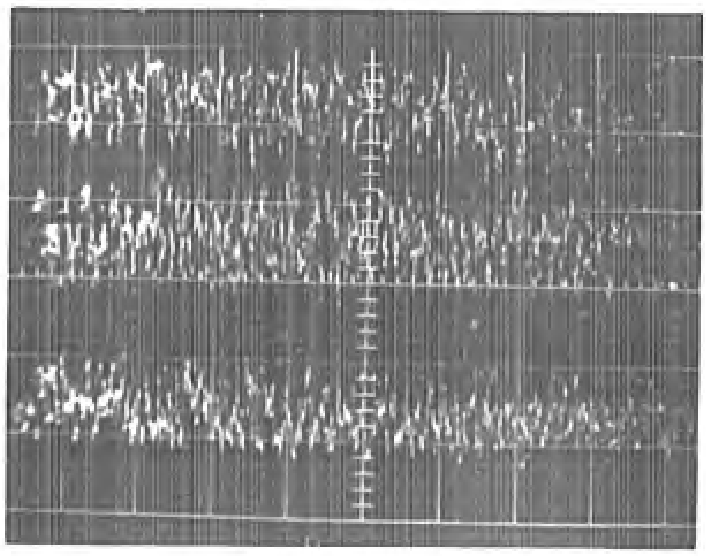

Distance
(inches)

a - 0.015

b - 0.010

c - 0.005

Figure B-3. Oscilloscope traces of the anemometer output for adiabatic, turbulent flow in close proximity to the wall with a Reynolds number of 6000.

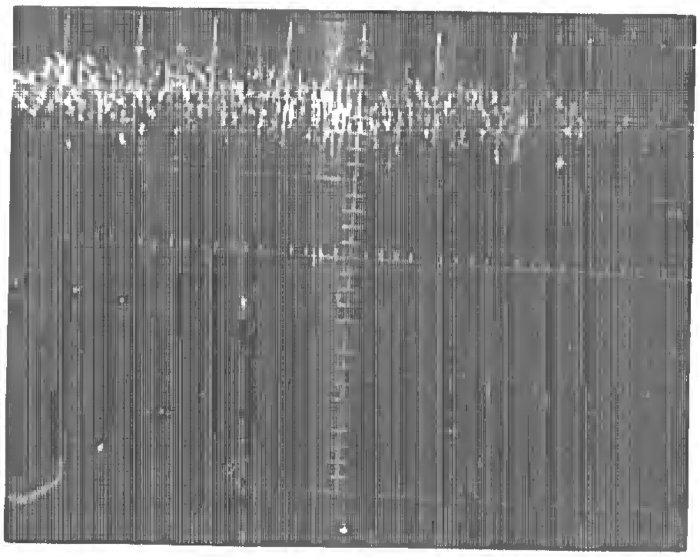

$q^{+} \approx 0.002$ with probe at centerline

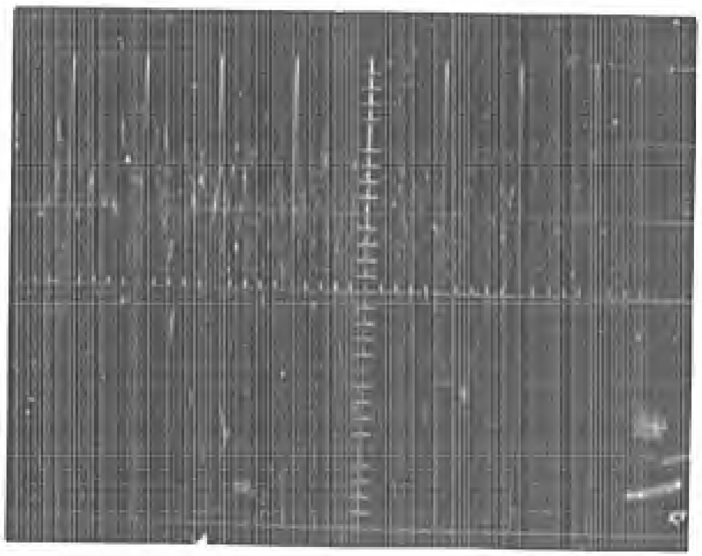

$q^{+} \approx 0.002$ with probe 0.090 inches from wall

Figure B-4. Oscilloscope traces of the anemometer output for heated turbulent flow at a local Reynolds Number of about 5000.

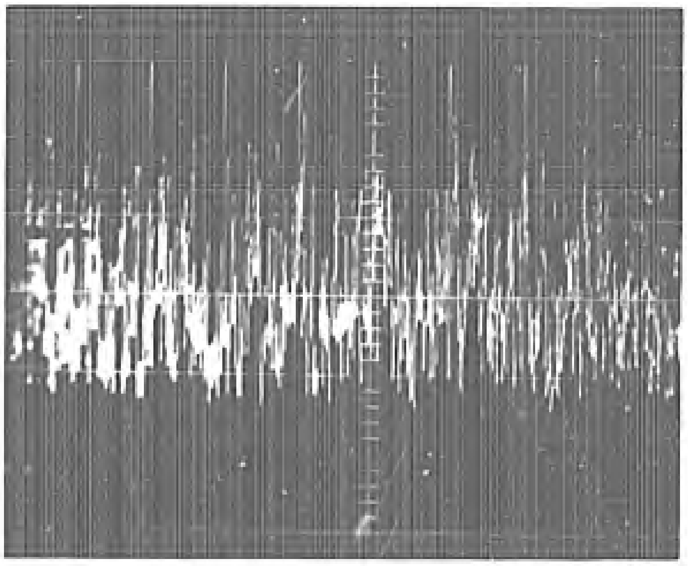

$q^+ \approx 0.002$, Re $\approx$ 5000 with probe 0.010 inches from wall

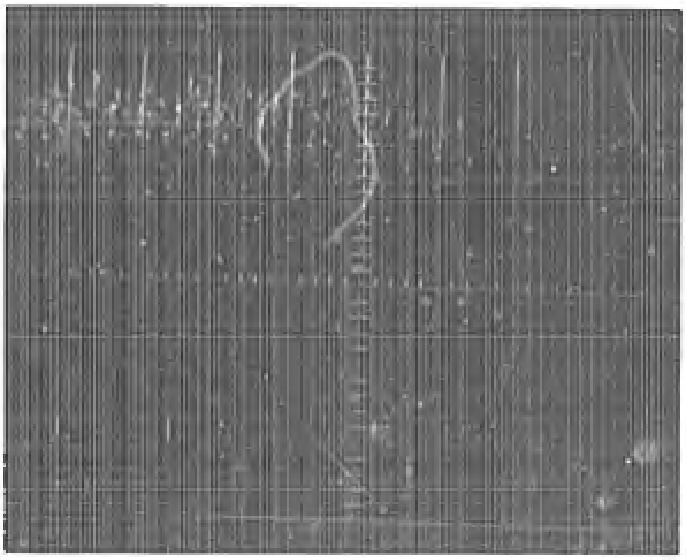

$q^+ \approx 0.004$, Re $\approx$ 4300 with probe at centerline

Figure B-5. Oscilloscope traces of the anemometer output for heated turbulent flow with two heating rates.

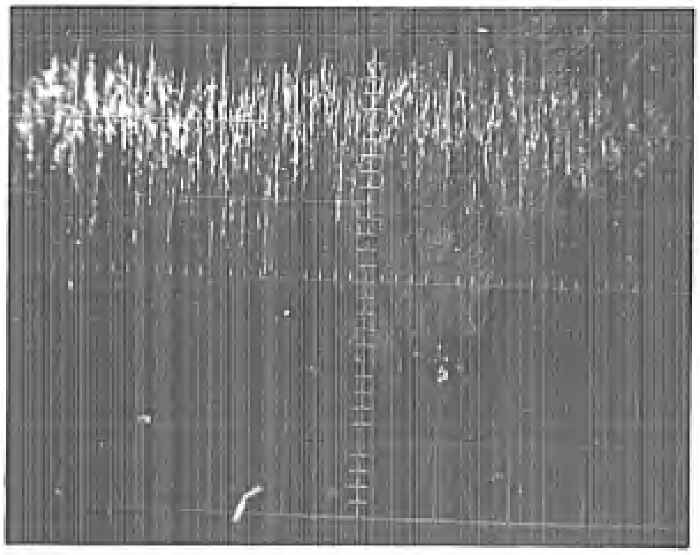

$q^{+} \approx 0.004$ with probe 0.190 inches from wall

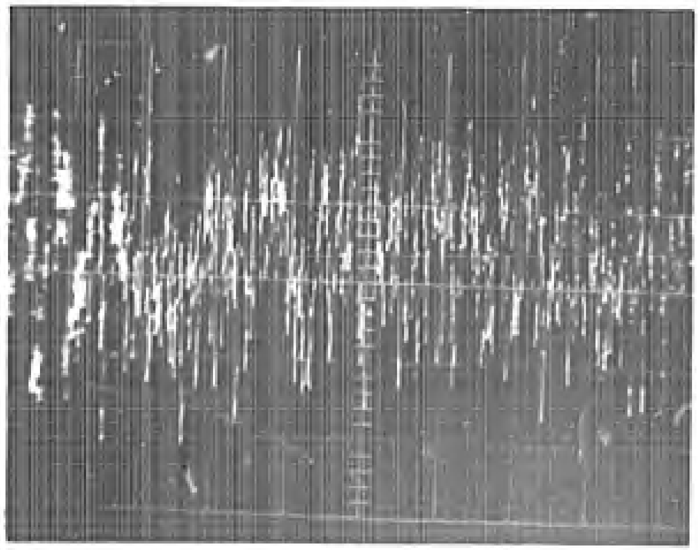

$q^{+} \approx 0.004$ with probe 0.090 inches from wall

Figure B-6. Oscilloscope traces of the anemometer output for heated turbulent flow at a local Reynolds Number of about 4300.

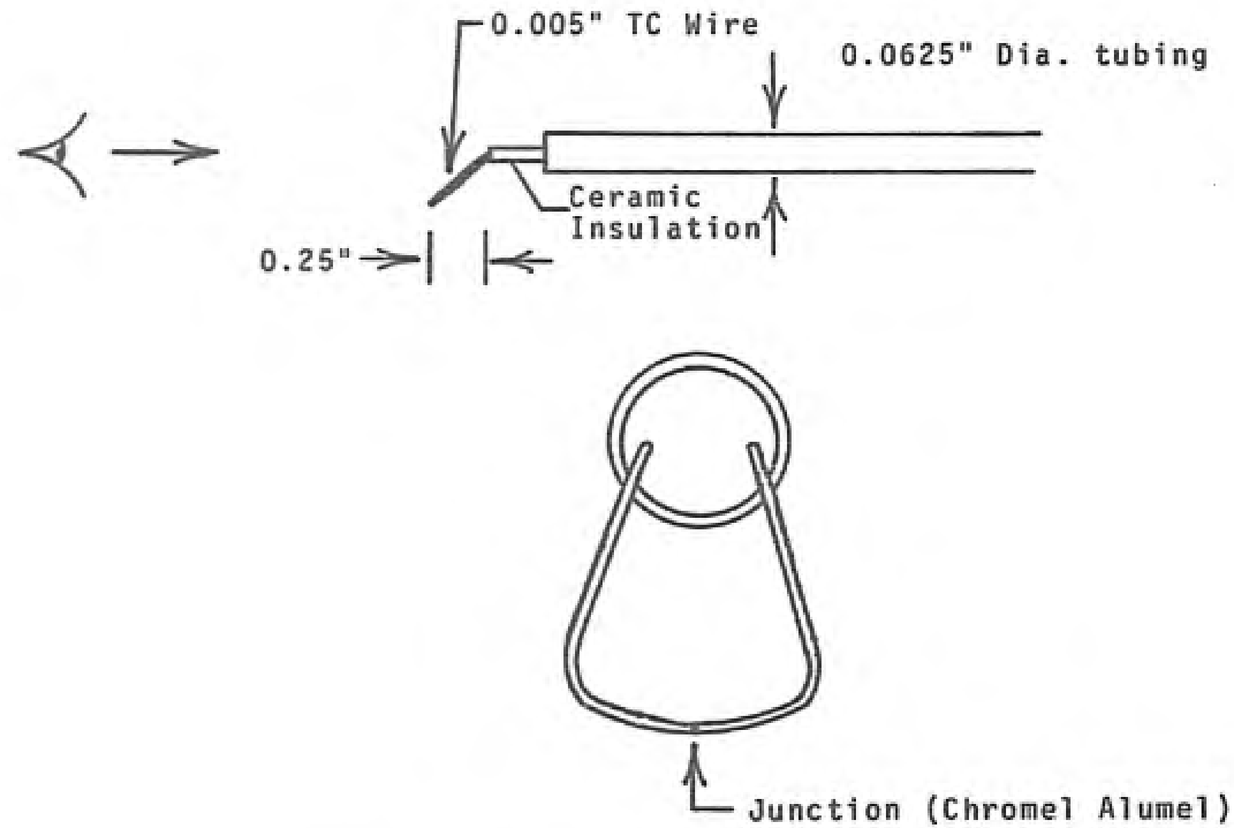

Figure B-7. Thermocouple probe

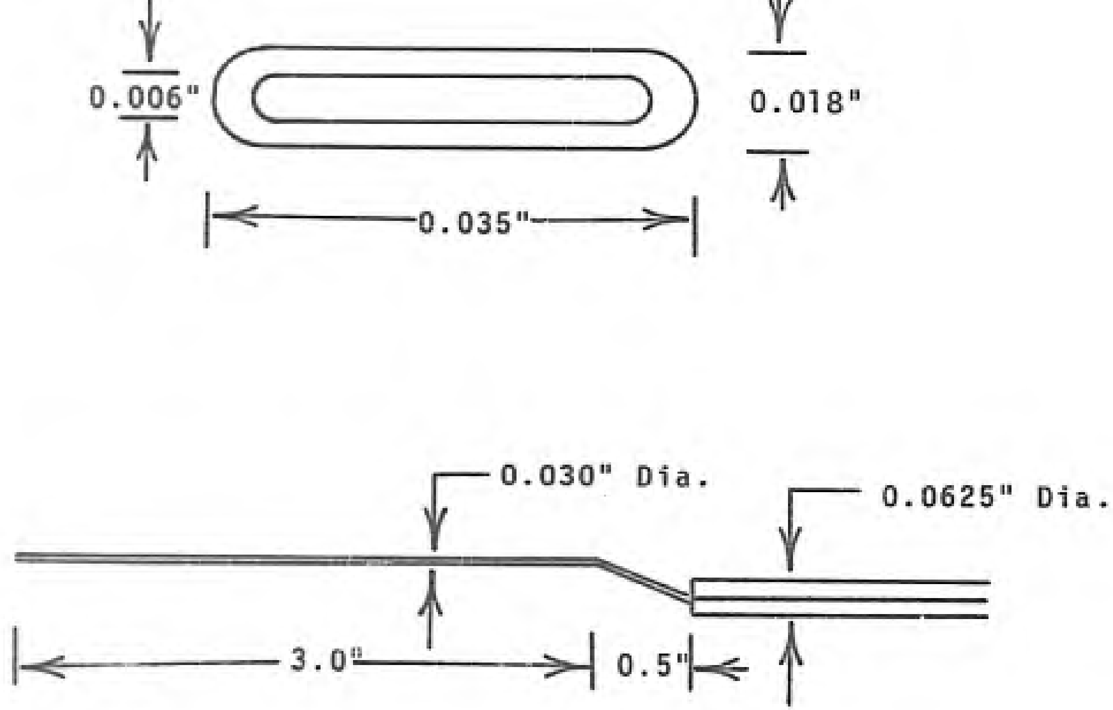

Figure B-8. Impact probe.

Table B-1. Mean Velocity and Temperature Profiles in Heated Flow

RUN 33 -- Approximate heating rate, $q^+ \cong 0.004$

Axial location, $x/D_H = 38.59$

Inner wall temperature $\cong$ 1120°F

r/r_w	Radial Position Distance from Wall (in.)	Velocity (ft/sec)	Temperature (°F)
0.964	0.009	15.01	1015.7
0.938	0.015	18.9	970.2
0.895	0.025	25.4	902.1
0.855	0.035	31.6	837.5
0.814	0.045	37.4	761.6
0.771	0.055	41.9	693.2
0.731	0.065	45.3	621.9
0.697	0.075	47.9	548.4
0.646	0.085	50.2	481.7
0.604	0.095	52.3	432.9
0.563	0.105	53.5	381.2
0.521	0.115	54.3	338.1
0.417	0.140	55.1	260.5
0.313	0.165	55.3	217.6
0.208	0.190	55.3	194.3
0.104	0.215	55.4	185.5
0.0	0.240	55.4	184.4

RUN 46 -- Approximate heating rate, $q^+ \cong 0.002$

Axial location, $x/D_H \cong 37.60$

Inner wall temperature $\cong$ 495°F

0.960	0.010	15.5	310.1
0.938	0.015	22.3	312.3
0.895	0.025	28.2	307.2
0.855	0.035	32.1	297.2
0.814	0.045	34.4	287.2
0.771	0.055	35.8	279.0
0.731	0.065	37.1	270.4
0.697	0.075	37.9	261.9
0.646	0.085	38.7	254.4
0.604	0.095	39.4	249.7
0.563	0.105	39.9	243.6
0.521	0.115	40.6	238.9
0.417	0.140	41.8	226.8
0.313	0.165	42.8	218.0
0.208	0.190	43.7	211.5
0.104	0.215	44.3	208.8
0.0	0.240	44.4	208.2

Table B-2. Summary of Hot Film Anemometer Signal Photographs

Heating Condition	Picture No.	Distance from Wall (in.)	"Cold" Resistance (ohm)	Overheat Ratio	Abscissa (sec/cm)	Ordinate (v/cm)	Large Amplitude Fluctuations 2v' (approx.)	Mean Bridge Output (v.)	Ratio of Fluc/Mean $\frac{2v'}{v}$	Comment
ADIABATIC	53	0.240	6.68	1.045	0.1	0.1	.003	0.525	-	No Flow
ADIABATIC	17	0.240	6.62	1.5	0.1	0.2	.012	-	-	$Re_D \cong 2000$
	25									
ADIABATIC	a	0.240	6.59	1.37	0.1	0.1	.03	1.89	.016	$Re_D \cong 6000$
	b	0.215	6.59	1.37	0.1	0.1	.035	1.89	.018	
	c	0.190	6.59	1.37	0.1	0.1	.04	1.88	.021	
ADIABATIC	43									
	a	0.090	6.65	1.3	0.1	0.1	.055	1.735	.032	
	b	0.065	6.65	1.3	0.1	0.1	.07	1.725	.040	$Re_D \cong 6000$
	c	0.040	6.65	1.3	0.1	0.1	.10	1.710	.058	
ADIABATIC	44									
	a	0.015	6.65	1.3	0.1	0.1	.12	1.655	.073	
	b	0.010	6.65	1.3	0.1	0.1	.125	1.625	.077	$Re_D \cong 6000$
	c	0.005	6.65	1.3	0.1	0.1	.1	1.570	.064	
$q^+ \cong 0.002$	27	0.240	7.64	1.37	0.1	0.1	.19	2.097	.090	
$q^+ \cong 0.002$	46	0.090	8.31	1.30	0.1	0.1	.3	2.000	.15	$Re_{D,i} \cong 6000$
$q^+ \cong 0.002$	50	0.010	9.35	1.25	0.1	0.1	.36	1.78	.20	$Re_x \approx 5000$
$q^+ \cong 0.004$	32	0.240	7.79	1.37	0.1	0.1	.23	2.175	.11	
$q^+ \cong 0.004$	33	0.190	7.85	1.37	0.1	0.1	.31	2.180	.14	$Re_{D,i} \cong 6000$
$q^+ \cong 0.004$	36	0.090	9.85	1.22	0.1	0.2	.7	1.84	.38	$Re_x \approx 4300$

APPENDIX C

MEASUREMENTS OF THREE-DIMENSIONAL GAS FLOW

K. R. Perkins[1], K. W. Schade[2] and D. M. McEligot[3]

Experiments in a vertical, rounded corner square duct are reported for heating rates which cause significant property variation in helium and nitrogen. In laminar flow, effects on local heat transfer parameters are slight but local friction factors vary strongly as the wall-to-bulk temperature ratio varies. Data concentrated in the range $3000 < Re_i < 10^4$ are examined to determine heating rates which cause premature laminarization as the Reynolds number decreases axially along the tube. The laminarization criteria evolved correspond to values of the "critical" acceleration parameter for two-dimensional, accelerated, external flows.

---

1. Research Assistant
2. NDEA Fellow.
3. Professor.

Table B-2. Summary of Hot Film Anemometer Signal Photographs

Heating Condition	Picture No.	Distance from Wall (in.)	"Cold" Resistance (ohm)	Overheat Ratio	Abscissa (sec/cm)	Ordinate (v/cm)	Large Amplitude Fluctuations $2v'$ (approx.)	Mean Bridge Output (v.)	Ratio of Fluc/Mean $\frac{2v'}{v}$	Comment
ADIABATIC	53	0.240	6.68	1.045	0.1	0.1	.003	0.525	-	No Flow
ADIABATIC	17	0.240	6.62	1.5	0.1	0.2	.012	-	-	$Re_D \cong 2000$
	25									
ADIABATIC	a	0.240	6.59	1.37	0.1	0.1	.03	1.89	.016	$Re_D \cong 6000$
	b	0.215	6.59	1.37	0.1	0.1	.035	1.89	.018	
	c	0.190	6.59	1.37	0.1	0.1	.04	1.88	.021	
ADIABATIC	43									
	a	0.090	6.65	1.3	0.1	0.1	.055	1.735	.032	
	b	0.065	6.65	1.3	0.1	0.1	.07	1.725	.040	$Re_D \cong 6000$
	c	0.040	6.65	1.3	0.1	0.1	.10	1.710	.058	
ADIABATIC	44									
	a	0.015	6.65	1.3	0.1	0.1	.12	1.655	.073	
	b	0.010	6.65	1.3	0.1	0.1	.125	1.625	.077	$Re_D \cong 6000$
	c	0.005	6.65	1.3	0.1	0.1	.1	1.570	.064	
$q^+ \cong 0.002$	27	0.240	7.64	1.37	0.1	0.1	.19	2.097	.090	
$q^+ \cong 0.002$	46	0.090	8.31	1.30	0.1	0.1	.3	2.000	.15	$Re_{D,i} \cong 6000$
$q^+ \cong 0.002$	50	0.010	9.35	1.25	0.1	0.1	.36	1.78	.20	$Re_x \approx 5000$
$q^+ \cong 0.004$	32	0.240	7.79	1.37	0.1	0.1	.23	2.175	.11	
$q^+ \cong 0.004$	33	0.190	7.85	1.37	0.1	0.1	.31	2.180	.14	$Re_{D,i} \cong 6000$
$q^+ \cong 0.004$	36	0.090	9.85	1.22	0.1	0.2	.7	1.84	.38	$Re_x \approx 4300$

NOMENCLATURE

A_{cs}	cross sectional area
c_p	specific heat at constant pressure
D_h	hydraulic diameter
G	average mass flux, $\dot{m}/A_{cs}$
g_c	dimensional constant
h	convective heat transfer coefficient, $q_w'/P(T_w-T_m)$
i	electric current
k	thermal conductivity; surface roughness
$\dot{m}$	mass flow rate
P	perimeter
p	pressure
q_w'	heat transfer to gas per unit length
R'	electrical resistance per unit length
T	absolute temperature
t	wall thickness
V_b	gas bulk velocity
x	axial coordinate

Greek symbols

μ viscosity

ρ density

τ_w apparent wall shear stress, $-\frac{D_h}{4}\frac{d}{dx}\left[p + G^2/\rho g_c\right]$

Non-dimensional parameters

f apparent friction factor, $2g_c\tau_w\rho/G^2$

Gr_q modified Grashoff number, $Gr^* q^+ RePr$

Gr^* modified Grashoff number, $gD_h{}^3/\nu^2$

K thermal acceleration parameter, eq. (10)

Nu Nusselt number, hD_h/k

Pr Prandtl number, $\mu c_p/k$

Q^+ laminar wall heat flux parameter, $D_h q''_w/(2k_i T_i)$

q^+ turbulent wall heat flux parameter, $q''_w/(Gc_{p,i}T_i)$

Re Reynolds number, GD_h/μ

St Stanton number, h/Gc_p

x^+ axial distance, $2x/(D_h Re_m Pr_m)$

Subscripts

cp evaluated from constant property prediction

i inlet

m evaluated at local bulk temperature

w wall

INTRODUCTION

Non-circular ducts are used for regeneratively cooled rocket nozzles, gas cooled nuclear power reactors and in the processing industries in cases where the application involved often precludes use of circular ducts. From a thermal standpoint, turbulent flow is usually desirable, but pumping power restrictions and possible failure modes force consideration of transitional and laminar flow as well. In order to conserve both space and power effectively, one must have accurate design criteria. The purpose of this investigation is to provide, by experiments, design criteria for square tube applications where the temperature-dependent properties may vary significantly.

In many applications the tubing is small. Since commercial tubing is normally employed in production, the square ducts used typically have slightly rounded corners rather than the infinitely sharp corners idealized in most analyses for non-circular tubes. As the tube size becomes smaller, the corner curvature becomes more important. Accordingly, the test section chosen for these experiments is a commercially available square tube with a corner-radius-ratio (r/D_h) of about one tenth.

It is, conceptually, possible to solve the laminar problem using a numerical approach. Such methods are now used routinely for two-dimensional boundary layer problems [1]. However, with flow readjustment due to temperature-dependent viscosity and density, the heated duct problem becomes a three-dimensional one including significant spanwise diffusion terms. Thus, numerical methods for "three-dimensional" swept wings are not applicable.

The coupled, non-linear governing equations form a parabolic system which involves solution of an elliptic boundary value problem at each forward step in a numerical procedure. Currently, computer storage and time requirements to solve two-dimensional elliptic flow problems are extensive if not excessive. Although promising three-dimensional numerical methods are under development by Spalding and co-workers [2] and by Pierce and Klinksiek [3], it is unlikely that many design engineers will have adequate first generation computers readily available for the three-dimensional problem. Solution of the flow problem for the small commercial ducts will involve a further complication; for accuracy near the rounded corners it will probably be expeditious to introduce a circular grid along with the main rectangular grid.

Numerical solution of the turbulent and relaminarizing problem, for variable-property flow in square ducts, is subject to the difficulties described above and is also hampered by insufficient knowledge of the transport mechanisms. Although several existing turbulence models give reasonable predictions in the fully turbulent regime in circular tubes, their use for the relaminarizing regime yields inadequate results [4]. Accordingly, the present study is devoted to the experimental measurement of heat transfer and wall friction parameters for laminar flow and relaminarizing turbulent flow of strongly heated gases through square tubes. It is hoped that in the near future current turbulence research will have progressed to the point where these data can be used in the verification of a more generally valid turbulence model than is presently available.

Table 1 summarizes the range of variables covered in the present experiment.

PREVIOUS WORK

For laminar flow, geometry has a pronounced effect on heat-transfer and friction coefficients. This fact is well documented for fully developed flow under the idealization that fluid properties are constant [5]. Montgomery and Wibulswas [6] showed further that geometry also affects the thermal entry region in rectangular ducts. Assuming constant properties and a fully developed velocity profile, they performed a numerical analysis which showed heat transfer coefficients in the thermal entry region to vary by forty per cent as the aspect ratio ranged between one and four. Their results are not known to have been verified experimentally. For ethylene glycol, Hwang and Hong have considered the effect of viscosity variation in a "fully developed" analysis for laminar flow in a square duct; they also present measurements in a square tube counter-current heat exchanger with fair agreement [7].

For gaseous laminar flow in a circular tube, Worsoe-Schmidt and Leppert [8] developed a numerical solution accounting for property variation; it is quite consistent with existing data. Their results show only a slight increase in the Nusselt number but a large increase in the friction coefficient (maximum differences of six per cent and fifty per cent, respectively, at a peak $[T_w/T_m]$ of 1.5) when compared to constant property predictions in the thermal entrance region. Recent analyses for parallel plates and annuli show comparable property dependence [9, 10].

Gaseous variable property results for the square duct are apparently limited to experiment. Battista and H. C. Perkins [11] suggest that their data agree with correlations given by Campbell and H. C. Perkins [12] for a triangular duct. Their results, however, are limited to turbulent flow at Reynolds numbers greater than 10^4. Laminar and transitional flow in a square duct was tackled by Lowdermilk, Weiland and Livingood [13] as early as 1954 but they only obtained <u>average</u> parameters and, at the time, the phenomenon of relaminarization was not recognized.

Relaminarization--that is, apparent laminar behavior at local Reynolds numbers normally associated with turbulent flow--has been observed in strongly heated internal gas flows [14,15,16] and in accelerated "external" flows [17,18]. With internal flow in the low Reynolds number range, a slight change in the heating rate can lead to a striking change from turbulent downstream behavior to laminar behavior. The consequence is a substantial reduction in local heat transfer coefficient and an increase in wall temperature. The danger is obvious. Until turbulence models are developed to predict parameters through the axial relaminarization process accurately, the engineer needs design criteria to predict when it is imminent. For accelerated flows, critical relaminarization parameters have been presented by both Launder [17] and Moretti and Kays [18]. By a transformation to a heating parameter, McEligot, Coon and Perkins [19] have shown that the reverse-transition inside circular tubes can be predicted by using approximately the same value of the critical acceleration parameter suggested by Moretti and Kays. However, whether their observation is valid for all internal flows is yet to be shown. One might expect that in non-circular ducts the proximity of adjacent walls in the corner regions would hasten re-laminarization.

THE EXPERIMENT

The equipment used was a redesigned version of the heat transfer loop employed by Reynolds, Swearingen and McEligot [20]. The essentials are illustrated in Figure 1. Test gas (helium or nitrogen) flows from commercial gas cylinders through a series of three pressure regulators, the last being a Honeywell "Precision Pressure Regulator," to keep pressure fluctuations to a minimum. The gas passes through one of two Brooks rotameters, which are used in setting the desired flow rates, and then enters a mixing chamber where the bulk temperature is measured. This chamber leads to the entrance to a vertical test section, which is heated resistively by a.c. current from a Sorensen line voltage stabilizer, an adjustable transformer and a 20-to-1 transformer. After leaving the test section, the gas is cooled to room temperature by a countercurrent water heat exchanger so that the flow rate can be measured more accurately. It then passes through the flow control valve and into a Parkinson-Cowan Type D1 positive displacement flow meter which is specified to provide half per cent accuracy at ambient conditions.

A Hewlett Packard Model 3450A digital voltmeter measures thermocouple e.m.f. Power is measured with a 0.01 per cent Fluke Model 883AB differential voltmeter in conjunction with a quarter per cent Weston Model 370 ammeter. Axial pressure differences are obtained with an MKS Baratron Pressure Meter, Model 77, with 1mm Hg differential pressure transducer, having a sensitivity of 1×10^{-5} torr, or with a Meriam micromanometer or inclined manometer, as appropriate. Pressure levels below 2 atmospheres are determined with vertical mercury or water manometers, while a Heise gage ($\pm$ 0.2 psi specified accuracy) is employed for higher pressures.

A vacuum environment is provided in an inverted bell jar, 40 in. x 18 in. dia. (100 cm x 55 cm), in order to minimize heat loss effects while allowing a localized radiant heat loss calibration. The vacuum also reduces the response time necessary to reach steady conditions with heating.

Test Section

The test section consists of a commercially available, seamless, extruded, Inconel 600 tube having a nominally square shape. From examination of metallograph pictures at 25x magnification, it was found to have a cross-sectional area of 5.87 square millimeters (0.0091 square inches), a hydraulic diameter of 2.49 millimeters (0.098 inches), and a wall thickness of 0.38 millimeters (0.015 inches). The small diameter minimized the possibility of natural connection effects which otherwise could be a problem at low Reynolds numbers. The radius of curvature at the corners is approximately 0.2 millimeters (0.008 inches). Tubing from the same manufacturer's run was used by Battista and Perkins [11].

Of the three electrodes shown in Figure 1 only the two upper ones were used for reported data. During heat loss calibration, power can be applied across the bottom electrode and the top electrode so that the center electrode acts as a radiating thermal sink and its conduction heat loss may be calibrated via extended fin analysis. In the normal flow run configuration with power across the upper two electrodes, the hydrodynamic entry length is 188 hydraulic diameters and the heated section is 121 hydraulic diameters long. Thermal expansion is accommodated by supporting the test section at its upper end only and simply passing the lower, adiabatic section through a pair of Teflon guides to maintain vertical alignment.

The heat transfer surface texture is described as bright, smooth and uniform by the manufacturer. Inner surface roughness is claimed to be 125 micro-inches RMS ($\sim 3\ \mu$). Roughness measurements with an industrial profilometer yielded an estimate of 20 to 30 micro-inches RMS ($\sim 1/2\ \mu$). However, optical viewing of a fresh piece of tubing at 1000 x showed roughness elements about 200 micro-inches ($\sim 5\ \mu$) apart and, by roughly calibrating the travel of the microscope drive, depths of 100-200 micro-inches. With the aid of stereoscopic photographs at 700x and 7000x on a Cambridge "Stereoscan 600" scanning electron microscope, heights were found to be about 2 to 3 μ ($\sim$ 100 micro-inches). The scanning electron microscope was also used to examine a well-used sample of the test section employed by Battista and Perkins [11]; its appearance was comparable to the proverbial sand grains with the largest being of the order of 400 micro-inches (10 μ). The photographs are presented elsewhere [21]. Since their test section was always used for air flow at moderate to high pressures when heated, it is believed that the surface texture observed on that sample would be an upper bound on the roughness of the present test section which normally employed helium or nitrogen as the test gas. Thus, relative roughness, k/D_h, was estimated to be in the range 0.001 to 0.004.

Premium grade chromel-alumel thermocouples of 0.005 inch ($\sim$ 0.13 mm) diameter were spot welded to the test section along the centerline of one face. The parallel-type configuration was employed to minimize thermocouple error due to finite junction area. At a number of locations additional thermocouples were attached at a corner to measure the circumferential temperature variation. Pressure tap orifices were about 5 mil ($\sim$ 0.13 mm) holes which were electrostatically drilled after the pressure taps were attached to obtain burr-less holes. Thus, the ratio of hole diameter to test section diameter was less than 1:10.

From the reduced data, it was found that local axial heating rate to the gas could be represented approximately as a step increase, followed by a gradual decrease as the heat loss increased axially with the wall temperature. The percentage change depended on the test gas, Reynolds number and heating rate. The measured deviation from a constant peripheral wall temperature was found to be within 2°F (1°C) for these tests. This observation is consistent with the correlation of $(T_{corner} - T_{center})/(T_{center} - T_m)$ vs. Nu/S* developed by Lowdermilk, Weiland and Livingood [13] for predominantly turbulent flows. In the present experiment the wall conduction parameter,

$$S^* = k_{wall}\, t/(k_{gas}\, D_h) \tag{1}$$

is about 10 for helium and about 70 for nitrogen. Thus, the experimental boundary conditions approached the analytical idealization of a specified axial heating rate with locally constant temperature around the circumference.

Procedure

A number of preliminary experiments were conducted to calibrate the equipment and to insure that it was functioning properly. Of these, the initial tests were adiabatic friction measurements, which will be described later under Results.

The second group of experiments were heat loss calibrations conducted by heating the test section without internal gas flow. These runs provided data for a number of calibrations. Test section emissivity, $\epsilon(x,T_w)$, was determined locally. As mentioned earlier, the electrode conduction heat loss could be calibrated. In data reduction for flow runs, the local energy generation is calculated from the i^2R' product so data for the resistance calibration, $R'(T_w)$, were also obtained during the heat loss runs. Several runs of this type included internal thermocouple probe measurements to calibrate the "radiating thermocouple conduction error," i.e., the temperature depression caused by axial conduction to the wall thermocouples which act as radiating fins [22].

Once preliminary results were obtained, a procedure evolved to obtain the data for flow with heating. First, the system was checked for leaks, thermocouple readouts were checked, and all manometers to be used were zeroed. Usually an adiabatic flow run was then conducted at the desired flow rate and comparisons were made to previous adiabatic runs. If all was in order, power was applied to the test section by establishing a constant voltage setting on the adjustable transformer. When thermal equilibrium was reached, measurements were taken. Since the response of the small pressure tap orifices in the test section was relatively slow, temperatures, power and flow rate were measured both before and after each set of axial pressure difference measurements to insure that the system had not suffered from some disturbance during the test.

Data were reduced at the C.D.C. 6400 computer facility of The University of Arizona. The basic computer program is described elsewhere [12,14] and details of modification for the vacuum environment are presented by Reynolds [23]. Discussion of the deduced parameters for non-circular ducts is provided by Campbell and Perkins [12] and their definitions are presented in the Nomenclature.

Experimental Uncertainties

Laminar flow measurements pose a severe test of internal, forced convective heat transfer apparatus since percent uncertainties for most deduced parameters increase as the Reynolds number is lowered. For the present study, uncertainty analyses based on the method of Kline and McLintock [24] were performed for a number of experimental runs. Typical estimates for the uncertainty of deduced Nusselt numbers and friction factors are listed in Table 2.

Heat transfer parameters are strongly dependent on the q_w' uncertainty which depends, in turn, on the ratio of the external radiative resistance to the internal convective resistance. Since the radiative resistance is a relatively fixed function of temperature, this uncertainty is primarily reduced by increasing the convective heat transfer coefficient. At a fixed Reynolds number, the Nusselt number (hD_h/k) does not vary widely as the heating rate is varied, so h may be increased by decreasing D_h and increasing k. Thus, the small size of the test section helps. For laminar flow we also found it necessary to take advantage of the higher thermal conductivity of helium compared to nitrogen. Increasing h also reduces the axial change in q_w', so using helium actually provided a more constant axial heating rate for the laminar runs than for turbulent data with nitrogen.

The uncertainty in duct diameter enters the friction factor calculations quite differently from the Nusselt number. Taking a sharp-cornered duct for convenience, one can see the calculations are

$$f = \frac{-g_c \rho_m D_h^5}{2\dot{m}^2} \frac{d}{dx} \left[p + \frac{\dot{m}^2}{g_c \rho_m D_h^4} \right] \tag{2}$$

and

$$Nu = q_w' / [4 k_m (T_w - T_m)] \tag{3}$$

in terms of "measured" quantities. So the Nusselt number is not directly dependent on the uncertainty in D_h while the friction factor is strongly sensitive. Accordingly, results demonstrating the effect of property variation on wall friction will be presented in normalized form, $f \cdot Re/(f \cdot Re)_{cp}$ with $(f \cdot Re)_{cp}$ measured on the same duct, to reduce the effect of the uncertainty due to diameter measurement. When normalized, the dominant uncertainty in the friction factor is the uncertainty in pressure differences between closely spaced pressure taps.

Concerning heat transfer, axial conduction losses tended to increase the Nusselt number uncertainty significantly near the electrodes despite calibration. At the upper end of the test section ($x/D_H > 80$), uncertainty in the Nusselt number was also increased by an increase in the percentage uncertainty of the temperature difference,

$$\frac{\delta(T_w - T_m)}{T_w - T_m} \approx \frac{\sqrt{\left(\frac{T_w}{T_m}\right)^2 \left(\frac{\delta T_w}{T_w}\right)^2 + \left(\frac{\delta T_m}{T_m}\right)^2}}{\frac{T_w}{T_m} - 1} \tag{4}$$

as T_w/T_m approaches unity.

In addition to Table 2, estimated uncertainties are indicated by light bracketed lines on some of the figures presenting the experimental results.

RESULTS

Adiabatic flow

Throughout the period of testing, unheated flow measurements were conducted in the range $400 \gtrsim Re \lesssim 30{,}000$ with helium and nitrogen. For laminar flow in our rounded-corner square duct, these correlated as

$$(f \cdot Re)_{cp} = 15.7 \tag{5}$$

which is close to the analytic value for a circular tube. For a sharp-cornered square tube, one would expect $f \cdot Re = 14.2$ [5]. Since overall pressure differences were used to calculate the friction factor, the experimental uncertainty in $(f \cdot Re)_{cp}$ is primarily dependent on the hydraulic diameter measurement which is believed to be known within one per cent. Accordingly, the uncertainty of $(f \cdot Re)_{cp}$ is estimated as about four per cent.

In the turbulent range, friction factors were greater than the correlation for a smooth tube. Comparison to predictions by Moody [25] show the data would correspond to a relative sand roughness factor, k_s/D_h, of about 0.001. This value agrees with the observations of Battista and Perkins [11] with similar tubing, but is slightly smaller than expected from our microscopic examinations.

Heat transfer in laminar flow

To minimize uncertainties in the Nusselt number, all heated laminar runs were made with helium as the test gas. For these data the axial variation of q_w' was about 14 per cent or less. Results are reported in Fig. 2. For $x^+ > 0.05$ they agree quite closely with the constant property analysis of Montgomery and Wibulswas [6] for a constant axial heating rate to gases flowing in a square duct. Downstream the variable property measurements are predicted well by the asymptotic calculations of Montgomery and Wibulswas and by the numerical solution of Clark and Kays [26] for fully established conditions under the usual constant property idealization. However, for $x^+ < 0.05$ there is evidently an increase in the heat transfer coefficient of about ten per cent.

The differences in the immediate thermal entry may be examined in more detail with the aid of a Leveque analysis as conducted by Worsoe-Schmidt for annuli [27]. At x^+ sufficiently small so that the thermal boundary layer thickness is much smaller than D_h, the problem may be treated as two-dimensional. In order to estimate the average peripheral Nusselt number, the wall velocity gradient is taken as the value corresponding to the average peripheral friction factor. Then one can show that, with a constant wall heat flux as the boundary condition, the Leveque solution would be given by

$$Nu \cong 0.652\ (f\cdot Re_{D_h})^{1/3}\ [2x/(D_h Re_{D_h} Pr)]^{-1/3} \tag{6}$$

This prediction is plotted on Fig. 2 for the sharp-cornered square duct ($f\cdot Re_{D_h} = 14.2$), the circular tube (16) and parallel plates (24). The numerical analysis of Montgomery and Wibulswas appears to be confirmed at $x^+ = 0.01$, the lowest value they present.

Since the present rounded-corner test section led to adiabatic friction factors which agreed with circular tube predictions, the Nusselt number in the immediate thermal entry may be compared to the Leveque solution for $f\cdot Re_{D_h} \cong 16$. The difference between the measurements with property variation and the constant property prediction is then about six per cent, which is slightly greater than the estimate of the experimental uncertainty. To put this effect into perspective, it should be noted that the fluid properties varied by up to 60 per cent across the tube in the thermal entry region.

One may conclude that for square ducts the effect of gas property variation is a slight increase of the Nusselt number in the thermal entry and a negligible effect downstream. This observation is consistent with the numerical results for symmetric circular tubes [8]. Concerning the effect of the rounded corners, it appears that at $(r/D_h) \approx 0.1$ the thermal entry behavior is predicted by circular tube analyses while downstream results conform with "sharp-corner" analyses for fully established conditions. Since the thermal resistance is distributed across the cross section in fully-developed laminar flow, instead of being concentrated near the wall as in turbulent flow, it is reasonable that the corner radius would have less effect when the thermal boundary layer extends across the duct. Thus, the constant property prediction of Montgomery and Wibulswas may be used for conservative design; however, their presentation is by means of a small graph which is difficult to read. Accordingly, we have correlated their results to within three per cent as

$$Nu = \left[\frac{1}{Nu_\infty} - 0.152 \exp \{-19.3x^+\} \right]^{-1} \qquad (6)$$

for $x^+ \gtrsim 0.015$ with Nu_∞ taken as 3.63.

Wall friction in laminar flow

Experimental friction factors were calculated from pressure drop measurements via the definition of the "apparent" wall shear stress,

$$\tau_w = \frac{-D_H}{4} \frac{d}{dx} (p + G^2/\rho_m g_c) \qquad (7)$$

As mentioned under Experimental Uncertainties, the effect of gas property variation is demonstrated by normalizing the results as $f \cdot Re_m / (f \cdot Re)_{cp}$. Whenever possible, the value of $(f \cdot Re)_{cp}$ was taken from the adiabatic flow run preceding each heated run, in order to reduce the propagation of experimental uncertainties in flow rate and in diameter measurement. It should be noted, however, that the difference in the day-to-day results was three per cent or less.

Results are presented in Fig. 3. In contrast with the heat transfer data, there is a strong dependence on gas property variation across the duct (expressed as T_w/T_m). For comparison the correlation by Davenport and Leppert [28], for laminar flow in circular tubes,

$$(f/f_{cp}) = (T_w/T_m)^{1.35} \tag{8}$$

is shown as well. It appears that their correlation may be extended to square ducts for design purposes, although a lower exponent might be justified

Heat transfer in turbulent flow

Since the square test section employed by Battista and Perkins [11] was a bare tube hung in atmospheric air, heat loss was greater in their experiment than in the present report. Consequently, their axial heating rate also could be described as a step change followed by a decreasing ramp function; in their worst case, at $Re_i \approx 21000$, the variation was about 26 per cent. In contrast, the present apparatus has only an axial variation in $q_w'(x)$ of about six per cent at the same Reynolds number with nitrogen flow. Their local heat transfer results were correlated as

$$Nu = 0.021\, re^{0.8} Pr^{0.4} \left(\frac{T_w}{T_m}\right)^{-0.7} \left[1 + \left(\frac{x}{D_h}\right)^{-0.7} \left(\frac{T_w}{T_b}\right)^{0.7}\right] \tag{9}$$

(a printing omission occurs on the last exponent in their printed version).

With reduced experimental uncertainties, our data verified the above equation for runs in the range $4 \times 10^3 < Re < 2.5 \times 10^4$ and

q^+ to 0.003 provided the acceleration parameter was less than 10^{-6}. In the next section, obvious divergence from this correlation is related to relaminarization, i.e., axial turbulent-to-laminar transition along the duct.

Relaminarization

As mentioned in the Introduction, the retransition regime can be extremely important since a sudden decrease in heat exchanger performance may occur in this region. In fact, Coon [29] reports a pair of experimental runs at identical conditions--same heating rate and flow rate--where one remained turbulent and the other evidently laminarized.

The most obvious way of testing for this condition might appear to be to insert a hot-wire anemometer into the flow. This approach would not be possible in the present apparatus without greatly altering the flow since the tube is only about 2.5 millimeters (0.1 in.) wide. More importantly, turbulence level measurements may not show the "point of retransition," i.e., the conditions where viscous effects dominate despite turbulent fluctuations and, in turn, lead to wall parameters which agree with laminar predictions. In a separate, unpublished experiment with a larger, circular tube at The University of Arizona, R. J. Pederson found that oscilloscope traces from a hot wire anemometer apparently showed normal turbulent flow although wall parameters indicated that laminarization had taken place.

Bankston [15] has demonstrated that local Stanton number measurements can give a clear indication of whether retransition occurs; Fig. 4 is an example. In these figures, local Re drops as x increases due to increased viscosity so successive axial measurements proceed from right to left. The upper sub figure shows an experimental run which agrees with the turbulent, variable properties correlation of Battista and Perkins [11]. Beyond the thermal entry the data drop below the fully-developed, constant properties turbulent curve, due to the effect of property variation and then, as T_w/T_m approaches unity, they approach the curve gradually. The lower sub figure shows a run which laminarizes; the thermal entry behavior continues until the data reach the downstream laminar prediction. The middle sub figure represents an intermediate, or "questionable" run.

Having established confidence in the heat transfer data in turbulent flow with Re > 10^4 and in laminar flow, we conducted additional heated flow runs in the retransition regime of McEligot, Coon and Perkins [19] to determine a criterion for laminarization in square ducts. As shown in Fig. 4, runs were classified either as turbulent, laminarizing or questionable. Results are plotted in Fig. 5. The data agree qualitatively with the classification of McEligot, Coon and Perkins. However, by concentrating more experimental runs in their transition range, the uncertainty in the relaminarization criterion has been reduced for the present square tube.

Alternatively, the data could be plotted using a suitably defined acceleration parameter instead of the heat flux parameter shown. However, as McEligot, Coon and Perkins have shown, the two approaches are closely related. In particular, for low Mach number flow of a strongly heated perfect gas, one can show that the acceleration parameter is related to the heat flux parameter as

$$K_i = \frac{\nu}{V_b^{\,2}} \left.\frac{dV_b}{dx}\right)_i \approx \frac{4q^+}{Re_{D_h,i}} \qquad (10)$$

for any uniformly heated duct of arbitrary shape. With these approximations, the critical acceleration factor suggested by Coon [29] for a circular tube has also been plotted in Fig. 5.

The question-of whether adjacent walls significantly increase the Reynolds number at which laminarization of a turbulent flow occurs - is answered. They evidently do not. While the viscous sublayer is likely thickened by strong heating (as shown by numerical predictions, which account for property variation), it appears that it is not thickened enough in this range to interfere with the hydraulic diameter analogy - which depends on the thermal resistance being concentrated near the wall.

Coon's correlation apparently predicts laminarization at higher Re in a circular tube than the present data do for a square duct. However, the difference probably lies in the methods of evaluating the parameters. Coon evaluated K near the exit of his tube ($x/D \approx 90$) - after his Nusselt numbers began to agree with the prediction for <u>fully developed</u>, laminar flow. Since it is not clear at what axial station viscous effects become dominant, the present work interprets the criterion as that set of initial and boundary conditions (i.e., K_i or q_i^+ and Re_i) which will lead to relaminarization. Accordingly, we effectively evaluate K_i near the start of heating. Coon's figures show that K decreased by a factor of two along the tube in some of his transitional and laminar runs. Thus, if his acceleration parameter were calculated in the same manner as the present study, the agreement would be closer.

For the range of data shown on Fig. 5, we may take the separation between those runs which are "questionable" and those which laminarize as a criterion for laminarization. This locus may be correlated as

$$q^+_{i,trans} \approx 3.9 \times 10^{-8} \, Re_i^{4/3} \tag{11}$$

as shown on Fig. 5. Alternatively, this correlation could be phrased

$$K_{i,trans} \cong 1.6 \times 10^{-7} \, Re_i^{1/3} \tag{12}$$

At $Re_i = 4000$, we then have $K_{i,trans} \cong 2.6 \times 10^{-6}$ which falls between the values suggested by Moretti and Kays [18] and Back and Seban [30] for external flows. If divergence from the turbulent correlation is preferred as a criterion, the heating rate $q^+_{i,trans}$ would be lower, e.g., about 35 per cent lower for a 15 per cent divergence as shown by our other locus on the figure.

CONCLUSIONS

This investigation indicates that the numerical analysis of Montgomery and Wibulswas [6], for heat transfer to laminar flow in sharp-cornered square ducts with constant properties, is substantially correct. For a duct with rounded corners instead, the peripheral average Nusselt number is slightly higher in the thermal entry. Gas property variation affects the Nusselt number only slightly; the effect on the friction factor was found to be much greater than on the heat transfer parameters, and Davenport and Leppert's correlation [28] for round tubes is recommended for square ducts as well.

With a thermal boundary condition of a gradually decreasing wall heat flux in the range $0.0015 < q_w''/Gc_{pi}T_i < 0.004$, the criterion for laminarization in a square duct may be approximated by equation (11). The values represented by this result are in agreement with criteria established for laminarization of accelerated, external turbulent boundary layers.

ACKNOWLEDGMENTS

The authors wish to acknowledge the financial support contributed by the U. S. Army Research Office - Durham as well as the U. S. Army Mobility Equipment Research and Development Center at Fort Belvoir. Thanks are also due to Dr. R. W. Shumway, and Messrs. E. Ek and G. Hasen for their valuable assistance.

REFERENCES

1. K. W. SCHADE and D. M. McELIGOT, "Cartesian Graetz Problems with Air Property Variation," Int. J. Heat Mass Transfer, 14, 653-666 (1971).
2. L. S. CARETTO, R. M. CURR and D. B. SPALDING, "Two numerical methods for three-dimensional boundary layers," Tech. Rept. EF/TN/A/40, Imperial College (July 1971).
3. F. J. PIERCE and W. F. KLINKSIEK, "An Implicit Numerical Solution of the Turbulent Three-Dimensional Incompressible Boundary Layer Equations," Tech. Rept. VPI-E-71-14, Virginia Polytechnic Institute (July 1971).
4. D. M. McELIGOT and C. A. BANKSTON, "Numerical Predictions for Circular Tube Laminarization by Heating," ASME paper 69-HT-52 (1969).
5. W. M. KAYS, Convective Heat and Mass Transfer, New York: McGraw-Hill (1966).
6. S. R. MONTGOMERY and P. WIBULSWAS, "Laminar Flow Heat Transfer in Ducts of Rectangular Cross-section," Proc., Third Intl. Heat Transfer Conf., Vol. 1, 107-112 (1966).
7. S. T. HWANG and S. W. HONG, "Effect of Variable Viscosity on Laminar Heat Transfer in a Rectangular Duct," A.I.Ch.E. paper 8, Natl. Heat Transfer Conf., Minneapolis (1969).
8. P. M. WORSOE-SCHMIDT and G. LEPPERT, "Heat Transfer and Friction for Laminar Flow of a Gas in a Circular Tube at High Heating Rate," Int. J. Heat Mass Transfer, 8, 1281-1301 (1965).
9. T. B. SWEARINGEN and D. M. McELIGOT, "Internal Laminar Heat Transfer with Gas Property Variation," J. Heat Transfer, 93, 432-440 (1971).
10. R. W. SHUMWAY and D. M. McELIGOT, "Laminar Gas Flow in Annuli with Property Variation," Nuc. Sci. Eng., 46, 394-407 (1971).
11. E. BATTISTA and H. C. PERKINS, "Turbulent Heat and Momentum Transfer in a Square Duct with Moderate Property Variation," Int. J. Heat Mass Transfer, 13, 1063 (1970).

12. D. A. CAMPBELL and H. C. PERKINS, "Variable Property Turbulent Heat and Momentum Transfer for Air in a Vertical Rounded Corner Triangular Duct," Int. J. Heat Mass Transfer, 11, 1003-1012 (1968).

13. W. H. LOWDERMILK, W. F. WEILAND and J. N. B. LIVINGOOD, "Measurements of Heat Transfer and Friction Coefficient for Flow of Air in Non-circular Ducts at High Surface Temperature," NACA RM E53J07 (1954).

14. D. M. McELIGOT, "The Effect of Large Temperature Gradients on Turbulent Flow of Gases in the Downstream Regions of Tubes," Ph.D. thesis, Stanford Univ., TID-19446 (1963).

15. C. A. BANKSTON, "Fluid Friction, Heat Transfer, Turbulence and Interchannel Flow Stability in the Transition from Turbulent to Laminar Flow in Tubes," Sc.D. thesis, University of New Mexico (1965).

16. C. W. COON and H. C. PERKINS, "Transition from the Turbulent to the Laminar Regime for Internal Convective Flow with Large Property Variations," J. Heat Transfer, 92, 506-512 (1970).

17. B. E. LAUNDER, "Laminarization of the Turbulent Boundary Layer in a Severe Acceleration," J. App. Mech., 31, 707-8 (Dec. 1964).

18. P. M. MORETTI and W. M. KAYS, "Heat Transfer Through an Incompressible Turbulent Boundary Layer with Varying Freestream Velocity and Varying Surface Temperature - an Experimental Study," Int. J. Heat Mass Transfer, 8, 1187-1202 (1965).

19. D. M. McELIGOT, C. W. COON and H. C. PERKINS, "Relaminarization in Tubes," Int. J. Heat Mass Transfer, 13, 431-433 (1970).

20. H. C. REYNOLDS, T. B. SWEARINGEN and D. M. McELIGOT, "Thermal Entry for Low Reynolds Number Turbulent Flow," J. Basic Eng., 91, 87-94 (1969).

21. K. R. PERKINS and D. M. McELIGOT, "Roughness of Heat Transfer Surfaces," Int. J. Heat Mass Transfer, (in press).

22. W. G. HESS, A. F. DEARDORFF and D. M. McELIGOT, "Radiating Thermocouple Conduction Error," Appendix F.

23. H. C. REYNOLDS, "Internal Low Reynolds Number Turbulent Heat Transfer," Ph.D. thesis, Univ. of Arizona. (1968) DDC AD 669 254.

24. S. J. KLINE and F. A. McLINTOCK, "The Description of Uncertainties in Single Sample Experiments," Mech. Eng., 75, 38 (1953).

25. L. F. MOODY, "Friction Factors for Pipe Flow," Trans., ASME, 66, 671 (1944).

26. S. H. CLARK and W. M. KAYS, "Laminar Flow Forced Convection in Rectangular Tubes," Trans., ASME, 75, 859-866 (1953).

27. P. M. WORSOE-SCHMIDT, "Heat Transfer in the Thermal Entrance Region of Circular Tubes and Annular Passages with Fully Developed Laminar Flow," Int. J. Heat Mass Transfer, 10, 541-551 (1967).

28. M. E. DAVENPORT and G. LEPPERT, "The Effect of Transverse Temperature Gradients on the Heat Transfer and Friction for Laminar Flow of Gases," J. Heat Transfer, 87, 191-196 (1965).

29. C. W. COON, "The Transition from the Turbulent to the Laminar Regime for Internal Convective Flow with Large Property Variations," Ph.D. thesis, Univ. of Arizona (1968).

30. L. H. BACK and R. A. SEBAN, "Flow and Heat Transfer in a Turbulent Boundary Layer with Large Acceleration Parameter," Heat Transfer and Fluid Mechanics Institute (1967).

	Nitrogen	Helium
Experimental Runs	16	12
Inlet Bulk Reynolds Number	3200-25400	1100-4600
Exit Bulk Reynolds Number	1900-16500	630-2600
Maximum T_w/T_i	3.4	3.4
Maximum $T_w(^{o}R)$	1810	1820
Maximum q^+ (turbulent)	0.0040	0.0030
Maximum Q^+ (laminar)	-	2.5
Maximum Gr_q/Re_i^2 (turbulent)	1.5×10^{-3}	2.1×10^{-5}
Maximum Gr_i^*/Re_i (laminar), ref [8]	-	0.03
Maximum Mach Number	0.29	0.24
Corner Radius of Curvature/Hydraulic diameter	0.08	0.08
x/D_H for Heat-Transfer Coefficients	3.0-109	3.0-109
x/D_H for Friction Factors	-	6.8-92

Range of Variables in the Present Experiment

Table 1

Table 2. Estimated experimental uncertainties

	Gas	Re_i	Max. q^+	Axial range	Estimated uncertainty	
f	He	> 1,000	0.005	$0.013 < x^+ < 0.4$	7%	Laminar
Nu	He	900 - 1400	0.005	$0.009 < x^+ < 0.2$	4	Laminar
Nu	He	1,400 - 2,000	0.004	$0.006 < x^+ < 0.15$	3	Laminar
Nu	N_2	2,000 - 3,500	0.003	$3 < x/D_h < 108$	7	Relaminarizing
Nu	N_2	3,500 - 5,500	0.004	$3 < x/D_h < 108$	7	Relaminarizing
Nu	N_2	5,000 - 10,000	0.003	$3 < x/D_h < 108$	5	Turbulent

FIGURE CAPTIONS

1. Schematic diagram of experimental apparatus.
2. Local heat transfer in laminar flow.
3. Local apparent friction factor in laminar flow. Symbols as in Figure 2.
4. Local heat transfer data demonstrating axial variation for the three classes of typical runs. Comparison is to predictions for fully established conditions.
5. Flow regime classification for square duct. Symbols as in Figure 4.

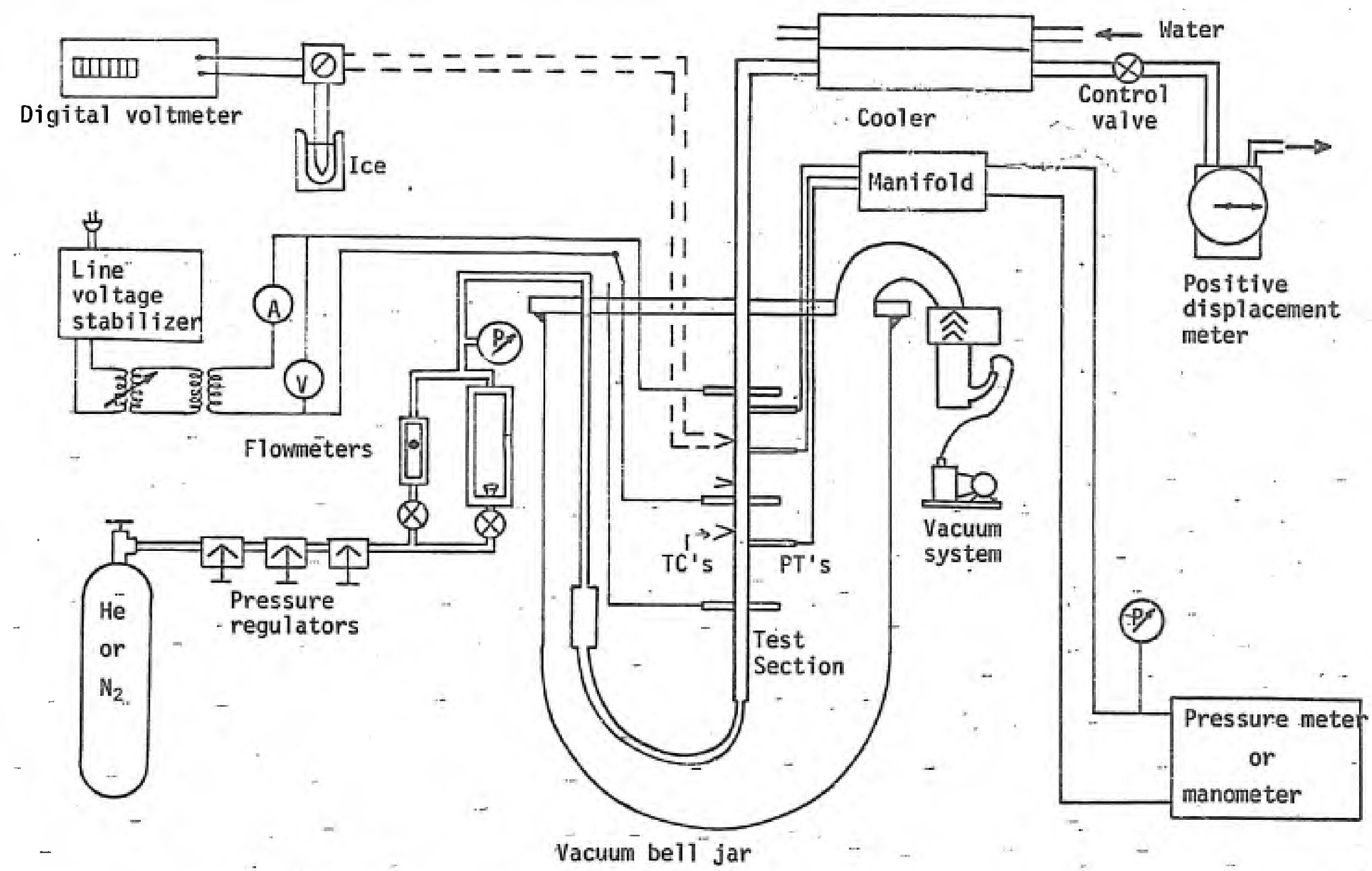

Figure 1. Schematic diagram of experimental apparatus

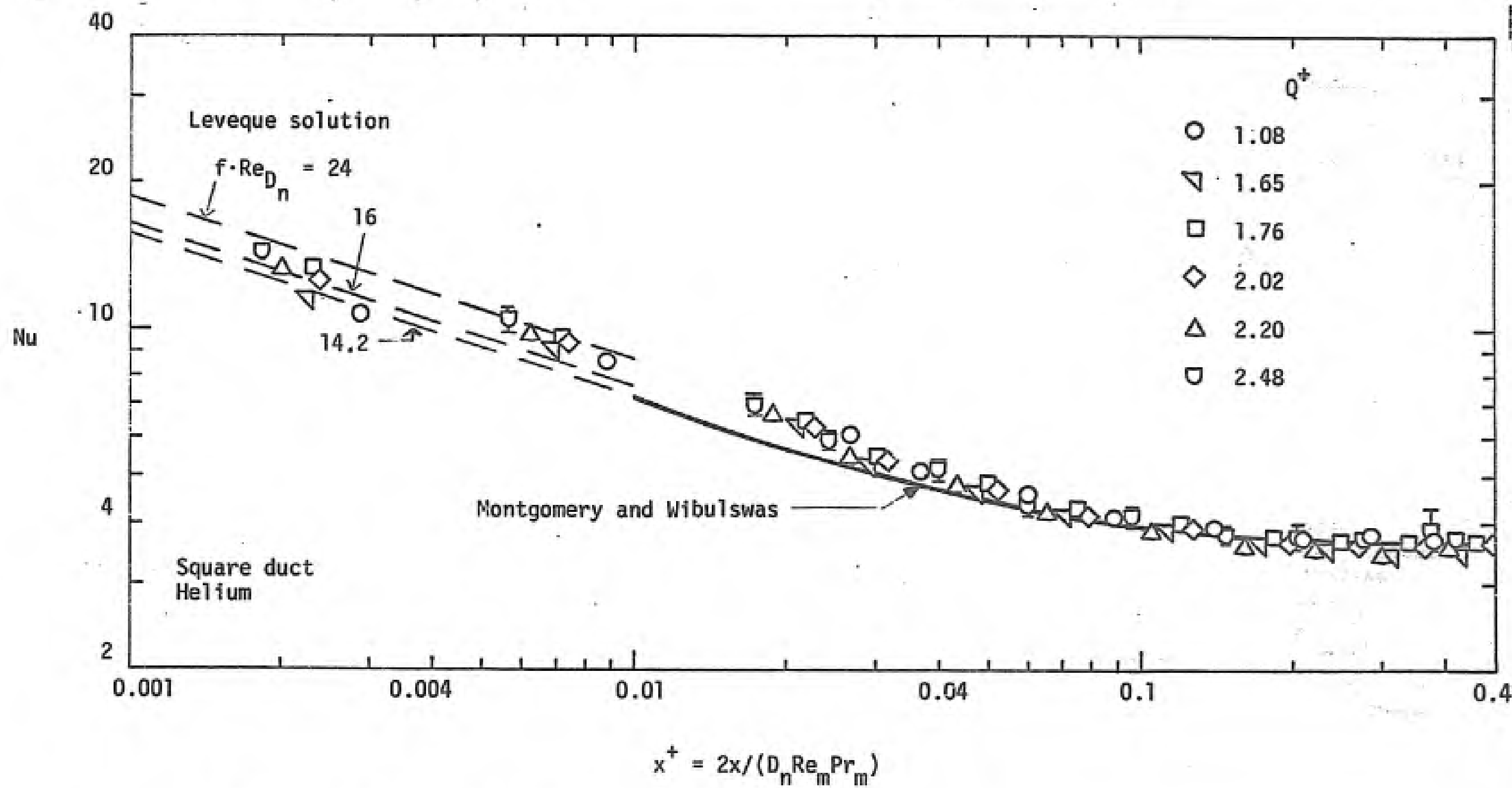

Figure 2. Local heat transfer in laminar flow.

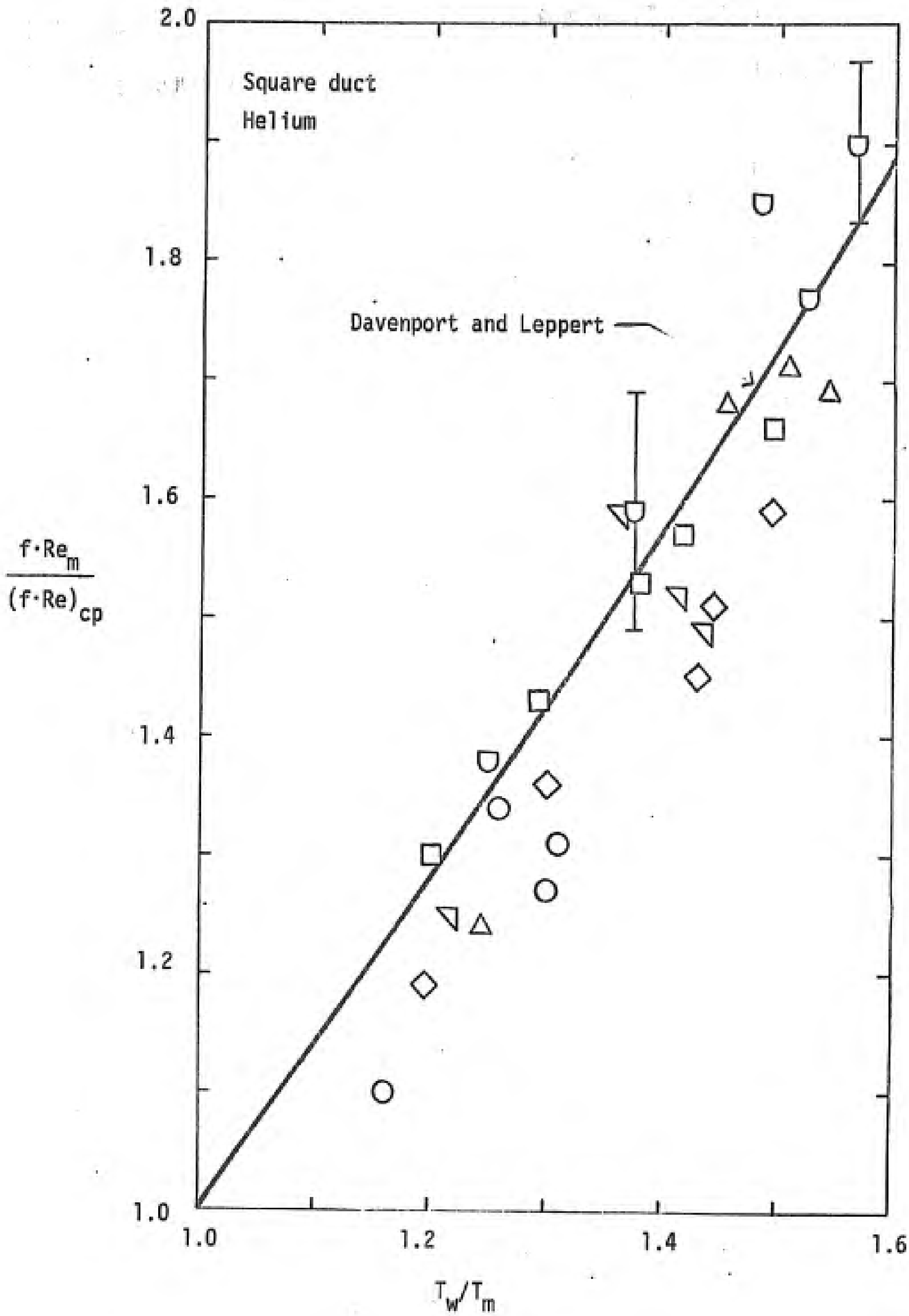

Figure 3. Local apparent friction factor in laminar flow. Symbols as in Figure 2.

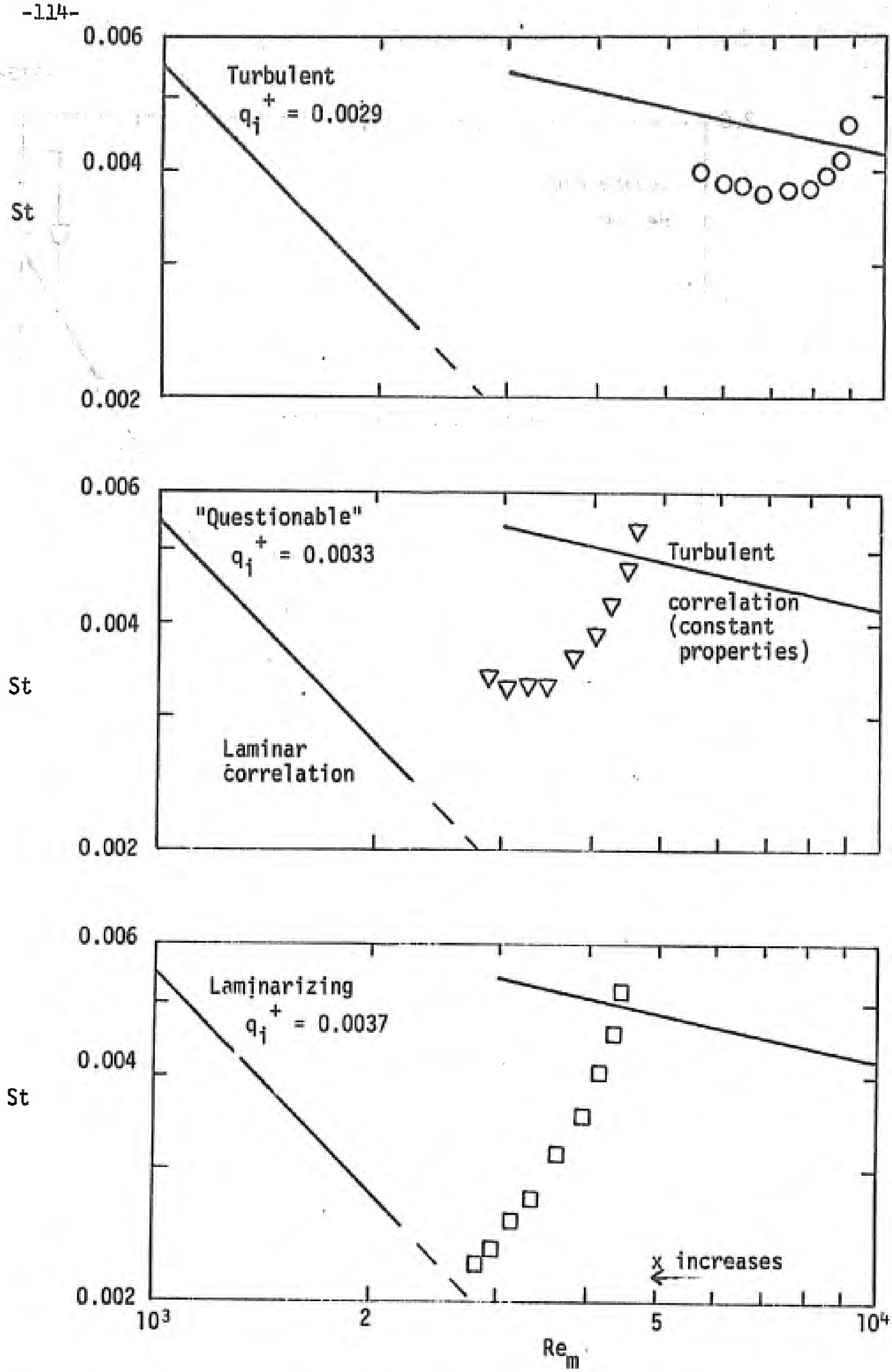

Figure 4. Local heat transfer data demonstrating axial variation for the three classes of typical runs. Comparison is to predictions for fully established conditions.

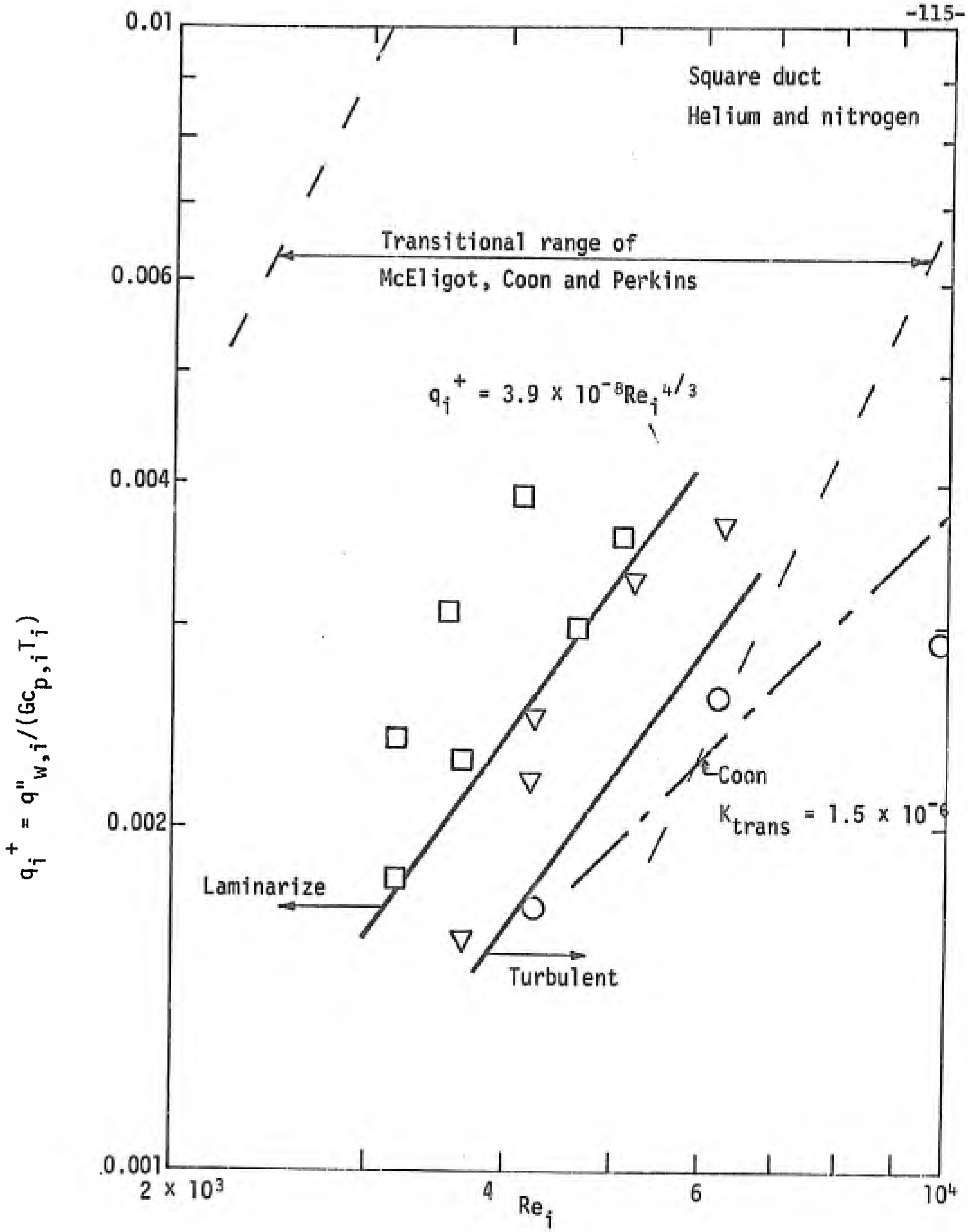

Figure 5. Flow regime classification for square duct. Symbols as in Figure 4.

APPENDIX D

DATA FOR HEATED FLOW IN A SQUARE DUCT

K. R. Perkins[1]

The following data are summaries of the results obtained from heat transfer experiments in a nominally square duct. The most pertinent information, from each successful run, has been reduced by a version of the computer program developed by Reynolds (Ph.D. thesis, University of Arizona, 1969; DDC AD 669 254). A full discussion of the apparatus and the implications of these results is included in the report by Perkins, Schade and McEligot (Appendix C).

It should be noted, however, that extreme care had to be exercised in the design of the experiment in order to insure that valid results could be obtained for low Reynolds number flow. The second column from the left gives a measure of the success of this design effort, in that it shows when the heat loss becomes too large compared to the heat transfer to the gas. When this ratio approaches the order of unity the inherent errors in determining the size of the heat loss make the deduced wall heat flux very uncertain at that position.

The same test section was used for all the experimental runs. It had a cross-sectional area of 0.0091 square inches and a hydraulic diameter of 0.0981 inches. The variables presented in the output are summarized in the following list.

---

1. Research Assistant.

NOMENCLATURE

X/D	axial distance divided by the hydraulic diameter
QP,L/QP,G	heat loss divided by heat transferred to gas
REYNOLDS	bulk Reynolds number, $GD_h/\mu m$
XPLUS	dimensionless distance, $2x/(D_H Re_m Pr_m)$
TW/TB	wall-to-bulk temperature ratio
NUSSELT	bulk Nusselt number, $q'_w D_h/[k_m P(T_w - T_m)]$
QPLAMIN	laminar wall heat flux parameter, $D_H q''_w/(2k_i T_i)$
QPTURB	turbulent heat flux parameter, $q''_w/(G\ c_{p,i} T_i)$
STANTON	bulk Stanton number, $Nu_m/(Re_m Pr_m)$
FRICTION FACTOR	apparent friction factor, $- g_c \rho_m D_h \frac{d}{dx} (p + \rho_m V_m^2)/2G^2$

Table 1. A Summary of Experimental Conditions

Run No.	*Gas*	*Re*	Q^+	q^+
		(conditions at $x/D_h = 1.0$)		
13	Helium	1302	1.87	0.00416
14	Helium	1269	2.15	0.00435
15	Helium	1905	0.29	0.00046
16	Helium	1890	0.58	0.00091
17	Helium	1659	2.62	0.00454
18	Helium	1345	Invalid - wrong electrode connected.	
19	Helium	1053	1.14	0.00312
21	Helium	1339	1.72	0.00370
22	Helium	1509	2.31	0.00441
23	Nitrogen	29725	17.28	0.00191
24	Nitrogen	22070	23.91	0.00294
25	Nitrogen	9468	10.72	0.00306
26	Nitrogen	4931	6.81	0.00371
27	Nitrogen	3376	4.46	0.00353
28	Nitrogen	3919	6.69	0.00452
29	Nitrogen	4836	7.40	0.00406
30	Nitrogen	5894	9.02	0.00406
31	Nitrogen	5939	6.33	0.00287
32	Nitrogen	4058	4.29	0.00284
33	Nitrogen	3056	3.18	0.00280
34	Nitrogen	4088	2.75	0.00182
35	Nitrogen	4025	3.65	0.00244
36	Nitrogen	3081	2.26	0.00198
37	Nitrogen	3545	2.36	0.00180
38	Nitrogen	3518	3.37	0.00257
39	Nitrogen	4763	6.03	0.00338
40	Helium	4553	4.66	0.00302

RUN 12 HELIUM FLOW= .79 LBS/HR TEST SECTION VOLTAGE=1.580 CURRENT=21.25 AMPS
INLET TEMPERATURE=74.77 F INLET PRESSURE=18.13 PSIA

*** HEAT TRANSFER DATA ***

POSITION (X/D)	HEAT LOSS (QP.L/QP.G)	BULK REYNOLDS	XPLUS	TW/TB	BULK NUSSELT	DIMENSIONLESS HEATING QPLAMIN	DIMENSIONLESS HEATING QPTURB	BULK STANTON
1.0	-.019	2133	.00141	1.03	19.90	.3300	.000463	.014041
3.0	.017	2127	.00428	1.04	14.63	.3185	.000446	.010351
8.8	.010	2113	.01248	1.06	10.11	.3208	.000449	.007200
11.9	.017	2106	.01697	1.07	8.77	.3185	.000446	.006265
18.5	.008	2090	.02660	1.08	8.03	.3211	.000450	.005776
26.1	.011	2073	.03790	1.08	7.38	.3202	.000449	.005354
38.6	.007	2044	.05685	1.08	6.98	.3214	.000450	.005136
53.9	.010	2010	.08070	1.09	6.38	.3205	.000449	.004777
68.8	.011	1978	.1[illegible]474	1.[illegible]9	5.91	.32[illegible]3	.000449	.004494
85.7	.012	1944	.13275	1.[illegible]9	5.45	.3197	.000448	.004223
1[illegible]7.7	.015	1912	.17[illegible]57	1.1[illegible]	5.0[illegible]	.3188	.000447	.003959
116.3	.[illegible]78	1886	.18578	1.10	4.59	.3001	.000421	.003565
12[illegible].1	-.006	1880	.19251	1.06	8.23	.3256	.000456	.006596

*** FRICTION DATA ***

POSITION (X/D)	TW/TB	BULK FRICTION FACTOR	BULK REYNOLDS
1.9	1.04	.0113	2130
6.8	1.06	.0123	2118
14.6	1.07	.0123	2100
29.9	1.08	.0121	2064
60.6	1.09	.0123	1996
91.4	1.09	.0118	1933

RUN 13 HELIUM FLOW= .50 LBS/HR TEST SECTION VOLTAGE=3.855 CURRENT=50.30 AMPS
INLET TEMPERATURE=75.55 F INLET PRESSURE=25.1[illegible] PSIA

*** HEAT TRANSFER DATA ***

POSITION (X/D)	HEAT LOSS (QP,L/QP,G)	BULK REYNOLDS	XPLUS	TW/TB	BULK NUSSELT	DIMENSIONLESS HEATING QPLAMIN	DIMENSIONLESS HEATING QPTURB	BULK STANTON
1.0	-.020	1302	.00231	1.26	13.32	1.8733	.004159	.015392
3.0	.048	1275	.00716	1.31	9.62	1.7505	.003887	.011351
8.8	.039	1209	.02188	1.41	6.46	1.7642	.003917	.008049
11.9	.052	1177	.03048	1.45	5.51	1.7428	.003870	.007056
18.5	.041	1117	.05003	1.45	4.85	1.7583	.003904	.006539
26.2	.057	1056	.07474	1.44	4.30	1.7320	.003846	.006136
38.8	.054	972	.12025	1.38	4.02	1.7346	.003851	.006235
54.2	.079	892	.18318	1.32	3.77	1.6929	.003759	.006372
69.3	.098	828	.25195	1.27	3.69	1.6615	.003689	.006718
86.3	.140	770	.33806	1.22	3.65	1.5994	.003551	.007146
108.6	.212	698	.46101	1.17	3.66	1.5016	.003334	.007768
117.6	.507	687	.51234	1.14	3.21	1.2075	.002681	.006998
121.4	.062	683	.53424	1.02	30.32	1.7161	.003810	.066695

*** FRICTION DATA ***

POSITION (X/D)	TW/TB	BULK FRICTION FACTOR	BULK REYNOLDS
1.9	1.28	.0105	1290
6.8	1.38	.0196	1231
14.6	1.45	.0227	1152
30.0	1.42	.0240	1027
60.9	1.29	.0262	861
92.1	1.20	.0271	754

RUN 14 HELIUM FLOW= .49 LBS/HR TEST SECTION VOLTAGE=4.180 CURRENT=54.20 AMPS
INLET TEMPERATURE=79.01 F INLET PRESSURE=23.94 PSIA

*** HEAT TRANSFER DATA ***

POSITION (X/D)	HEAT LOSS (QP,L/QP,G)	BULK REYNOLDS	XPLUS	TW/TB	BULK NUSSELT	DIMENSIONLESS HEATING QPLAMIN	QPTURB	BULK STANTON
1.0	-.015	1269	.00237	1.31	12.49	2.1535	.004853	.014815
3.0	.050	1239	.00737	1.36	9.33	2.0209	.004553	.011334
8.8	.046	1166	.02271	1.46	6.29	2.0254	.004564	.008123
11.9	.058	1133	.03171	1.50	5.38	2.0002	.004507	.007160
18.6	.051	1068	.05234	1.49	4.71	2.0129	.004536	.006637
26.2	.069	1001	.07901	1.47	4.17	1.9773	.004455	.006284
38.8	.070	917	.12758	1.40	3.90	1.9737	.004447	.006400
54.3	.104	835	.19570	1.33	3.63	1.9108	.004306	.006554
69.4	.130	772	.27074	1.27	3.60	1.8639	.004200	.007032
86.5	.190	708	.36425	1.21	3.57	1.7685	.003985	.007508
108.9	.293	659	.49807	1.16	3.61	1.6255	.003663	.008253
118.1	.597	641	.55495	1.13	3.29	1.3156	.002964	.007741
121.9	.113	635	.57853	1.01	45.71	1.8895	.004258	.108496

*** FRICTION DATA ***

POSITION (X/D)	TW/TB	BULK FRICTION FACTOR	BULK REYNOLDS
1.9	1.33	.0091	1256
6.8	1.43	.0192	1190
14.6	1.50	.0227	1105
30.0	1.45	.0244	974
61.0	1.30	.0266	806
92.3	1.20	.0273	688

RUN 15 HELIUM FLOW= .70 LBS/HR TEST SECTION VOLTAGE=1.420 CURRENT=19.76 AMPS
INLET TEMPERATURE=69.19 F INLET PRESSURE=19.25 PSIA

*** HEAT TRANSFER DATA ***

POSITION (X/D)	HEAT LOSS (QP.L/QP.G)	BULK REYNOLDS	XPLUS	TW/TB	BULK NUSSELT	DIMENSIONLESS HEATING QPLAMIN	QPTURB	BULK STANTON
1.0	-.054	1905	.00158	1.04	15.43	.2911	.000458	.012189
3.9	-.019	1901	.00480	1.05	11.79	.29[illegible]3	.000441	.009268
8.8	-.023	1889	.01397	1.07	8.13	.2817	.000443	.006482
11.9	-.015	1882	.01900	1.08	7.06	.2794	.000440	.005648
18.5	-.024	1868	.02977	1.08	6.46	.2821	.000444	.005203
26.1	-.022	1852	.04241	1.09	5.98	.2814	.000443	.004857
38.6	-.025	1827	.06358	1.09	5.64	.2822	.000444	.004643
53.9	-.023	1797	.09024	1.09	5.37	.2815	.000443	.004495
68.8	-.023	1769	.11709	1.09	5.20	.2814	.000443	.004422
85.7	-.021	1738	.14842	1.09	5.10	.2809	.000442	.004414
107.7	-.022	1701	.19065	1.08	5.19	.2811	.000442	.004599
116.3	.053	1687	.20763	1.09	4.39	.2611	.000411	.003917
120.1	-.035	1682	.21514	1.05	8.20	.2849	.000448	.007347

*** FRICTION DATA ***

POSITION (X/D)	TW/TB	BULK FRICTION FACTOR	BULK REYNOLDS
1.9	1.04	.0101	1903
6.8	1.06	.0107	1893
14.6	1.08	.0110	1876
29.9	1.09	.0112	1845
60.6	1.09	.0116	1785
91.4	1.09	.0117	1729

RUN 16 HELIUM FLOW= .70 LBS/HR TEST SECTION VOLTAGE=2.050 CURRENT=27.70 AMPS
INLET TEMPERATURE=68.30 F INLET PRESSURE=19.45 PSIA

*** HEAT TRANSFER DATA ***

POSITION (X/D)	HEAT LOSS (QP.L/QP.G)	BULK REYNOLDS	XPLUS	TW/TB	BULK NUSSELT	DIMENSIONLESS HEATING QPLAMIN	DIMENSIONLESS HEATING QPTURB	BULK STANTON
1.0	-.031	1890	.00159	1.08	15.31	.5758	.000909	.012193
3.0	.013	1881	.00485	1.10	11.26	.5505	.000870	.009009
8.8	.004	1857	.01421	1.14	7.71	.5551	.000877	.006242
11.9	.014	1845	.01938	1.16	6.61	.5498	.000868	.005387
18.5	.004	1818	.03059	1.17	5.90	.5554	.000877	.004883
26.1	.007	1789	.04394	1.18	5.31	.5532	.000874	.004464
38.6	.003	1743	.06674	1.18	4.87	.5554	.000877	.004204
53.9	.007	1691	.09607	1.18	4.50	.5531	.000874	.004006
68.9	.008	1644	.12628	1.18	4.28	.5526	.000873	.003924
85.8	.011	1596	.16201	1.17	4.13	.5508	.000870	.003900
107.8	.017	1539	.21118	1.16	4.06	.5473	.000865	.003975
116.5	.122	1518	.23113	1.14	3.95	.4961	.000784	.003915
120.3	-.044	1510	.23995	1.07	9.80	.5823	.000920	.009780

*** FRICTION DATA ***

POSITION (X/D)	TW/TB	BULK FRICTION FACTOR	BULK REYNOLDS
1.9	1.08	.0101	1886
6.8	1.12	.0117	1865
14.6	1.16	.0121	1834
29.9	1.18	.0124	1775
60.6	1.18	.0132	1669
91.5	1.17	.0133	1581

RUN 17 HELIUM FLOW= .63 LBS/HR TEST SECTION VOLTAGE=4.525 CURRENT=59.10 AMPS
INLET TEMPERATURE=70.53 F INLET PRESSURE=20.89 PSIA

*** HEAT TRANSFER DATA ***

POSITION (X/D)	HEAT LOSS (QP.L/QP.G)	BULK REYNOLDS	XPLUS	TW/TB	BULK NUSSELT	DIMENSIONLESS HEATING QPLAMIN	DIMENSIONLESS HEATING QPTURB	BULK STANTON
1.0	-.018	1659	.00182	1.33	14.40	2.6157	.004543	.013055
3.0	.044	1622	.00563	1.40	10.50	2.4602	.004273	.009734
8.8	.035	1531	.01729	1.52	7.01	2.4772	.004303	.006899
11.9	.048	1487	.02415	1.57	5.96	2.4465	.004249	.006040
18.6	[illegible]	1406	.03979	1.57	5.20	2.4656	.004282	.005577
26.2	.054	1323	.05977	1.55	4.60	2.4285	.004218	.005237
38.8	.055	1212	.09653	1.48	4.17	2.4233	.004209	.005179
54.3	.082	1107	.14780	1.41	3.81	2.3584	.004096	.005194
69.4	.102	1025	.20403	1.34	3.76	2.3152	.004021	.005523
86.6	.143	950	.27460	1.27	3.76	2.2293	.003872	.005958
109.0	.209	869	.37573	1.20	3.91	2.1053	.003657	.006745
118.1	.404	849	.41931	1.17	3.75	1.8115	.003146	.006650
121.9	.075	840	.43735	1.04	19.61	2.3707	.004118	.035164

*** FRICTION DATA ***

POSITION (X/D)	TW/TB	BULK FRICTION FACTOR	BULK REYNOLDS
1.9	1.36	.0090	1643
6.8	1.48	.0186	1561
14.6	1.57	.0206	1452
30.0	1.53	.0217	1285
61.0	1.38	.0234	1068
92.3	1.25	.0236	923

RUN 18   HELIUM FLOW= .50 LBS/HR   TEST SECTION VOLTAGE=5.320   CURRENT=45.80 AMPS
INLET TEMPERATURE=83.38 F   INLET PRESSURE=26.58 PSIA

*** HEAT TRANSFER DATA ***

POSITION (X/D)	HEAT LOSS (QP.L/QP.G)	BULK REYNOLDS	XPLUS	TW/TB	BULK NUSSELT	DIMENSIONLESS HEATING QPLAMIN	DIMENSIONLESS HEATING QPTURB	BULK STANTON

Invalid - wrong electrode connected.

*** FRICTION DATA ***

POSITION (X/D)	TW/TB	BULK FRICTION FACTOR	BULK REYNOLDS

Invalid - wrong electrode connected.

RUN 19 HELIUM FLOW= .41 LBS/HR TEST SECTION VOLTAGE=3.000 CURRENT=39.70 AMPS
INLET TEMPERATURE=82.62 F INLET PRESSURE=22.22 PSIA

*** HEAT TRANSFER DATA ***

POSITION (X/D)	HEAT LOSS (QP.L/QP.G)	BULK REYNOLDS	XPLUS	TW/TB	BULK NUSSELT	DIMENSIONLESS HEATING QPLAMIN	QPTURB	BULK STANTON
1.3	-.025	1053	.00286	1.19	10.79	1.1399	.003124	.015414
3.0	.026	1037	.00880	1.22	8.58	1.0821	.002965	.012449
8.8	.022	995	.02657	1.28	6.09	1.0857	.002975	.009218
11.9	.042	975	.03678	1.31	5.14	1.0646	.002917	.007950
18.5	.028	935	.05970	1.31	4.62	1.0787	.002956	.007438
26.2	.041	895	.08818	1.31	4.13	1.0643	.002916	.006950
38.7	.036	835	.13993	1.28	3.92	1.0691	.002930	.007085
54.1	.055	777	.20980	1.24	3.74	1.0491	.002875	.007260
69.1	.066	730	.28560	1.20	3.77	1.0377	.002843	.007795
86.1	.095	684	.37916	1.17	3.70	1.0089	.002765	.008139
108.3	.152	636	.51306	1.14	3.58	.9586	.002627	.008485
117.3	.489	622	.56864	1.11	3.30	.7411	.002031	.007991
121.1	-.001	616	.59253	1.00	*5.93	1.1061	.003031	.503871

*** FRICTION DATA ***

POSITION (X/D)	TW/TB	BULK FRICTION FACTOR	BULK REYNOLDS
1.9	1.20	.0128	1046
6.8	1.26	.0214	1009
14.6	1.31	.0221	957
30.0	1.30	.0233	876
60.8	1.22	.0267	755
91.8	1.16	.0266	671

RUN 21 HELIUM FLOW= .52 LBS/HR TEST SECTION VOLTAGE=3.756 CURRENT=49.00 AMPS
INLET TEMPERATURE=83.92 F INLET PRESSURE=26.65 PSIA

*** HEAT TRANSFER DATA ***

POSITION (X/D)	HEAT LOSS (QP.L/QP.G)	BULK REYNOLDS	XPLUS	TW/TB	BULK NUSSELT	DIMENSIONLESS HEATING QPLAMIN	QPTURB	BULK STANTON
1.0	-.012	1339	.00225	1.27	11.60	1.7245	.003699	.013029
3.0	.039	1315	.00694	1.31	9.14	1.6400	.003517	.010462
6.8	.034	1254	.02111	1.39	6.38	1.6466	.003532	.007662
11.9	.057	1223	.02933	1.43	5.30	1.6092	.003451	.006533
18.5	.042	1168	.04788	1.44	4.72	1.6316	.003499	.006094
26.2	.057	1109	.07116	1.43	4.19	1.6070	.003446	.005689
38.8	.054	1027	.11384	1.38	3.90	1.6104	.003454	.005716
54.2	.077	948	.17229	1.33	3.63	1.5739	.003376	.005769
69.3	.095	884	.23598	1.28	3.52	1.5475	.003319	.005992
86.3	.132	825	.31519	1.23	3.43	1.4950	.003206	.006269
108.6	.194	759	.42850	1.18	3.46	1.4166	.003038	.006821
117.7	.456	731	.47624	1.15	3.15	1.1593	.002486	.006369
121.5	.043	727	.49627	1.03	22.99	1.6232	.003481	.046971

*** FRICTION DATA ***

POSITION (X/D)	TW/TB	BULK FRICTION FACTOR	BULK REYNOLDS
1.9	1.28	.0100	1329
6.8	1.36	.0192	1274
14.6	1.44	.0192	1200
30.0	1.41	.0216	1082
60.9	1.31	.0245	918
92.1	1.22	.0239	808

RUN 22 HELIUM FLOW= .59 LBS/HR TEST SECTION VOLTAGE=4.351 CURRENT=56.80 AMPS
INLET TEMPERATURE=84.81 F INLET PRESSURE=25.24 PSIA

*** HEAT TRANSFER DATA ***

POSITION (X/D)	HEAT LOSS (QP.L/QP.G)	BULK REYNOLDS	XPLUS	TW/TB	BULK NUSSELT	DIMENSIONLESS HEATING QPLAMIN	QPTURB	BULK STANTON
1.0	-.019	1509	.00200	1.31	13.19	2.3134	.004405	.013155
3.0	.044	1476	.00619	1.38	9.73	2.1727	.004137	.009920
8.8	.032	1396	.01898	1.49	6.63	2.1970	.004184	.007157
11.9	.056	1357	.02645	1.54	5.47	2.1457	.004086	.006073
18.6	.042	1286	.04350	1.55	4.80	2.1722	.004136	.005622
26.2	.060	1210	.06535	1.53	4.21	2.1332	.004062	.005243
38.8	.061	1113	.10515	1.47	3.86	2.1300	.004056	.005230
54.3	.091	1018	.16069	1.39	3.57	2.0691	.003940	.005279
69.4	.112	944	.22142	1.33	3.49	2.0263	.003859	.005572
86.6	.162	878	.29743	1.27	3.41	1.9377	.003690	.005855
109.0	.234	804	.40617	1.20	3.55	1.8220	.003470	.006624
118.3	.451	786	.45350	1.16	3.44	1.5492	.002950	.006587
122.1	.079	778	.47288	1.04	20.11	2.0880	.003976	.038938

*** FRICTION DATA ***

POSITION (X/D)	TW/TB	BULK FRICTION FACTOR	BULK REYNOLDS
1.9	1.34	.0089	1495
6.8	1.46	.0187	1422
14.6	1.54	.0201	1327
30.0	1.51	.0230	1178
61.1	1.36	.0247	984
92.4	1.25	.0231	851

RUN 23 NITROGEN FLOW=8.65 LBS/HR TEST SECTION VOLTAGE=4.754 CURRENT=63.40 AMPS
INLET TEMPERATURE=76.87 F INLET PRESSURE=38.80 PSIA

*** HEAT TRANSFER DATA ***

POSITION (X/D)	HEAT LOSS (QP.L/QP.G)	BULK REYNOLDS	XPLUS	TW/TB	BULK NUSSELT	DIMENSIONLESS HEATING QPLAMIN	DIMENSIONLESS HEATING QPTURB	BULK STANTON
1.0	-.011	24725	.00011	1.32	*4.93	17.2780	.001913	.005987
3.0	.016	24438	.00035	1.37	84.87	16.8129	.001862	.004907
8.8	.01[illegible]	23705	.00105	1.46	63.11	16.8983	.001871	.003778
11.9	.017	23328	.00145	1.50	56.28	16.7765	.001858	.003432
18.5	.00[illegible]	22580	.00235	1.48	54.71	16.9871	.001881	.003463
26.2	.01[illegible]	21795	.00345	1.48	49.81	16.8835	.001870	.003282
38.8	.006	20657	.00542	1.45	46.15	16.9434	.001876	.003230
54.1	.009	19467	.00809	1.42	43.50	16.8910	.001871	.003251
69.1	.009	18476	.01094	1.38	41.48	16.8713	.001868	.003282
86.1	.013	17515	.01442	1.35	39.76	16.8071	.001861	.003330
108.3	.019	16469	.01932	1.32	37.45	16.6900	.001848	.003342
117.0	.09[illegible]	16121	.02134	1.30	35.18	15.6031	.001728	.003207
120.8	-.026	16000	.02220	1.12	*3.87	17.4825	.001936	.009540

*** FRICTION DATA ***

POSITION (X/D)	TW/TB	BULK FRICTION FACTOR	BULK REYNOLDS
1.9	1.34	.0059	24602
6.8	1.43	.0084	23952
14.6	1.49	.0078	23011
30.0	1.47	.0079	21429
60.8	1.40	.0082	19006
91.8	1.34	.0076	17233

RUN 24 NITROGEN FLOW=7.84 LBS/HR TEST SECTION VOLTAGE=5.680 CURRENT=74.80 AMPS
INLET TEMPERATURE=73.79 F INLET PRESSURE=38.96 PSIA

*** HEAT TRANSFER DATA ***

POSITION (X/D)	HEAT LOSS (QP,L/QP,G)	BULK REYNOLDS	XPLUS	TW/TB	BULK NUSSELT	DIMENSIONLESS HEATING QPLAMIN	QPTURB	BULK STANTON
1.0	-.008	22070	.00013	1.46	97.49	23.9115	.002935	.006245
3.0	.029	21698	.00040	1.54	75.92	23.0465	.002829	.004958
8.8	.022	20730	.00121	1.69	53.91	23.1683	.002844	.003709
11.9	.029	20259	.00168	1.73	47.57	22.9896	.002822	.003360
18.6	.017	19344	.00277	1.71	44.43	23.2603	.002855	.003307
26.3	.025	18420	.00413	1.69	40.22	23.0666	.002832	.003163
38.9	.022	17143	.00661	1.63	36.52	23.1170	.002838	.003108
54.3	.030	15879	.01003	1.56	33.54	22.9158	.002813	.003097
69.4	.034	14890	.01371	1.49	32.12	22.8174	.002801	.003172
86.5	.045	13954	.01823	1.43	30.76	22.5576	.002769	.003239
108.9	.061	12992	.02455	1.37	29.74	22.1883	.002724	.003353
117.9	.093	12664	.02723	1.34	29.31	21.5381	.002644	.003385
121.7	-.002	12563	.02831	1.13	90.06	23.6478	.002903	.010479

*** FRICTION DATA ***

POSITION (X/D)	TW/TB	BULK FRICTION FACTOR	BULK REYNOLDS
1.9	1.49	.0053	21910
6.8	1.64	.0086	21052
14.7	1.72	.0081	19873
30.1	1.67	.0082	18009
61.1	1.53	.0085	15416
92.3	1.42	.0079	13690

RUN 25 NITROGEN FLOW=3.38 LBS/HR TEST SECTION VOLTAGE=3.763 CURRENT=49.70 AMPS
INLET TEMPERATURE=79.19 F INLET PRESSURE=37.90 PSIA

*** HEAT TRANSFER DATA ***

POSITION (X/D)	HEAT LOSS (QP,L/QF,G)	BULK REYNOLDS	XPLUS	TW/TB	BULK NUSSELT	DIMENSIONLESS HEATING QPLAMIN	QPTURB	BULK STANTON
1.0	-.028	9468	.00030	1.35	55.41	10.7225	.003062	.008281
3.0	.036	9305	.00093	1.42	41.87	10.0525	.002870	.006383
8.8	.036	8887	.00282	1.55	28.70	10.0443	.002868	.004612
11.9	.045	8686	.00393	1.59	25.17	9.9472	.002840	.004151
18.6	.032	8293	.00645	1.58	22.84	10.0673	.002875	.003969
26.2	.045	7895	.00963	1.56	20.75	9.9403	.002838	.003810
38.8	.041	7349	.01542	1.51	19.04	9.9693	.002847	.003781
54.2	.060	6809	.02336	1.45	17.36	9.7814	.002793	.003741
69.3	.07[illegible]	6383	.03192	1.39	16.69	9.6886	.002767	.003842
86.4	.096	5991	.04236	1.34	15.79	9.4518	.002699	.003872
108.6	.133	5585	.05699	1.29	15.22	9.1341	.002608	.003993
117.6	.235	5450	.06311	1.26	14.37	8.3787	.002393	.003855
121.4	-.006	5405	.06564	1.07	69.38	10.4257	.002977	.018755

*** FRICTION DATA ***

POSITION (X/D)	TW/TB	BULK FRICTION FACTOR	BULK REYNOLDS
1.9	1.38	.0060	9398
6.8	1.51	.0099	9025
14.6	1.59	.0092	8519
30.0	1.54	.0090	7720
61.0	1.42	.0094	6611
92.1	1.33	.0088	5879

RUN 26 NITROGEN FLOW=1.78 LBS/HR TEST SECTION VOLTAGE=2.970 CURRENT=39.10 AMPS
INLET TEMPERATURE=80.17 F INLET PRESSURE=38.34 PSIA

*** HEAT TRANSFER DATA ***

POSITION (X/D)	HEAT LOSS (QP.L/QP.G)	BULK REYNOLDS	XPLUS	TW/TB	BULK NUSSELT	DIMENSIONLESS HEATING QPLAMIN	QPTURB	BULK STANTON
1.0	-.057	4931	.00058	1.33	36.90	6.8108	.003710	.010601
3.0	.050	4831	.00178	1.40	26.20	6.1097	.003328	.007705
8.8	.059	4588	.00548	1.54	17.03	6.0552	.003299	.005311
11.9	.072	4471	.00765	1.58	14.59	5.9747	.003255	.004688
18.6	.069	4249	.01262	1.60	12.36	5.9916	.003264	.004204
26.2	.101	4029	.01893	1.60	10.60	5.8127	.003167	.003825
38.8	.112	3734	.03044	1.57	8.98	5.7456	.003130	.003519
54.3	.181	3455	.04612	1.53	7.52	5.4061	.002945	.003196
69.4	.221	3242	.06292	1.47	6.92	5.2262	.002847	.003138
86.6	.299	3050	.08330	1.41	6.39	4.9077	.002673	.003077
109.0	.402	2857	.11156	1.34	6.01	4.5443	.002476	.003077
118.0	.542	2795	.12325	1.32	5.49	4.1282	.002249	.002866
121.8	.020	2773	.12811	1.06	39.75	6.2584	.003409	.020905

*** FRICTION DATA ***

POSITION (X/D)	TW/TB	BULK FRICTION FACTOR	BULK REYNOLDS
1.9	1.36	.0073	4888
6.8	1.49	.0127	4667
14.6	1.59	.0121	4376
30.0	1.59	.0116	3933
61.0	1.50	.0109	3354
92.4	1.39	.0096	2996

RUN 27   NITROGEN FLOW=1.23 LBS/HR   TEST SECTION VOLTAGE=2.420   CURRENT=31.70 AMPS
INLET TEMPERATURE=83.29 F   INLET PRESSURE=37.96 PSIA

*** HEAT TRANSFER DATA ***

POSITION (X/D)	HEAT LOSS (QP,L/QP,G)	BULK REYNOLDS	XPLUS	TW/TB	BULK NUSSELT	DIMENSIONLESS HEATING QPLAMIN	DIMENSIONLESS HEATING QPTURB	BULK STANTON
1.0	-.062	3376	.00084	1.29	26.91	4.4630	.003530	.011314
3.0	.056	3312	.00261	1.34	19.72	3.9652	.003137	.008475
8.8	.073	3157	.00798	1.44	13.17	3.8982	.003084	.005977
11.9	.093	3082	.01111	1.48	11.26	3.8249	.003026	.005251
18.5	.086	2940	.01824	1.50	9.55	3.8378	.003036	.004697
26.2	.127	2798	.02724	1.50	8.13	3.7046	.002930	.004222
38.8	.144	2605	.04357	1.50	6.70	3.6433	.002882	.003763
54.2	.25[illegible]	2424	.06565	1.49	5.26	3.3312	.002635	.003183
69.3	.316	2286	.08910	1.45	4.62	3.1572	.002497	.002968
86.4	.443	2163	.11736	1.40	4.07	2.8824	.002280	.002764
108.8	.588	2040	.15630	1.34	3.77	2.6170	.002070	.002706
118.3	.966	2001	.17295	1.31	3.17	2.1114	.001670	.002319
122.1	-.006	1986	.17980	1.08	24.62	4.1985	.003321	.018130

*** FRICTION DATA ***

POSITION (X/D)	TW/TB	BULK FRICTION FACTOR	BULK REYNOLDS
1.9	1.31	.0077	3348
6.8	1.41	.0142	3208
14.6	1.49	.0143	3021
30.0	1.50	.0133	2735
61.0	1.47	.0124	2359
92.2	1.39	.0105	2130

RUN 28 NITROGEN FLOW=1.43 LBS/HR TEST SECTION VOLTAGE=2.944 CURRENT=38.70 AMPS
INLET TEMPERATURE=79.90 F INLET PRESSURE=38.38 PSIA

*** HEAT TRANSFER DATA ***

POSITION (X/D)	HEAT LOSS (QP.L/QP.S)	BULK REYNOLDS	XPLUS	TW/TB	BULK NUSSELT	DIMENSIONLESS HEATING QPLAMIN	QPTURB.	BULK STANTON
1.0	-.070	3919	.00073	1.38	30.40	6.6920	.004522	.011013
3.0	.053	3825	.00226	1.45	21.47	5.9049	.003990	.007997
8.8	.072	3605	.00701	1.60	13.75	5.7953	.003916	.005478
11.9	.095	3501	.00982	1.64	11.57	5.6657	.003829	.004766
18.6	.101	3307	.01630	1.68	9.52	5.6340	.003807	.004175
26.3	.167	3123	.02454	1.68	7.75	5.3092	.003588	.003621
38.9	.209	2884	.03956	1.66	6.25	5.1147	.003456	.003182
54.4	.351	2668	.05990	1.61	4.95	4.5720	.003090	.002729
69.6	.441	2509	.08147	1.54	4.42	4.2850	.002896	.002586
86.9	.599	2370	.10746	1.47	3.96	3.8594	.002608	.002445
109.7	.752	2232	.14340	1.38	3.80	3.5192	.002378	.002481
119.6	.938	2184	.15941	1.34	3.59	3.1808	.002150	.002392
123.4	.048	2168	.16553	1.07	29.70	5.9027	.003989	.019923

*** FRICTION DATA ***

POSITION (X/D)	TW/TB	BULK FRICTION FACTOR	BULK REYNOLDS
1.9	1.41	.0072	3879
6.8	1.55	.0147	3677
14.7	1.66	.0141	3418
30.1	1.67	.0128	3045
61.2	1.58	.0122	2594
92.8	1.44	.0101	2332

RUN 29 NITROGEN FLOW=1.75 LBS/HR TEST SECTION VOLTAGE=3.085 CURRENT=40.70 AMPS
INLET TEMPERATURE=76.78 F INLET PRESSURE=17.40 PSIA

*** HEAT TRANSFER DATA ***

POSITION (X/D)	HEAT LOSS (QP,L/QP,G)	BULK REYNOLDS	XPLUS	TW/TB	BULK NUSSELT	DIMENSIONLESS HEATING QPLAMIN	QPTURB	BULK STANTON
1.0	-.066	4836	.00059	1.38	34.23	7.4032	.004064	.010036
3.0	.042	4731	.00183	1.44	24.96	6.6732	.003664	.007506
8.8	.056	4476	.00563	1.59	16.28	6.5768	.003611	.005214
11.9	.076	4354	.00788	1.64	13.79	6.4491	.003541	.004556
18.6	.074	4126	.01303	1.67	11.51	6.4540	.003543	.004040
26.3	.122	3903	.01959	1.67	9.55	6.1766	.003391	.003561
38.9	.148	3611	.03153	1.66	7.80	6.0274	.003309	.003163
54.3	.251	3339	.04781	1.61	6.24	5.5245	.003033	.002745
69.5	.327	3137	.06511	1.56	5.45	5.2023	.002856	.002551
86.7	.469	2961	.08596	1.50	4.72	4.6972	.002579	.002337
109.4	.624	2787	.11468	1.42	4.30	4.2438	.002330	.002252
119.3	.774	2726	.12764	1.39	4.09	3.8849	.002133	.002187
123.1	.038	2706	.13258	1.12	22.93	6.6633	.003658	.012348

*** FRICTION DATA ***

POSITION (X/D)	TW/TB	BULK FRICTION FACTOR	BULK REYNOLDS
1.9	1.41	.0067	4791
6.8	1.54	.0131	4559
14.6	1.65	.0128	4257
30.1	1.66	.0117	3809
61.1	1.59	.0109	3245
92.6	1.48	.0090	2913

RUN 30 NITROGEN FLOW=2.14 LBS/HR TEST SECTION VOLTAGE=3.434 CURRENT=45.20 AMPS
INLET TEMPERATURE=76.33 F INLET PRESSURE=22.78 PSIA

*** HEAT TRANSFER DATA ***

POSITION (X/D)	HEAT LOSS (QP.L/QP.G)	BULK REYNOLDS	XPLUS	TW/TB	BULK NUSSELT	DIMENSIONLESS HEATING QPLAMIN	DIMENSIONLESS HEATING QPTURB	BULK STANTON
1.0	-.047	5894	.00048	1.41	38.50	9.0178	.004063	.009260
3.0	.041	5764	.00150	1.48	28.61	8.2523	.003718	.007059
8.8	.052	5449	.00463	1.63	18.89	8.1566	.003675	.004970
11.9	.070	5297	.00648	1.67	16.07	8.0100	.003609	.004366
18.6	.066	5014	.01073	1.70	13.58	8.0331	.003619	.003922
26.3	.107	4739	.01615	1.69	11.40	7.7280	.003482	.003506
38.9	.123	4376	.02604	1.66	9.64	7.6107	.003429	.003227
54.4	.191	4035	.03960	1.59	8.23	7.1716	.003231	.002997
69.6	.227	3779	.05410	1.51	7.75	6.9556	.003134	.003013
86.9	.29[illegible]	3548	.07176	1.42	7.52	6.6104	.002978	.003107
109.6	.349	3312	.09648	1.32	7.96	6.3169	.002846	.003503
119.5	.479	3229	.10770	1.27	7.90	5.7607	.002595	.003558
123.3	.029	3202	.11192	1.05	58.59	8.3076	.003743	.026583

*** FRICTION DATA ***

POSITION (X/D)	TW/TB	BULK FRICTION FACTOR	BULK REYNOLDS
1.9	1.44	.0065	5838
6.8	1.58	.0124	5551
14.7	1.69	.0114	5177
30.1	1.68	.0109	4622
61.2	1.55	.0100	3916
92.7	1.39	.0087	3482

RUN 31 NITROGEN FLOW=2.12 LBS/HR TEST SECTION VOLTAGE=2.865 CURRENT=37.80 AMPS
INLET TEMPERATURE=76.78 F INLET PRESSURE=22.84 PSIA

*** HEAT TRANSFER DATA ***

POSITION (X/D)	HEAT LOSS (QP.L/QP.G)	BULK REYNOLDS	XPLUS	TW/TB	BULK NUSSELT	DIMENSIONLESS HEATING QPLAMIN	DIMENSIONLESS HEATING QPTURB	BULK STANTON
1.0	-.038	5939	.00048	1.30	37.71	6.3347	.002870	.008984
3.0	.040	5844	.00147	1.35	28.99	5.8568	.002654	.007034
8.8	.045	5603	.00448	1.45	20.26	5.8282	.002641	.005180
11.9	.059	5486	.00621	1.49	17.63	5.7474	.002604	.004600
18.5	.046	5256	.01016	1.50	15.66	5.8129	.002634	.004288
26.2	.066	5023	.01510	1.49	13.90	5.7038	.002585	.004006
38.8	.060	4698	.02406	1.46	12.71	5.7292	.002596	.003944
54.2	.086	4374	.03628	1.40	11.67	5.5889	.002532	.003911
69.2	.098	4117	.04938	1.35	11.29	5.5247	.002503	.004027
86.2	.136	3878	.06537	1.31	10.48	5.3366	.002418	.003970
108.5	.194	3628	.08774	1.27	9.92	5.0921	.002307	.004010
117.4	.463	3551	.09691	1.24	8.34	4.1418	.001877	.003444
121.2	-.022	3523	.10079	1.07	46.06	6.2040	.002811	.019152

*** FRICTION DATA ***

POSITION (X/D)	TW/TB	BULK FRICTION FACTOR	BULK REYNOLDS
1.9	1.32	.0068	5898
6.8	1.42	.0110	5683
14.6	1.49	.0104	5389
30.0	1.48	.0102	4919
53.9	1.38	.0103	4254
92.0	1.30	.0096	3808

RUN 32 NITROGEN FLOW=1.45 LBS/HR TEST SECTION VOLTAGE=2.338 CURRENT=30.80 AMPS
INLET TEMPERATURE=75.88 F INLET PRESSURE=22.84 PSIA

*** HEAT TRANSFER DATA ***

POSITION (X/D)	HEAT LOSS (QP.L/QP.G)	BULK REYNOLDS	XPLUS	TW/TB	BULK NUSSELT	DIMENSIONLESS HEATING QPLAMIN	DIMENSIONLESS HEATING QPTURB	BULK STANTON
1.0	-.051	4058	.00070	1.26	29.87	4.2874	.002837	.010420
3.0	.048	3995	.00215	1.30	22.50	3.8829	.002569	.007991
8.8	.058	3836	.00654	1.39	15.53	3.8430	.002543	.005777
11.9	.070	3759	.00906	1.42	13.54	3.7986	.002514	.005155
18.5	.066	3606	.01479	1.44	11.78	3.8304	.002535	.004701
26.2	.087	3453	.02135	1.44	10.22	3.7336	.002471	.004282
38.8	.084	3236	.03489	1.42	9.07	3.7429	.002477	.004082
54.1	.124	3021	.05246	1.38	8.05	3.6080	.002387	.003902
69.2	.145	2851	.07123	1.35	7.56	3.5383	.002341	.003892
86.2	.205	2693	.09427	1.32	6.78	3.3611	.002224	.003699
108.4	.293	2539	.12581	1.28	6.07	3.1283	.002070	.003520
117.3	.616	2481	.13876	1.26	4.87	2.5022	.001656	.002882
121.1	-.048	2460	.14434	1.05	44.98	4.2556	.002816	.026815

*** FRICTION DATA ***

POSITION (X/D)	TW/TB	BULK FRICTION FACTOR	BULK REYNOLDS
1.9	1.28	.0077	4031
6.8	1.36	.0128	3889
14.6	1.43	.0121	3695
30.0	1.44	.0114	3383
60.9	1.37	.0111	2941
91.9	1.31	.0101	2648

RUN 33   NITROGEN FLOW=1.10 LBS/HR   TEST SECTION VOLTAGE=2.027   CURRENT=26.40 AMPS
INLET TEMPERATURE=79.01 F   INLET PRESSURE=23.26 PSIA

*** HEAT TRANSFER DATA ***

POSITION (X/D)	HEAT LOSS (QP,L/QP,G)	BULK REYNOLDS	XPLUS	TW/TB	BULK NUSSELT	DIMENSIONLESS HEATING QPLAMIN	DIMENSIONLESS HEATING QPTURB	BULK STANTON
1.0	-.059	3056	.00093	1.22	25.83	3.1770	.002797	.011973
3.0	.073	3009	.00286	1.26	18.52	2.7843	.002451	.008735
8.8	.081	2895	.00866	1.34	12.65	2.7638	.002433	.006238
11.9	.095	2839	.01200	1.37	10.97	2.7266	.002400	.005527
18.5	.084	2728	.01954	1.40	9.48	2.7539	.002424	.005000
26.2	.117	2616	.02895	1.41	8.09	2.6709	.002351	.004471
38.7	.119	2458	.04589	1.41	6.85	2.6633	.002345	.004057
54.1	.19[illegible]	2302	.06880	1.40	5.55	2.5023	.002203	.003527
69.1	.237	2180	.09309	1.38	4.84	2.4045	.002117	.003260
86.2	.340	2067	.12250	1.36	4.13	2.2190	.001954	.002936
108.4	.456	1953	.16312	1.32	3.74	2.0408	.001797	.002815
117.3	1.036	1920	.17948	1.30	2.69	1.4592	.001285	.002059
121.1	-.066	1906	.18661	1.07	23.77	3.1890	.002808	.018314

*** FRICTION DATA ***

POSITION (X/D)	TW/TB	BULK FRICTION FACTOR	BULK REYNOLDS
1.9	1.24	.0083	3036
6.8	1.32	.0139	2933
14.6	1.38	.0135	2792
30.0	1.41	.0127	2565
60.8	1.39	.0126	2245
91.9	1.35	.0112	2036

RUN 34 NITROGEN FLOW=1.45 LBS/HR TEST SECTION VOLTAGE=1.860 CURRENT=24.80 AMPS
INLET TEMPERATURE=74.10 F INLET PRESSURE=23.23 PSIA

*** HEAT TRANSFER DATA ***

POSITION (X/D)	HEAT LOSS (QP.L/QP.G)	BULK REYNOLDS	XPLUS	TW/TB	BULK NUSSELT	DIMENSIONLESS HEATING QPLAMIN	DIMENSIONLESS HEATING QPTURB	BULK STANTON
1.0	-.043	4088	.00069	1.19	26.95	2.7535	.001823	.009316
3.0	.016	4046	.00212	1.21	22.48	2.5934	.001717	.007865
8.8	.038	3937	.00634	1.26	16.25	2.5380	.001680	.005864
11.9	.051	3881	.00873	1.28	14.37	2.5046	.001658	.005273
18.5	.036	3770	.01404	1.29	13.07	2.5365	.001679	.004958
26.2	.048	3653	.02057	1.29	12.10	2.5119	.001663	.004755
38.7	.041	3480	.03213	1.28	11.25	2.5266	.001673	.004669
54.0	.060	3297	.04762	1.26	10.43	2.4804	.001642	.004598
69.0	.068	3144	.06407	1.23	10.00	2.4613	.001629	.004664
85.9	.093	2996	.08405	1.22	9.28	2.4040	.001591	.004540
108.0	.123	2834	.11196	1.19	9.05	2.3378	.001548	.004688
116.7	1.222	2790	.12294	1.18	4.53	1.1816	.000782	.002383
120.6	-.115	2771	.12783	1.04	56.83	2.9688	.001965	.030133

*** FRICTION DATA ***

POSITION (X/D)	TW/TB	BULK FRICTION FACTOR	BULK REYNOLDS
1.9	1.20	.0070	4070
6.8	1.24	.0103	3974
14.6	1.29	.0114	3834
29.9	1.28	.0103	3597
60.7	1.25	.0108	3226
91.6	1.21	.0109	2951

RUN 35 NITROGEN FLOW=1.44 LBS/HR TEST SECTION VOLTAGE=2.150 CURRENT=28.40 AMPS
INLET TEMPERATURE=74.55 F INLET PRESSURE=23.22 PSIA

*** HEAT TRANSFER DATA ***

POSITION (X/D)	HEAT LOSS (QP.L/QP.G)	BULK REYNOLDS	XPLUS	TW/TB	BULK NUSSELT	DIMENSIONLESS HEATING QPLAMIN	QPTURB	BULK STANTON
1.0	-.045	4025	.00070	1.23	28.66	3.6502	.002440	.010071
3.0	.036	3971	.00216	1.26	22.38	3.3512	.002240	.007988
8.8	.051	3833	.00653	1.34	15.69	3.3042	.002209	.005833
11.9	.064	3763	.00903	1.36	13.73	3.2619	.002181	.005210
18.5	.052	3629	.01465	1.38	12.14	3.2983	.002205	.004801
26.2	.073	3489	.02165	1.38	10.73	3.2327	.002161	.004437
38.7	.066	3289	.03420	1.36	9.78	3.2513	.002174	.004319
54.1	.094	3086	.05121	1.33	8.95	3.1649	.002116	.004238
69.1	.108	2921	.06938	1.29	8.57	3.1242	.002089	.004305
86.1	.146	2766	.09143	1.27	7.91	3.0135	.002015	.004201
108.2	.206	2601	.12228	1.23	7.36	2.8655	.001916	.004157
117.0	.872	2554	.13463	1.22	4.75	1.8463	.001234	.002733
120.8	-.078	2536	.13997	1.05	45.87	3.7562	.002511	.026565

*** FRICTION DATA ***

POSITION (X/D)	TW/TB	BULK FRICTION FACTOR	BULK REYNOLDS
1.9	1.24	.0076	4002
6.8	1.31	.0122	3879
14.6	1.37	.0118	3707
30.0	1.38	.0107	3425
60.8	1.31	.0111	3009
91.8	1.26	.0108	2720

RUN 36 NITROGEN FLOW=1.09 LBS/HR TEST SECTION VOLTAGE=1.684 CURRENT=22.20 AMPS
INLET TEMPERATURE=74.55 F INLET PRESSURE=23.29 PSIA

*** HEAT TRANSFER DATA ***

POSITION (X/D)	HEAT LOSS (QP.L/QP.G)	BULK REYNOLDS	XPLUS	TW/TB	BULK NUSSELT	DIMENSIONLESS HEATING QPLAMIN	QPTURB	BULK STANTON
1.0	-.055	3081	.00092	1.18	23.29	2.2551	.001978	.010688
3.0	.047	3048	.00282	1.20	18.17	2.0446	.001793	.008442
8.8	.056	2962	.00843	1.26	12.94	2.0158	.001768	.006214
11.9	.077	2918	.01162	1.28	11.25	1.9775	.001734	.005496
18.5	.066	2831	.01871	1.30	10.05	2.0082	.001761	.005077
26.2	.076	2740	.02745	1.30	8.96	1.9730	.001730	.004699
38.7	.071	2606	.04294	1.30	8.05	1.9859	.001742	.004466
54.0	.105	2467	.06373	1.29	7.01	1.9232	.001687	.004133
69.0	.124	2351	.08576	1.28	6.32	1.8906	.001658	.003928
86.0	.179	2241	.11245	1.28	5.34	1.8003	.001579	.003494
108.1	.261	2124	.14946	1.27	4.52	1.6825	.001476	.003127
116.8	1.937	2094	.16392	1.26	1.89	.7221	.000633	.001328
120.6	-.146	2081	.17039	1.07	23.11	2.4882	.002182	.016325

*** FRICTION DATA ***

POSITION (X/D)	TW/TB	BULK FRICTION FACTOR	BULK REYNOLDS
1.9	1.19	.0086	3067
6.8	1.24	.0130	2991
14.6	1.29	.0129	2881
29.9	1.30	.0120	2697
60.7	1.28	.0122	2413
91.7	1.27	.0113	2209

RUN 37 NITROGEN FLOW=1.26 LBS/HR TEST SECTION VOLTAGE=1.733 CURRENT=22.90 AMPS
INLET TEMPERATURE=76.33 F INLET PRESSURE=23.18 PSIA

*** HEAT TRANSFER DATA ***

POSITION (X/D)	HEAT LOSS (QP.L/QP.G)	BULK REYNOLDS	XPLUS	TW/TB	BULK NUSSELT	DIMENSIONLESS HEATING QPLAMIN	QPTURB	BULK STANTON
1.0	-.045	3545	.00080	1.18	24.65	2.3556	.001800	.009829
3.0	.032	3510	.00245	1.20	19.90	2.1805	.001666	.008030
8.8	.052	3417	.00730	1.25	14.21	2.1365	.001633	.005910
11.9	.067	3370	.01005	1.27	12.50	2.1060	.001610	.005284
18.5	.051	3276	.01616	1.29	11.29	2.1372	.001633	.004928
26.2	.068	3177	.02365	1.29	10.20	2.1041	.001608	.004611
38.7	.058	3030	.03689	1.28	9.49	2.1222	.001622	.004522
54.0	.081	2875	.05460	1.26	8.76	2.0768	.001587	.004426
69.0	.096	2745	.07338	1.24	8.35	2.0581	.001573	.004438
85.9	.121	2618	.09615	1.23	7.61	2.0010	.001529	.004258
108.0	.164	2480	.12789	1.21	6.97	1.9257	.001472	.004127
116.7	1.848	2445	.14021	1.21	2.75	.7868	.000601	.001649
120.5	-.138	2430	.14572	1.04	41.42	2.6025	.001989	.025038

*** FRICTION DATA ***

POSITION (X/D)	TW/TB	BULK FRICTION FACTOR	BULK REYNOLDS
1.9	1.18	.0081	3530
6.8	1.23	.0121	3448
14.6	1.28	.0117	3330
29.9	1.29	.0108	3130
60.7	1.25	.0114	2814
91.6	1.22	.0111	2580

RUN 38 NITROGEN FLOW=1.26 LBS/HR TEST SECTION VOLTAGE=2.093 CURRENT=27.30 AMPS
INLET TEMPERATURE=76.55 F INLET PRESSURE=23.21 PSIA

HEAT TRANSFER DATA

POSITION (X/D)	HEAT LOSS (QP.L/QP.G)	BULK REYNOLDS	XPLUS	TW/TB	BULK NUSSELT	DIMENSIONLESS HEATING QPLAMIN	QPTURB	BULK STANTON
1.0	-.044	3518	.00081	1.24	25.62	3.3718	.002570	.010315
3.0	.053	3468	.00248	1.27	19.87	3.0607	.002333	.008128
8.8	.062	3343	.00750	1.34	14.13	3.0328	.002312	.006031
11.9	.087	3281	.01037	1.37	12.14	2.9631	.002259	.005290
18.5	.072	3161	.01685	1.39	10.67	3.0024	.002288	.004851
26.2	.097	3036	.02491	1.39	9.33	2.9324	.002235	.004437
36.7	.093	2860	.03940	1.38	8.26	2.9414	.002242	.004201
54.1	.136	2681	.05902	1.36	7.14	2.8281	.002156	.003897
69.1	.168	2539	.07988	1.34	6.32	2.7495	.002096	.003655
86.1	.251	2406	.10516	1.34	5.24	2.5659	.001956	.003203
108.3	.367	2271	.14013	1.31	4.41	2.3462	.001788	.002855
117.1	.843	2231	.15422	1.30	3.22	1.7389	.001325	.002119
120.9	-.065	2215	.16032	1.08	24.23	3.4354	.002619	.016059

FRICTION DATA

POSITION (X/D)	TW/TB	BULK FRICTION FACTOR	BULK REYNOLDS
1.9	1.25	.0076	3497
6.8	1.31	.0128	3385
14.6	1.38	.0124	3231
30.0	1.39	.0112	2980
60.8	1.35	.0116	2615
91.8	1.33	.0109	2370

RUN 39 NITROGEN FLOW=1.72 LBS/HR TEST SECTION VOLTAGE=2.816 CURRENT=36.80 AMPS
INLET TEMPERATURE=79.01 F INLET PRESSURE=17.40 PSIA

HEAT TRANSFER DATA

POSITION (X/D)	HEAT LOSS (QP.L/QP.G)	BULK REYNOLDS	XPLUS	TW/TB	BULK NUSSELT	DIMENSIONLESS HEATING QPLAMIN	QPTURB	BULK STANTON
1.0	-.044	4763	.00060	1.33	32.84	6.0299	.003382	.009772
3.0	.048	4675	.00185	1.38	24.82	5.5010	.003086	.007544
8.8	.061	4458	.00564	1.49	16.75	5.4288	.003045	.005376
11.9	.076	4353	.00786	1.53	14.38	5.3402	.002996	.004742
18.5	.070	4152	.01290	1.55	12.32	5.3761	.003016	.004285
26.2	.104	3951	.01928	1.56	10.48	5.2072	.002921	.003851
38.8	.109	3677	.03085	1.54	9.01	5.1786	.002905	.003583
54.2	.170	3414	.04661	1.50	7.59	4.9023	.002750	.003264
69.3	.208	3210	.06348	1.45	6.93	4.7473	.002663	.003174
86.4	.285	3026	.08391	1.40	6.28	4.4572	.002500	.003046
108.8	.392	2840	.11221	1.34	5.74	4.1131	.002307	.002961
117.8	.583	2780	.12397	1.32	5.10	3.6160	.002028	.002685
121.6	.008	2759	.12886	1.09	29.54	5.6934	.003194	.015652

FRICTION DATA

POSITION (X/D)	TW/TB	BULK FRICTION FACTOR	BULK REYNOLDS
1.9	1.35	.0071	4725
6.8	1.45	.0128	4528
14.6	1.54	.0121	4266
30.0	1.55	.0113	3862
61.0	1.48	.0111	3319
92.2	1.38	.0098	2975

RUN 40 HELIUM FLOW=1.71 LBS/HR TEST SECTION VOLTAGE=6.101 CURRENT=80.40 AMPS
INLET TEMPERATURE=76.33 F INLET PRESSURE=26.15 PSIA

*** HEAT TRANSFER DATA ***

POSITION (X/D)	HEAT LOSS (QP,L/QP,G)	BULK REYNOLDS	XPLUS	TW/TB	BULK NUSSELT	DIMENSIONLESS HEATING QPLAMIN	QPTURB	BULK STANTON
1.0	-.003	4553	.00066	1.31	29.23	4.6597	.003022	.009657
3.0	.029	4483	.00203	1.39	21.50	4.5136	.002927	.007212
8.8	.015	4299	.00615	1.52	14.94	4.5700	.002964	.005230
11.9	.023	4205	.00853	1.58	12.57	4.5308	.002938	.004499
18.5	.013	4026	.01388	1.60	10.96	4.5719	.002965	.004102
26.2	.020	3846	.02055	1.63	9.25	4.5410	.002945	.003626
38.8	.017	3586	.03259	1.63	7.81	4.5465	.002949	.003280
54.2	.028	3320	.04918	1.62	6.45	4.4910	.002913	.002927
69.3	.040	3114	.06711	1.61	5.56	4.4364	.002877	.002691
86.4	.061	2914	.08938	1.57	4.93	4.3400	.002815	.002547
108.9	.087	2704	.12127	1.50	4.63	4.2333	.002745	.002578
118.0	.115	2631	.13517	1.46	4.56	4.1259	.002676	.002612
121.8	.010	2610	.14069	1.23	10.14	4.5664	.002961	.005856

*** FRICTION DATA ***

POSITION (X/D)	TW/TB	BULK FRICTION FACTOR	BULK REYNOLDS
1.9	1.35	.0100	4523
6.8	1.48	.0137	4360
14.6	1.59	.0132	4130
30.0	1.63	.0126	3764
61.0	1.62	.0128	3225
92.2	1.55	.0121	2857

APPENDIX E

USE OF SCANNING ELECTRON MICROSCOPE TO EXAMINE HEAT TRANSFER SURFACES

K. R. Perkins[1] and D. M. McEligot[2]

In convective heat transfer experiments within small diameter commercial tubing, surface roughness can have a significant effect in turbulent flow, even when the surface is carefully prepared. The magnitude of this roughness effect depends on the ratio of roughness height to hydraulic diameter. In general, the roughness elements are not homogeneous in either size or distribution, and the roughness is usually categorized in terms of a relative roughness ratio, (ϵ/D_h), suggested by Nikuradse [1]. In this case ϵ must be defined as an "equivalent sand grain diameter" as given by Moody [2]. The value of ϵ will depend on the size, shape, flow orientation, and distribution of the actual elements. Typically, to avoid the problem of accurately describing the detailed texture of the surface, adiabatic friction factor measurements are conducted and the results are compared to the so-called Moody diagram in order to obtain the equivalent sand grain roughness. If one has complete faith in his measurements and covers a wide range of Reynolds numbers, this approach is quite reasonable. However, in many cases the investigator is limited in flow range and would like to use the adiabatic results to

---

[1]Research Assistant

[2]Professor

verify his equipment performance. If the adiabatic results are used to determine effective roughness, other effects, due to measurement error, may thereby be hidden. Further, for the design engineer, results of previous experiments will not be useful unless he knows a priori that the surface roughness has an identical character to the previous studies. From either standpoint, it is preferable to have a good surface characterization which is established independently from the experiment.

In industrial applications, the surface roughness is often measured by means of a profilometer. In typical practice, its conical tracer has a radius of curvature of about 0.0005 inches (0.0013 cm). As shown schematically in Fig. 1, this instrument will have the same response for a large variety of roughness elements with identical pitch when the elements are considerably smaller than the radius of the tracer point. Further, the vertical displacement of the tracer point can be very much smaller than the depth of the roughness elements if this situation occurs. For an idealized two-dimensional case as shown in Figs. 1a and 1b, the maximum displacement of the tracer point is given by

$$\frac{\Delta y}{r} = 1 - \sqrt{1 - \left(\frac{1}{1-R/r}\right)}$$

or, under a small angle approximation,

$$\frac{\Delta y}{r} \approx \frac{1}{2} \quad \frac{r}{R}$$

Thus, for a cylindrical roughness element of the order of 100 μin. ($\sim$ 0.0002 cm), the displacement would be approximately 10 μin. ($\sim$0.00002 cm). This method is clearly unsatisfactory if one is interested in determining the depth of roughness elements of smaller size than the tracer point. More importantly, a profilometer is almost useless in characterizing the distribution, orientation and shape of most roughness elements.

The optical microscope can be used to obtain some information concerning surface roughness. However, in order to examine surfaces with roughness on the scale of 100 μin. ($\sim$0.0002 cm), it is necessary to use magnifications of about 1000x. At these magnifications the depth of focus is so short that the shape of the roughness element usually is not clear. Only the outline of each element is visible and one cannot determine from the image whether a given outline represents a cavity, a projection or simply a discoloration. Such views will give a measure of the spacing, orientation and outline shape of the roughness elements if they are not simply discolorations, but cannot measure height or determine shape completely. Often simple measurements of the shape outlines are taken to be the size of roughness but this assumption is obviously in error unless the roughness elements happen to be spherical. It is possible to obtain order of magnitude estimates of the height (or depth) of roughness elements by calibrating the microscope's mechanical focus mechanism and then measuring the travel required to focus on the peaks of the projections, after having focused on the troughs of the cavities. However, from an examination of a Moody diagram [2], it is evident that better resolution is necessary if one is to expect accurate results; at $Re_{D_h} = 10^4$ and $\epsilon/D_h \approx 0.002$, doubling the roughness size leads to a 10% increase in friction factor but the difference in depth may not be discerned with the optical method. Additionally, the shape in the vertical plane may be important [1] and it can not be readily determined optically.

The scanning electron microscope offers great potential as a tool for heat transfer surface characterization. Its extremely long depth of field overcomes the objections of the above methods. Shown in Fig. 2 are several photographs of surfaces being used for measurement of convective heat transfer coefficients in small non-circular ducts. The material is Inconel alloy 600 described by the manufacturer as having clean, bright, uniform outside and inside surfaces. It was temper-annealed before forming by extrusion. The inside surface is normally described by the manufacturer as having a 125 μin. RMS maximum surface roughness. Photographs are obtained with a Polaroid camera mounted on the video display of a Cambridge "Stereoscan 600" scanning electron microscope.

The two photographs on the left are at successively higher magnifications with a sample of the test section material still in the "as received" condition. The direction of the drawing and, hence, the flow direction in the tube are approximately in the vertical direction on the picture. While the contrast is not optimized, a number of ridges are visible in the flow direction. In the lower photograph, the region around one of the ridges has been magnified by another order of 10. The contrast is better here; one large ridge along the right-hand side is quite evident and a smaller, more jagged one appears down the center of the figure. By tilting the sample holder through five degrees, another photograph of the same view was obtained. Thus, it is possible to obtain three dimensional effects. By examining the two pictures in a stereoscopic viewer it is possible to assess the size, shape, orientation and distribution of the roughness elements. It should be noted that the angle between views must be small for the purpose of visualization, but in order to make three-dimensional measurements the angle between views should be larger. For the surfaces shown, the roughness elements are essentially oriented vertically with respect to the surface. Thus, only one picture is necessary to obtain the required measurements as long as the viewing angle is substantially off the perpendicular. In this particular case, with the surface oriented at an angle of 46° for the left-hand photos, trigonometric calculations indicate:

1. Scattered and irregularly shaped roughness elements as high as 3 microns.
2. Randomly spaced ridges about 2 to 3 microns in height, 4 to 5 microns in width, 5 to 10 microns in length and typically spaced about 5 microns apart.

Thus, the surface is comparable to longitudinally-finned tubing in some respects.

If the same material is heated in air, more illuminating pictures are obtained. The two figures on the right-hand side of the plate show views of the inner surface of the test section used by Battista and H. C. Perkins [3]. While the detailed temperature-time history was not recorded for this particular specimen, it has been estimated from memory that it was cycled from room temperature to approximately $1700^{\circ}R$ a number of times. The total heating time was probably of the order of several weeks. Heating experiments were conducted with pressurized air flowing through the tube. Despite the difference in contrast, it seems reasonably clear that the two photographs at magnifications of 700x show markedly different surface textures. One could quite readily characterize the heated surface as being represented by a "sand grain" type of roughness. Due to press of time, no stereoscopic photographs were taken of this sample, but it appears reasonable to claim that the depth dimension and the horizontal dimensions of these surface elements are approximately the same. Typical dimensions then would be about 7 microns (300 μin.). Since the hydraulic diameter of this test section was approximately 0.1

inches (0.25 cm) the relative roughness would be 0.003. From another assessment of the photographs, the typical spacing is found to be about 25 microns (1,000 μin.). Comparing these values to Schlichting's measurements [1], at this spacing we would expect the "equivalent sand grain roughness" to be about the same as our measurements of the roughness. However, Schlichting's results show significant variation with spacing in this range.

A scanning electron microscope was used mainly for order-of-magnitude measurements in the present study. Further, only a few measurements were possible due to the limited time the equipment was available. However, it seems clear that the scanning electron microscope offers considerable potential for more complete characterization of the texture of the surfaces employed in convective heat transfer applications. By using electronic signal processing, it is likely that useful measurements of the size spectra could be readily recorded and reduced. The improved characterization of the shape is also valuable.

ACKNOWLEDGMENT

The authors are particularly grateful to Mssrs. C. E. Birgensmith and R. P. Jernigan of Kent Cambridge Scientific, Inc. who graciously donated time on their equipment.

REFERENCES

1. H. SCHLICHTING, Boundary Layer Theory, 4th ed., McGraw-Hill, New York (1960).
2. L. F. MOODY, Friction factors for pipe flow, Trans. A.S.M.E., 66, 671 (1944).
3. E. BATTISTA and H. C. PERKINS, Turbulent heat and momentum transfer in a square duct with moderate property variations, Int. J. Heat Mass Transfer, 13, 1063-1065 (1970).

Figure Captions

1. Examples of surfaces causing identical profilometer point displacement, Δy, when $R >> r$.

2. Scanning electron microscope comparison of a fresh surface (left) with surface after use in moderate temperature convective heat transfer experiment (right). In upper photographs, small black rectangle is 20 μ across, while in lower two it represents 2 μ.

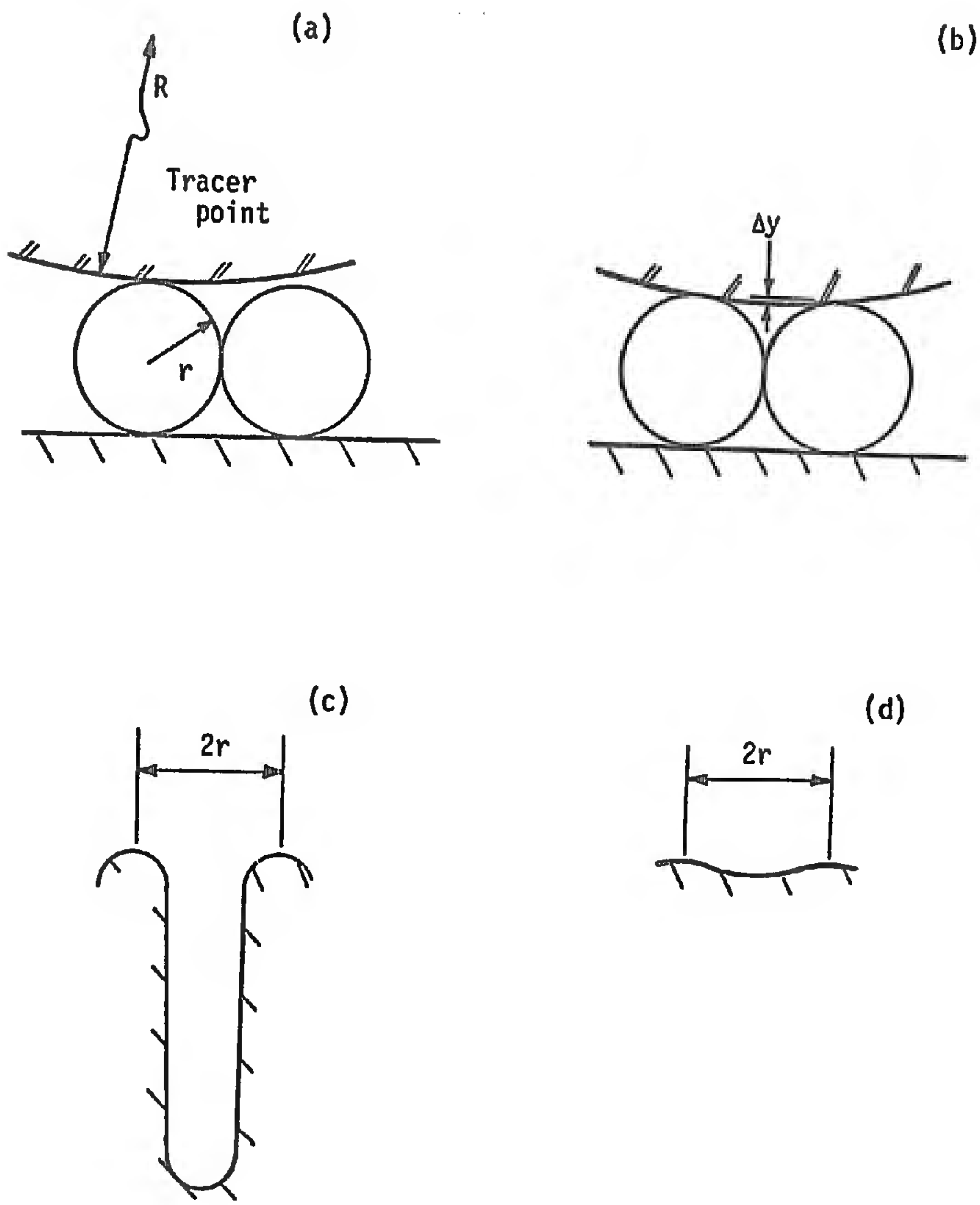

Figure 1. Examples of surfaces causing identical profilometer point displacement, Δy, when $R >> r$.

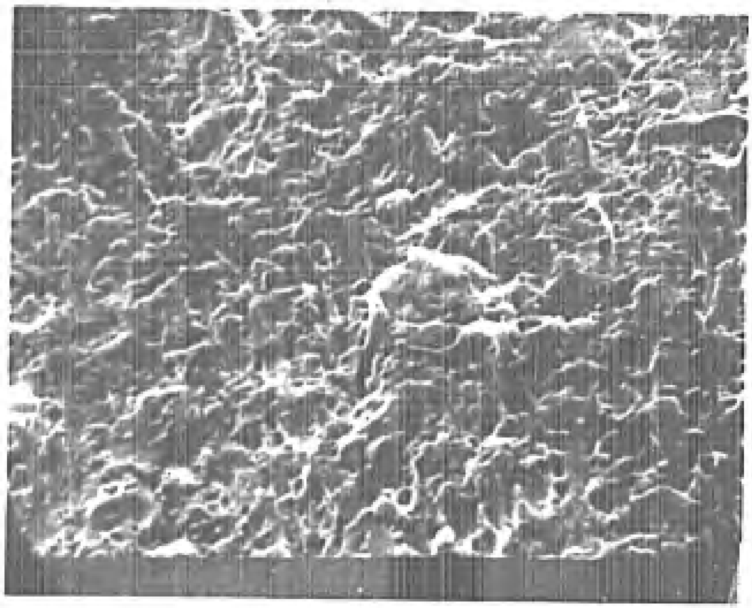

700X

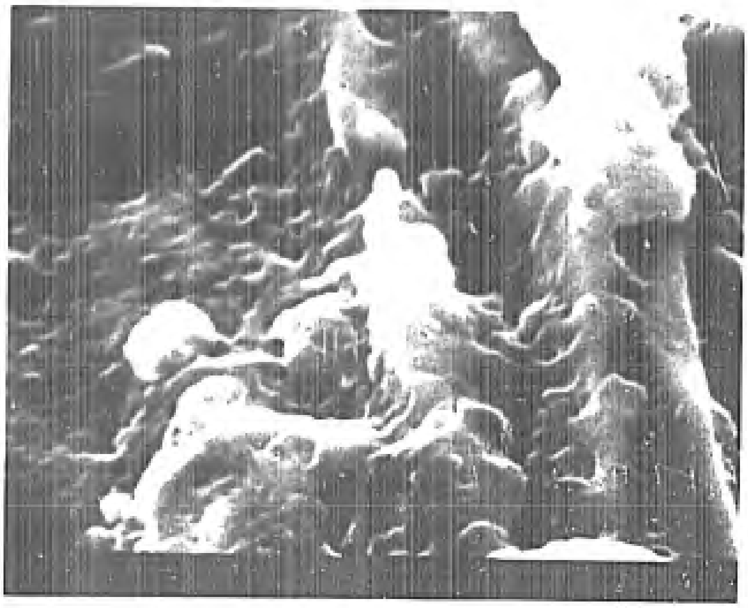

7000X

Figures 2a,2b. Scanning electron microscope photographs of an annealed surface in the "as received" condition. In the upper photograph the small black rectangle is 20μ across, while in the lower one it represents 2μ.

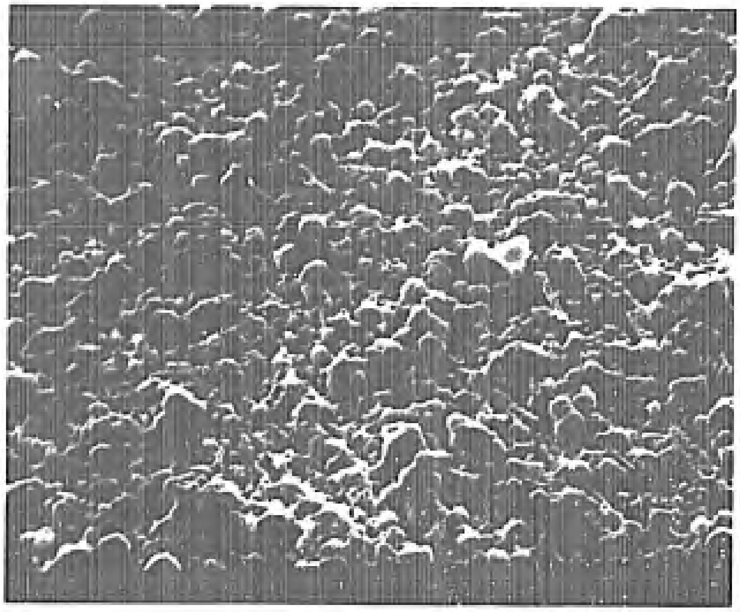

700X

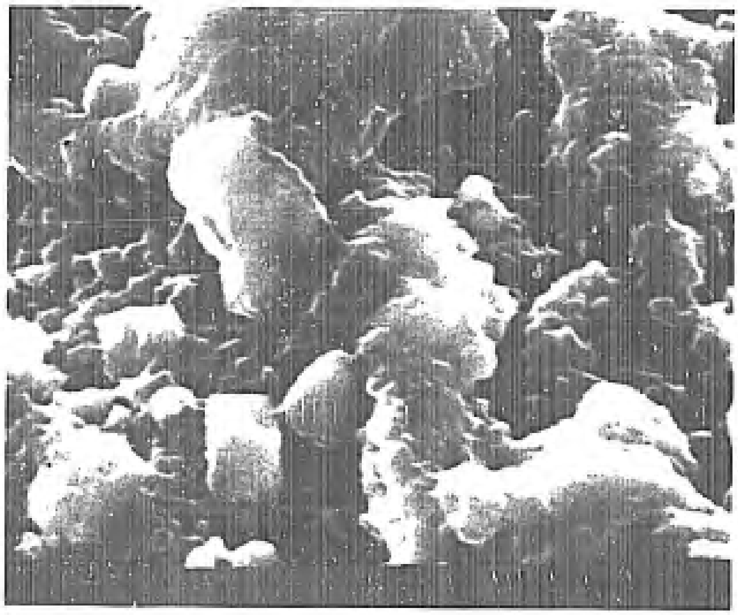

7000X

Figures 2c,2d. Scanning electron microscope photographs of the annealed surface after use in a moderate temperature convective heat transfer experiment. In the upper photograph the small black rectangle is 20μ across. while in the lower one it represents 2μ.

APPENDIX F

RADIATING THERMOCOUPLE CONDUCTION ERROR

W. G. Hess[1], A. F. Deardorff[2] and D. M. McEligot[3]

In space environments and space simulation chambers, temperatures are often measured with thermocouples attached to exposed surfaces. The primary means of energy exchange then are conduction through the solid material and thermal radiation. In our Laboratory, we also often use a vacuum environment to minimize and/or localize the heat loss from thin-walled tubes in which we perform internal convective heat transfer measurements [1]. In these situations the thermocouple attachment usually acts as a radiating fin which reduces the local surface temperature near the point of measurement. This systematic effect may be called the radiating thermocouple conduction error.

Schneider [2] presents an analysis to predict the thermocouple conduction error in a convective environment by idealizing the thermocouple as a cylinder mounted perpendicular to the surface at a single point.

---

1. Research Assistant. Now with Pratt and Whitney Aircraft Company, West Palm Beach, Florida.

2. Research Assistant. Now with Gulf General Atomics, La Jolla, California.

3. Professor.

Including energy generation in the wall by electrical resistive heating and energy transfer from the surface opposite the idealized thermocouple, one may extend Schneider's result to

$$\frac{T_{TC} - T_{w,u}}{T_{w,u} - T_{\infty}} = \frac{(h_o - h_{TC}) r\, K_o(\lambda r)}{(h_i + h_{TC}) r\, K_o(\lambda r) + 2\lambda k_w \delta K_1(\lambda r)} \quad (1)$$

where the heat transfer coefficients may represent convective or radiative processes as appropriate. In the case of infinite radiating thermocouple leads, the effective heat transfer coefficient over the contact area of the thermocouple may be shown to be

$$h_{TC} = \frac{k_{TC}\left[\frac{2\beta}{5}\left(T_{TC}^5 - 5T_{TC}T_{\infty}^4 + 4T_{\infty}^5\right)\right]^{\frac{1}{2}}}{T_{TC} - T_{\infty}} \quad (2)$$

if its emissivity and thermal conductivity are constant. Thus, provided that the material properties are known, prediction of the radiating thermocouple conduction error reduces to the problem of determining the effective thermocouple radius, r.

For many applications the parallel type thermocouple junction, shown in the figure insert, is more accurate than the more common cross type junction because the location of the measuring plane is effectively on the tube surface rather than being spread perpendicular to it [3]. Rather than satisfying the idealization of a single cylindrical interface between the thermocouple and the surface, the attachment region for the parallel junction consists of two roughly elliptical areas slightly separated from each other. Accordingly, the objectives of the present work were taken to be (1) to determine r for a parallel junction configuration and (2) to investigate the reproducibility of the conduction error when such thermocouples are produced by using normal laboratory standards for equipment construction.

Measurements were conducted on three circular test sections of 0.010 inch thick Inconel 600, two feet long. Premium grade bare Chromel and Alumel thermocouple wires of 0.005 inch diameter were spot welded to the test section by the electrical discharge technique. Circumferential distance between the two wires was approximately 1/8 inch and the attached area of each covered approximately one to two wire diameters. Tests included about fourteen such thermocouples with all wires taken from the same spools.

These resistively heated test sections were mounted in glass vacuum chambers. With no internal flow, h_i equals zero and h_o can be determined from the tube emissivity which one also deduces from the tests. "Undisturbed" tube wall temperatures, $T_{w,u}$, were determined with a traveling internal thermocouple probe, also of premium grade Chromel-Alumel, which measured the wall temperature profile axially between the thermocouples. Calculations show the maximum temperature drop through the wall to be less than 0.01 $^\circ$F so the thin wall idealization is valid. Readings were accepted without correction for deviation from standard N.B.S. emf tables since Hoskins Manufacturing Company certified the deviation as less than 1°F.

Results are demonstrated on Figure 1. The dashed curves are predictions based on equations (1) and (2) in conjunction with manufacturers' information for emissivities and thermal conductivities of the thermocouple wires and the tube. The solid curve represents predictions based on the measured emissivity of the Inconel tube used by Hess and on an effective thermocouple radius equal to the actual wire diameter; otherwise the bases are the same.

Hess' data points are averages of the thermocouple readings for the central portion of the tube and they show the effective radius to be approximately equal to the wire diameter or slightly less. The measurements of Swearingen and of Reynolds and Deardorff are from test sections with different thermal histories, hence emissivities, but of the same materials and dimensions. Their calibrations suggest that r is about one-half the wire diameter. Different welding jigs were used for each and, consequently, the region of attachment varied from test section to test section but would be approximately uniform for different thermocouples on the same test section. Accordingly, one would expect the level of the thermocouple conduction error to vary from test section to test section as it does in Figure 1.

We conclude that the effective radius of the thermocouple attachment is approximately one-half to one wire diameter when constructed in the manner described. One may use this observation with manufacturers' information and equations (1) and (2) to determine whether the systematic error will be significant in his specific application. (For the results shown, in an internal convective heating experiment with $T_w \approx 1000°F$ and $T_b \approx 900°F$, the resulting error in Nusselt number would be 5 to 10 per cent.) If such predictions indicate that the errors would be important, we recommend individual calibration since the values of a number of the pertinent input variables are not readily available.

REFERENCES

1. H. C. Reynolds, T. B. Swearingen and D. M. McEligot, "Thermal Entry for Low Reynolds Number Turbulent Flow," J. Basic Engr., 91, 67 (1969).

2. P. J. Schneider, Conduction Heat Transfer, Reading: Addison-Wesley, 1955.

3. W. K. Moen, "Surface Temperature Measurement," Inst. and Cont. Syst., 33, 70 (1960).

ACKNOWLEDGEMENT:

This work was also partially supported by the Engineering Experiment Station of the University of Arizona and by the Army Research Office - Durham.

NOMENCLATURE

h	Heat transfer coefficient; h_i, inner surface: h_o, outer (thermocouple) surface.
k	thermal conductivity
K_o, K_1	Bessel functions
r	effective thermocouple attachment radius
T_{TC}	temperature measured by thermocouple
$T_{w,u}$	"undisturbed" wall temperature
β	thermocouple heat transfer constant, $2\sigma\varepsilon/(k_{TC}r)$
δ	wall thickness
ε	emissivity
λ	wall heat transfer constant, $[h_o + h_i)/(k_w r)]^{\frac{1}{2}}$
σ	Stefan-Boltzman constant

FIGURE CAPTION

Figure 1. Radiating thermocouple conduction error for parallel type junction

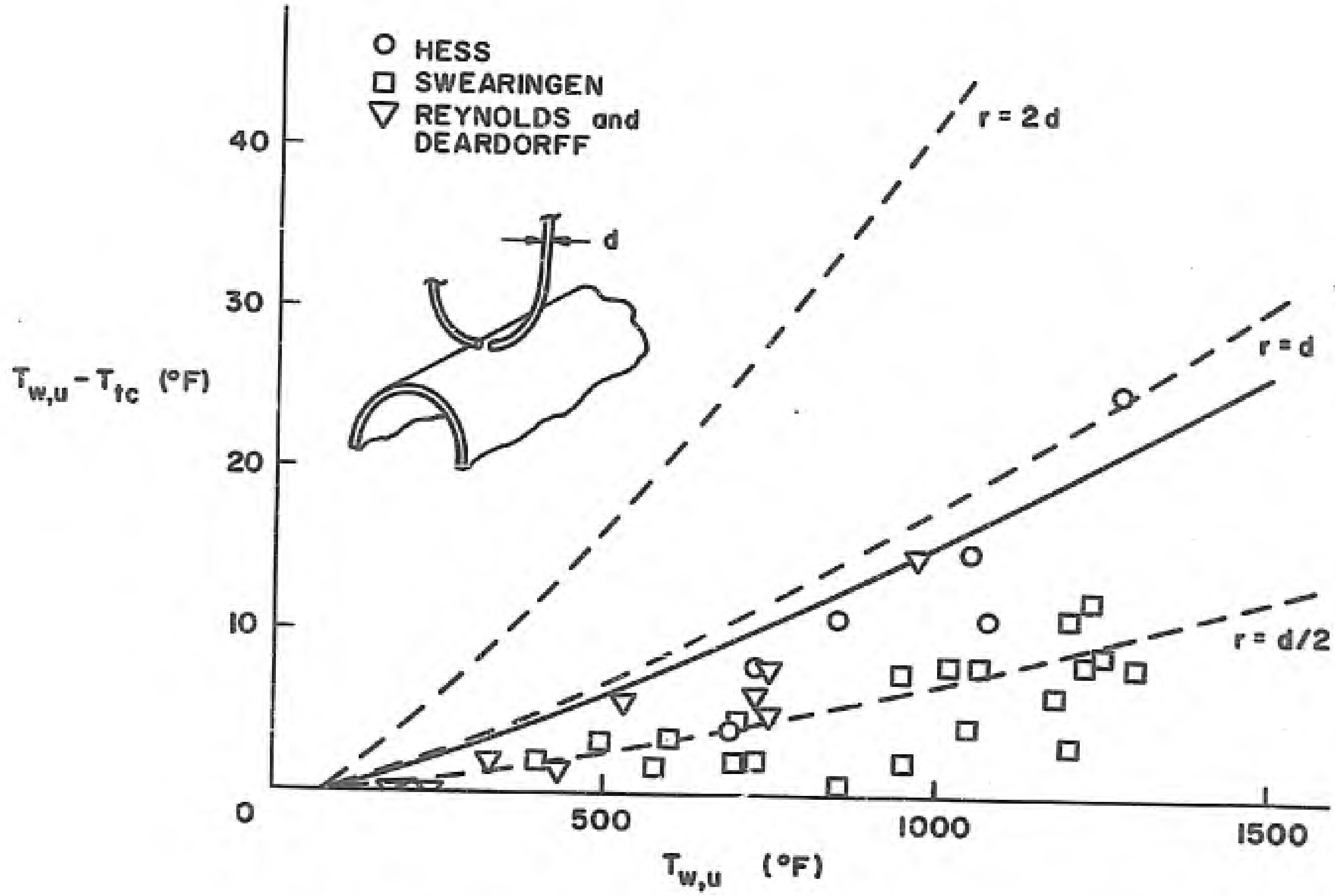

Figure 1. RADIATING THERMOCOUPLE CONDUCTION ERROR FOR PARALLEL TYPE JUNCTION

APPENDIX G

EFFECTS OF INLET TEMPERATURE ON THERMAL DEVELOPMENT FOR TURBULENT FLOW IN DUCTS HEATED ASYMMETRICALLY WITH AIR PROPERTY VARIATION

D. M. McEligot[1] and K. W. Schade[2]

---

1. Professor.

2. NDEA Fellow.

With symmetric conditions in a circular tube one cannot obtain axially-invariant temperature and velocity profiles when gas transport properties vary significantly. However, with annuli or parallel plates maintaining one wall at a constant temperature can eventually lead to fully established conditions downstream. Hatton [1] analytically treats this situation with constant fluid properties, both wall temperatures specified and fully developed turbulent flow before heating commences. He shows that when the non-dimensional temperature profiles are symmetric, i.e. the inlet temperature is the mean of the two wall temperatures, there is a striking reduction in the distance necessary to approach Nu_∞ closely. If this condition does not exist, Nu may still differ considerably from Nu_∞ even at $x/D_h \approx 100$.

Hall, Jackson and Khan [2] conducted an experimental study of heat transfer to supercritical carbon dioxide downstream in an apparatus with one wall heated at approximately constant heat flux and the other cooled by water flow. Their purpose was to examine a fully developed flow with strong property variation. In the present note their boundary conditions are studied by means of numerical solutions of the governing equations. Since air properties can be represented more easily than those of carbon dioxide near the "pseudo-critical temperature," they are treated here, but at a moderately high heating rate so that the properties do vary significantly.

The object of this note is to examine the trends in the heat transfer behavior as the inlet temperature is varied when property variation is included. Since a heating rate parameter, such as T_h/T_c or q''_{wh}/Gc_pT_i, and the inlet temperature are required to characterize the general problem as well as the Reynolds number, Prandtl number and idealized property-dependence functions, only one typical situation is examined. The extensive computer calculations otherwise necessary are beyond the scope of this brief report.

Method

The usual boundary layer approximations apply. The flow is by pure forced convection at low Mach number. Thermal boundary conditions are constant wall heat flux on the upper plate and constant wall temperature on the lower. Temperature and velocity are taken as uniform at the entrance and power laws represent the air properties.

Calculations use the numerical program of Schade [3], which solves the coupled, governing finite-difference-equations, derived by considering finite control elements, in the same manner as Bankston and McEligot [4]. Grid parameters were chosen to yield convergence of wall parameters to within about two per cent to conserve computer time.

To study a typical situation, inlet and heating conditions are adjusted to approach a downstream condition with Re $\sim 6 \times 10^4$ and $T_{h,\infty}/T_c \sim 2$. Entering temperatures are varied between $T_{h,\infty}$ and T_c.

Turbulence model

We chose a model which is expected to predict optimistically short entry lengths. Then, if the predicted distances are unreasonably long, we realize the situation would be worse in practice. The "van Driest-wall" mixing length

$$\ell = Ky\ [\ 1 - \exp(-y_w^+/y_\ell^+)]$$

is expected to be such a model. No history of the upstream turbulence behavior is represented by mixing length models directly. With strong heating in a tube the model appears to predict readjustment of flow more rapidly than observed [4]. Further, ℓ is allowed to increase, in accordance with equation (1), until near the center it exceeds the value calculated from the opposite wall, rather than truncating $\ell(y)$; thus, the predicted boundary layer should propagate into the core region more rapidly than in practice.

The turbulence model enters the finite-difference-equations as effective viscosity and effective thermal conductivity, based on the assumption of equal eddy diffusivities. One concern with a mixing length model is that where the velocity gradient is zero, the effective thermal conductivity will only have a molecular contribution. Theoretically, the fully-developed solution then would show an artificial region of high thermal resistance somewhere in the central region. However, the procedures of the computer program avoid this difficulty by taking k_{eff} at each control surface as the mean of k_{eff} at the two nearby nodes. A relatively coarse grid in the central region ensures that even if $k_{eff} = k$ at one node, its neighbor and, hence, the mean of the two will give strong turbulent contributions.

Results

We concentrate on the heated wall. As seen in Figure 1a, heating the inlet air can reduce the distance required to obtain an approximately constant Nusselt number. However, in contrast to Hatton's constant property results [1], the mean temperature is not best when the fluid properties vary in an unsymmetric manner. The gradual approach to Nu_∞ presents another design problem: as an example, the prediction for inlet temperature (normalized) of 0.4 varies only a few per cent over the range $40 < x/D_h < 80$, yet it is not yet near Nu_∞ . For "short" ducts of 100 D_h (200 x plate spacing) or so, a design based on the fully developed prediction can be considerably in error.

One of the primary objectives of experiments performed with the geometry and boundary conditions of this note is to obtain conditions where the eddy diffusivity for heat, or some equivalent quantity, may be determined directly - by measuring q''_w and a single temperature profile - from

$$q''_w = q''_y(y) = -(k + \rho c_p \varepsilon_h) \partial t/\partial y$$

In this case the appropriate criterion of fully developed flow is not Nu but whether $q''_y(y) \approx q''_w$. Accordingly, the maximum deviation from q''_w,

$$\left| \frac{q''_y(y) - q''_{wh}}{q''_{wh}} \right|_{max}$$

is plotted against axial position as Figure 1b. (A number of the curves show changes in slope where the transverse location of the maximum deviation shifts abruptly from the central region to the opposite wall.) Concentrating on the "best" curve, inlet temperature of 0.6, we see that the unbalance is about ten per cent at $x/D_h \approx 40$ although Nu is within a few per cent of Nu_∞. And at $x/D_h = 100$ there is still a five per cent error somewhere across the flow. Since the hydraulic diameter is twice the plate spacing and one inch is perhaps a reasonable minimum spacing for probe measurements without disturbing the flow significantly, rather long ducts would be required. Further, the locus of the curve is quite sensitive to the inlet temperature - and possibly to the turbulence model - so it would be a mistake to design an experiment with the length limited to the best conditions found in this sort of numerical calculation.

Thus, such experiments should be designed to measure $\varepsilon(x,y)$ since extremely long ducts would be necessary before $q''(y) \approx q''_w$ so that ε can be measured as a function of y only.

Acknowledgments

The calculations were performed while the first author was on sabbatical leave at Imperial College of Science and Technology, London. The aid of their Computer Centre is appreciated.

Subscripts

b	bulk
c	cold wall
h	hot wall
i	inlet conditions
w	wall, evaluated at wall temperature
y	in transverse direction
∞	fully developed

References

1 Hatton, A. P., "Heat Transfer in the Thermal Entrance Region with Turbulent Flow between Parallel Plates at Unequal Temperatures," *Appl. Sci. Res.*, A, Vol. 12, 1963, pp. 249 - 266.

2 Hall, W. B., Jackson, J. D. and Khan, S. A.,"An Investigation of Forced Convection Heat Transfer to Supercritical Pressure Carbon Dioxide," *Proceedings of the Third International Heat Transfer Conference,* Vol. I, 1966, pp. 257 - 266.

3 Schade, K. W. and McEligot, D. M., "Cartesian Graetz Problems with Air Property Variation," *Int. J. Heat Mass Transfer,* Vol 14, 1971, pp. 653-666.

4 Bankston, C. A. and McEligot, D. M., "Turbulent and Laminar Heat Transfer with Varying Properties in the Entry Region of Ducts," *Int. J. Heat Mass Transfer,* Vol. 13, 1970, pp. 319 - 344.

Figure Caption

Figure 1 Thermal Development between Parallel Plates with Asymmetric Thermal Boundary Conditions, Air Properties.

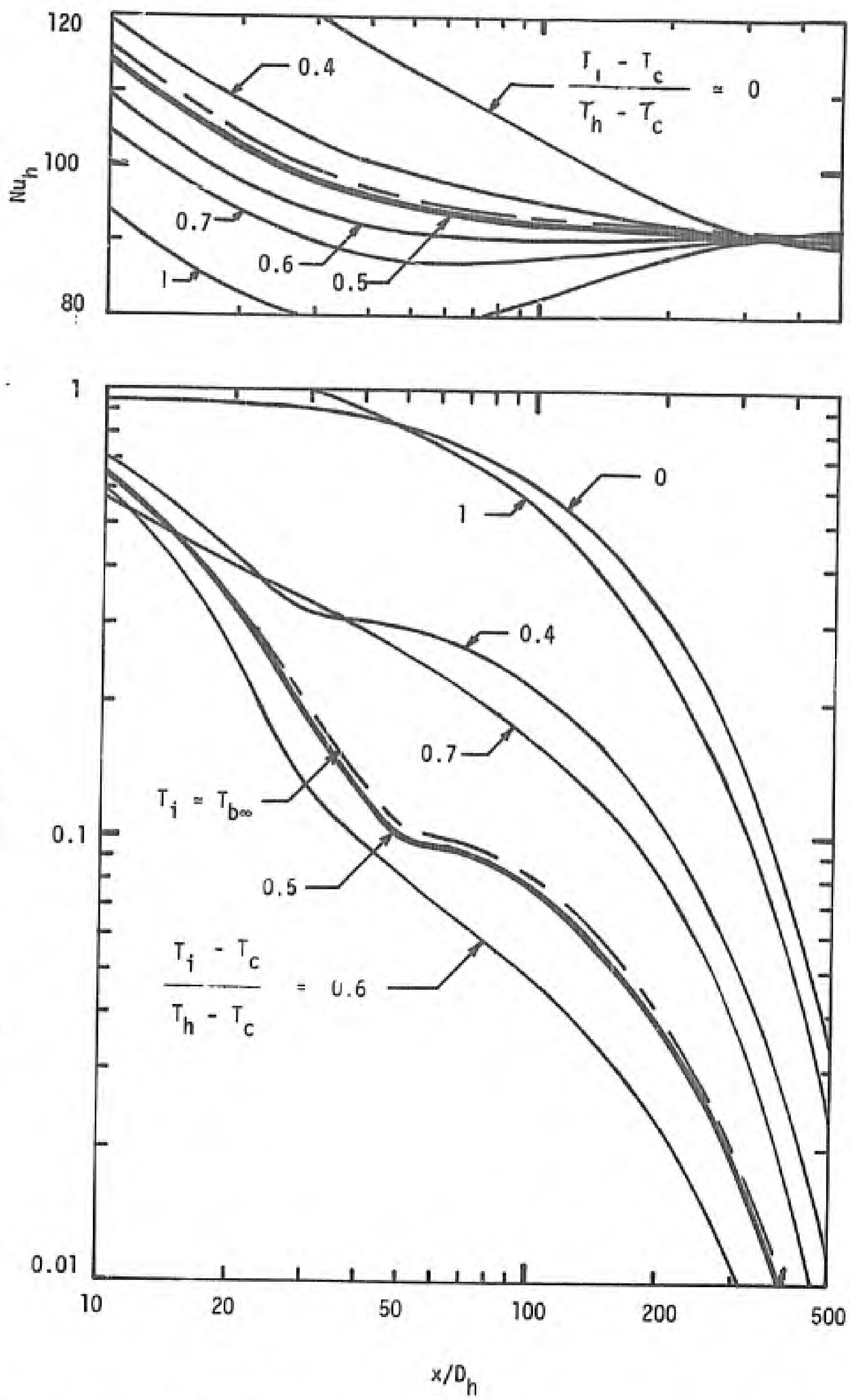

Figure 1 Thermal Development Between Parallel Plates with Asymmetric Thermal Boundary Conditions, Air Properties.